The Life Cycle of the pteropod *Limacina helicina* in Rivers Inlet (British Columbia, Canada)

by

Kang Wang

B.Sc., The University of British Columbia, 2009

A THESIS SUBMITTED IN PARTIAL FULFILLMENT OF

THE REQUIREMENTS FOR THE DEGREE OF

Master of Science

in

The Faculty of Graduate and Postdoctoral Studies

(Oceanography)

THE UNIVERSITY OF BRITISH COLUMBIA

(Vancouver)

April 2014

Abstract

The life cycle of *Limacina helicina* has been continuously debated within the literature. We believe the current lack of consensus regarding fundamental aspects of its life cycle (e.g. seasonal times of spawning, seasonal development of the population size structure, as well as the life cycle longevity) is primarily due to using datasets of low temporal resolution.

Using fort-nightly data, two population cohorts were identified using the `mixdist` statistical package and tracked for more than 400 days, throughout 2008 to 2010. From this, a life cycle longevity of 1.2–1.5 years was estimated for *L. helicina* in Rivers Inlet. Throughout the seasons, the population size structure showed a continually high presence of the smaller size-groups suggesting continuous spawning, however, based on total densities of > 600 ind.m^{-3}, the late spring was put forward as the period of peak spawning.

Continuous spawning was confirmed with the use of daily data. Identification of a summer peak spawning established late spring and summer as two periods of enhanced spawning, although continuous spawning occurred throughout the season (in a limited fashion). Short-term periods of significant growth were observed prior to peak spawning in late spring and summer. This was not directly coupled with chlorophyll concentrations, possibly due to the time lag between periods of high chlorophyll biomass and zooplankton response. At-

tempts were made to estimate the instantaneous mortality of *L. helicina*, and the seasonal changes experienced from spring to summer. Our estimates were complicated by a combination of 1.) inherent patchiness of *L. helicina*, 2.) advection, and 3.) merged recruits. Generally, there were no cases of significant mortality throughout the seasons however, short term mortality was observed after peak spawning. It is plausible that the smallest size-groups of *L. helicina* experiences the highest mortality after peak spawning.

Our findings show that in Rivers Inlet, *L. helicina* has a life cycle spanning 1–1.5 years with spring and summer peak spawning activities. The spring cohort is likely spawned by the summer cohort from the previous year. It utilizes the spring phytoplankton bloom to reach sexual maturity and spawn the summer cohort.

Preface

This thesis is ultimately a product of the collaborative effort of many investigators from the University of British Columbia, Point Grey campus, of the inter-disciplinary RIES - Rivers Inlet Ecosystem Study conducted from 2008 to 2010 (*riversinlet.eos.ubc.ca/People.html*). The aims of this thesis are separate and not directly connected with the main objectives of the RIES. Additional winter sampling from 2010–2011 was performed by Wayne Jacobson with direction from Brian Hunt and the Hakai Institute. Results from other studies in the RIES were used throughout Chapters 2 and 3 to help rationalize our findings.

Formalin preserved zooplankton samples for the bi-weekly and monthly sampling in Chapter 2, as well as the daily zooplankton samples used in Chapter 3, were processed by myself. Prior to being considered for this thesis, the daily zooplankton samples in Chapter 3 was used by an undergraduate student as the basis of a directed studies project, guided by Evgeny Pakhomov.

The cohort analysis in Chapters 2 and 3, performed using the `mixdist` statistical package (for the R statistical programming language), was conducted by myself with guidance from Evgeny Pakhomov and Brian Hunt. Complicated details concerning the use of `mixdist` were clarified through email communication with the author, Peter MacDonald.

Table of Contents

List of Tables

List of Figures

Acknowledgements

I want to thank Dr. Evgeny Pakhomov for giving me the opportunity to become involved in oceanographic research, even before I was an M.Sc. student. Your extensive expertise and patience has motivated me to keep pushing forward in the my search for the answers, and your calm demeanour during my times of difficulty have always reminded me to keep focused and proceed one step at a time.

Thank you Dr. Brian Hunt for all of your supporting help throughout this graduate degree. In particular, your meticulous attention to detail has provided me with the motivation to further improve my scientific writing in order to better communicate my thoughts and opinions, to the general public.

Additional thanks to my committee members, Dr. Christopher Harley and Dr. Mary O'Connor for giving me new perspectives throughout the challenging times of data interpretation. Thank you to Lora Pakhomov for all the support you've provided during field work. Moira Galbraith, Doug Yelland, and the rest of the scientific community of the C.C.G.S. John P. Tully, thanks for all your assistance in the field.

To all the members of the P-Lab Family, old and new, thank you all for your friendship as well as your positive and constructive feedback. Special thanks to

Desiree Tommasi for all of your support and encouragement, when it seemed like there was no one else, and to all the other oceanographers in the department. I have enjoyed many a lunchtimes with you, drinking tea/coffee, and talking non-science, as well as sharing many laughs.

Last but not least I want to thank my father for the unconditional help he has given me throughout my studies and in life.

Dedication

Dad, this thesis is dedicated to you. For your patience, for your spiritual (...and financial) support, and for your continued encouragement to pursue whichever path I choose.

Chapter 1

An Introductory Review

1.1 What Are Pteropods

Pteropods are pelagic snails (sea snails, sea slugs) and are one of five groups of holoplanktonic gastropods, ranging in size from 0.2 mm to $>$ 80 mm in length (Lalli and Gilmer, 1989). Living primarily within the euphotic zone, some pteropods (e.g. *Limacina trochiformes*) have been observed at depths of $\geq$ 2km (Lalli and Gilmer, 1989). The term "pteropod" refers to two taxonomic orders of gastropods, thecosomes and gymnosomes. Thecosomatous pteropods are housed within a calcareous shell while gymnosomes are shell-less (Lalli and Gilmer, 1989). Only the Thecosomes will be discussed as the remaining thesis focuses on species from this order.

Distributed throughout the oceans, thecosome diversity is highest in tropical waters where few species are found in high abundance (Lalli and Gilmer, 1989). Conversely, the waters of high-temperate and polar latitudes are home to a few species that occur in high abundance (Lalli and Gilmer, 1989; Kobayashi, 1974; Gannefors et al., 2005; Hunt et al., 2008; Bednaršek et al., 2012). *Limacina*

retroversa and *Limacina helicina* are two such species, with *L. retroversa* being observed only within the Atlantic. *L. helicina* was postulated as a bipolar species with the Northern Hemisphere *L. helicina helicina* (forma *acuta, helicina, and pacifica*) found in the waters of the polar Arctic, and *L. helicina antarctica* (forma *antarctica* and *rangi*) found in the Southern Oceans (Hunt et al., 2010). Subsequent molecular analysis in Hunt et al. (2010) revealed genetic differences between the Arctic and Antarctic forms of *L. helicina*, alluding to the two variants (e.g. *L. helicina helicina* and *L. helicina Antarctica*) being distinct. Both Northern and Southern variants appear to have a skewed distribution with a larger ratio of small juveniles to larger adults (Hunt et al., 2008). Bednaršek et al. (2012) reports the contribution of the larger size-fractions to be $\leq 2\%$ of the population.

1.2 Taxonomy

Two suborders comprise the Thecosome order, the calcareous Euthecosomata and the pseudoconch bearing Pseudothecosomata (Lalli and Gilmer, 1989). The following presents the classification from Lalli and Gilmer (1989).

Class Gastropoda

Subclass Opisthobranchia

Order Thecosomata

Suborder Euthecosomata

Family Limacinidae

Family Cavoliniidae

Suborder Pseudothecosomata

Family Peraclididae

Family Cymbuliidae

Family Desmopteridae

Order Gymnosomata

Suborder Gymnosomata

Family Pneumodermatidae

Family Notobranchadeidae

Family Cliopsidae

Family Clionidae

Suborder Gymnoptera

Family Hydromylidae

Family Laginiopsidae

The above scheme is deemed suitable such that suborders and families within Thecosomata are easily distinguished, visually.

1.3 Thecosome Morphology

Euthecosomes and Pseudotheosomes are differentiated by shell morphology and/or shell surface features (Lalli and Gilmer, 1989). In the Euthecosome suborder, the family Limacinidae are identified by a sinistrally coiled shell ($<$ 1 mm to 15 mm). (Lalli and Gilmer, 1989). Pseudothecosomes include species that possess a calcareous shell (Family Peraclididae), species lacking a calcareous shell but possessing a pseudoconch (Family Cymbuliidae), and species that lack both a calcareous shell and a pseudoconch (Family Desmopteridae) (Lalli and Gilmer, 1989). Similar to Limacinidae, Peraclididae are also characterized by a sinistrally coiled shell although Peraclididae feature distinctive ornamented patterns on the shell surface. The wings are also fused together into a single "wing

plate" whereas Limacinidae possess separate wings. Cymbuliidae are considerably larger (35 mm to 80 mm in length), with some species (in genera *Cymbulia, Corolla, Gleba*) lacking an external shell but possessing a pseudoconch (Lalli and Gilmer, 1989). Lacking a calcareous shell as well as a pseudoconch, Desmopteridae are characterized by a cylindrical body with fused wing plates attached and a single pair of symmetrical tentacles (Lalli and Gilmer, 1989)

1.4 Swimming and Buoyancy Regulation

Thecosome swimming is a process that involves phases of active swimming and passive sinking (Lalli and Gilmer, 1989). Conover and Paranjape (1977) define a "rest" and "active" stage of locomotion for *L. retroversa* and Gilmer and Harbison (1986) state that these two stages likely apply for all species of Thecosomes. Despite being thin and comparatively light, the calcareous shell is sufficiently heavy (50% of dry weight) to cause gradual sinking (Conover and Paranjape, 1977). In order for Thecosomes to maintain the same depth distribution, active swimming must be maintained for 25% of the swimming process (Conover and Paranjape, 1977). Sinking rates will differ depending on the method of buoyancy regulation (Lalli and Gilmer, 1989). Limacinidae have limited approaches to regulate buoyancy while Cavoliniidae are able to employ different strategies (Lalli and Gilmer, 1989). Cavoliniidae shells feature spines and curvatures that increase the surface area of the individual (Lalli and Gilmer, 1989). Moreover, many genera within Cavoliniidae (*Creseis, Hyalocylis, Styliola, Cuvierina, Clio*) are able to extend the mantle lining to the shell exterior, where mucous material is exuded to mitigate sinking (e.g. *Creseis acicula*, *Creseis virgula*) (Lalli and Gilmer, 1989). Additional methods include the ability to create a neutrally buoyant pseudoconch (Lalli and Gilmer, 1989). Lacking external shell features and a pseudoconch, Limacinidae utilizes a mucous feeding web to regulate buoy-

ancy (Lalli and Gilmer, 1989; Hunt et al., 2008). When deployed the mucous web prevents sinking, with the buoyant period correlated to feeding (Lalli and Gilmer, 1989).

1.5 Food and Diet

The cessation of motion when neutrally buoyant prevents the disturbance of the deployed mucous web by movements of the paired-wings or the wing-plate (Lalli and Gilmer, 1989). Limacinidae are considered the least specialized of feeders, producing spherical feeding webs (Lalli and Gilmer, 1989). Cavoliniidae are also considered simple feeders but only for those genera exhibiting a conical shell (e.g. *Creseis, Clio, Hyalocylis, Styliola, Cuvierina*) (**?**)lalli1989pelagic). The size of the food web produced is size and species dependent, with some food webs of $\geq$ 2 m in diameter produced (Lalli and Gilmer, 1989). Pseudothecosomes produce funnel shaped feeding webs or flattened rectangular webs as opposed to the spherical webs produced by Euthecosomes (Lalli and Gilmer, 1989). Web production within *Limacina* is rapid with complete construction within 5 seconds (Lalli and Gilmer, 1989). Similarly, webs are retracted *via.* ciliary action in about 20 seconds, although they can discarded when the feeding individual is disturbed (Lalli and Gilmer, 1989). Comparatively slower, web production in *Cavolinia* can exceed 2 minutes while times of web ingestion range between 1–3 minutes (Lalli and Gilmer, 1989). When feeding, individuals are orientated with the ventral surface facing up towards the web, and the individual below (Lalli and Gilmer, 1989). Connection between the feeding individual and the feeding web is maintained by the proboscis (elongate appendage, Figure 25b in Lalli and Gilmer, 1989). Feeding webs are pulled into the gut by a small radula where solid material (e.g. diatom frustules) is crushed by gizzard action (Figure 27 in Lalli and Gilmer, 1989).

Phytoplankton is the main food source although the spectrum of food ingested can be quite diverse (Morton, 1954; Kobayashi, 1974; Gilmer and Harbison, 1991; Gannefors et al., 2005; Hunt et al., 2008; Bernard and Froneman, 2009; Bednaršek et al., 2012). Detritus, bacteria, small protozoa, to various types of phytoplankton (diatoms, dinoflagellates, tintinnids, coccolithophorids) have been found in the gut content of various species within *Limacina* (Lalli and Gilmer, 1989). Larger food items (foraminifera, zooplankton, molluscan larvae, heteropods, chaetognaths) have also been found in the gut content of various Limacinidae and Cavoliniidae species (Lalli and Gilmer, 1989).

1.6 Reproductive Biology

Developing first as males and maturing as females, Thecosomes are protandric hermaphrodites that reproduce sexually with the reciprocal exchange of spermatophores (Lalli and Gilmer, 1989). Although understudied, all species within the Thecosome order share similar reproductive biologies with minor differences in reproductive structures and behaviours (Lalli and Gilmer, 1989). The growth of *Limacina* has been thought to be uniform with the hypothesis that maturity is size dependent (Kobayashi, 1974; Lalli and Gilmer, 1989). Dadon and de Cidre (1992) argue against this with the contention that maturity is influenced by environmental conditions, resulting in occurrences of individuals of differing age despite being the same size. With the exception of *L. helicoides* and *L. inflata*, the ontological development of *Limacina* progresses through the male stage with sperm produced in the ovotestis and stored within the hermaphroditic duct (Figure 31 in Lalli and Gilmer, 1989). Once matured to the female stage, the subsequent eggs produced are fertilized within the hermaphroditic duct and eventually passed through the female accessory organ to be encased by mucous from the female mucous gland (Figure 31 in Lalli and Gilmer, 1989). The fe-

male accessory glands lead into the mantle area where the eggs are subsequently released (Figure 31 in Lalli and Gilmer, 1989). Eggs are packaged and released as transparent free-floating egg masses varying in length depending on species (Lalli and Gilmer, 1989). *L. retroversa* has been reported to produce egg-masses ranging from 2–4 mm in length while the larger *L. helicina* produces egg-masses up to 12 mm in length (Lalli and Gilmer, 1989). Paranjape (1968) reports of 600 eggs spawned per female, for *L. helicina* in the coastal waters off of Vancouver Island, while up to 10,000 eggs per female have been reported for *L. helicina* inhabiting polar waters (Lalli and Gilmer, 1989). Up to 260 eggs per female have been recorded for the smaller *L. retroversa* inhabiting boreal waters (Lalli and Gilmer, 1989). Table 13 in Lalli and Gilmer (1989) summarizes egg mass production by *L. helicina* and *L. retroversa*. *Limacina helicoides* is ovoviviparous, with the eggs produced hatching within the mantle of the parent, while *L. inflata* exhibits brood protection with the hatched young residing within the parent mantle until a suitable size is reached (Lalli and Wells, 1978; Lalli and Gilmer, 1989).

1.7 Ecological Role, Ecological Threats, and Knowledge Gaps

1.7.1 Ocean Acidification

Dubbed "*the other CO_2 problem*", ocean acidification is an increasing problem for calcareous organisms, especially in polar waters (Fabry et al., 2008; Doney et al., 2009). Housed within an metastable aragonite shell and primarily distributed in polar waters, *L. helicina* is especially susceptible to ocean acidification (parts of the Arctic Ocean are already seasonally undersaturated with respect to aragonite) (Yamamoto-Kawai et al., 2009). This makes *L. he-*

licina a key indicator species of ocean acidification and a proxy of ocean health (Hunt et al., 2008; Bednaršek et al., 2012). While some calcareous organisms show resilience to increased acidity, our understanding of the potential impacts to ecosystem processes are complicated by the synergistic effects of increasing acidity and seawater temperature (Dixson et al., 2010; Lischka and Riebesell, 2012).

Despite our current grasp of the underlying biology of *L. helicina*, there are considerable knowledge gaps surrounding fundamental aspects of its life cycle (Lalli and Gilmer, 1989; Kobayashi, 1974; Fabry, 1989; Gannefors et al., 2005; Hunt et al., 2008; Bednaršek et al., 2012). Questions surrounding the life cycle longevity, seasonal spawning, and the seasonal development of the population size structure have yet to be resolved despite various studies in different eco-regions (Kobayashi, 1974; Fabry, 1989; Gannefors et al., 2005; Hunt et al., 2008; Bednaršek et al., 2012). Additionally, seasonal growth as well as mortality has only been investigated by a few studies of *L. helicina* (Kobayashi, 1974; Lischka et al., 2010; Bednaršek et al., 2012).

1.7.2 Life Cycle of *L. helicina* – Knowledge Gaps

The lack of consensus surrounding the life cycle of *L. helicina* is complicated by the lack of comparability between studies. Additional problems are present in the implementation of different sampling protocols combined with the use of different sampling equipment for data collection. Noted in Hunt et al. (2008) and Bednaršek et al. (2012), the use of sampling nets with differing mesh sizes influences the size of the population captured. Furthermore, *L. helicina* is a species that spans many geographical zones which may further complicate life cycle interpretations.

The spatial and temporal scale of sampling will also impact how the data are

sampled and interpreted (Wiens, 1989). Defined in Wiens (1989), the ability to distinguish temporal patterns is dependent on both the area sampled and the organism studied. Investigations with large spatial extents will be accompanied by increased heterogeneity while studies on smaller scales may reveal phenomenon that cannot be generalized over larger scales (Wiens, 1989). For *L. helicina*, the temporal resolution of data collected appears to be an important factor when attempting to describe its life-cycle. It appears our lack of understanding may be due to an "incomplete picture" describing the seasonal evolution of *L. helicina*, although Northern and Southern variants may live differing life-cycles due to genetic differences (Hunt et al., 2010).

This thesis investigates the life cycle of *L. helicina* in an attempt to resolve the knowledge gaps concerning its life cycle dynamics. Datasets of high temporal resolution are used in two chapters to study differing aspects of the *L. helicina*— life cycle . In Chapter 2, fort-nightly and monthly resolution sampling over 3 years is used to determine the inter-annual variation of the *L. helicina* population in Rivers Inlet. Using inter-annual data for 3 years, we attempt to portray a relatively more "complete" picture of the life cycle of *L. helicina*. Chapter 3 uses daily data for over 100 days (e.g. from spring to summer) to resolve the seasonal dynamics of *L. helicina*. With daily resolution, we aim to provide accurate estimates of the seasonal growth and mortality experienced by *L. helicina*, and to describe how this changes from spring to summer. Moreover, with the addition of chlorophyll data, we hope to establish a definitive connection between food availability and *L. helicina* population abundance.

Chapter 2

Life-Cycle Dynamics of *Limacina helicina* in Rivers Inlet B.C.

2.1 Introduction

2.1.1 Research Aims

Limacina helicina is a prominent pelagic mollusk in polar and temperate waters and is a key component of the zooplankton community (Hunt et al., 2008; Lalli and Gilmer, 1989). Potentially a significant grazer, *L. helicina* also acts as prey for numerous organisms across various trophic levels (cetaceans, various fish species, sea-birds, and other zooplankton) (Lalli and Gilmer, 1989; Hunt et al., 2008; Bednaršek et al., 2012). Additionally, *L. helicina* is also a significant contributor to the flux of $CaCO_3$ to the deep sea (Fabry, 1989; Bednaršek et al., 2012; Maas et al., 2011).

Characterized by a wing-like parapodia, *L. helicina* is housed within an aragonite shell and swims in a jerky spiral motion, hence its name of *sea-butterflies* (Morton, 1954; Lalli and Gilmer, 1989). As aragonite is a metastable form of $CaCO_3$, it is more susceptible to dissolution than calcite and at shallower depths

(Mucci, 1981). With the increasing threat of ocean acidification, the associated challenges imposed on calcareous organisms (e.g. significant decreases in calcification rates, reduced shell mass and activity) can have detrimental effects on the growth, development, and reproduction of these organisms (Yamamoto-Kawai et al., 2009; Comeau et al., 2009). Investigations by Comeau et al. (2010) demonstrated that larval *Cavolinia inflexa* were deformed when exposed to lower pH and despite showing active movement, these malformed individuals did not produce shells, and exhibited reduced growth rates. Similar results were obtained in experiments on Arctic *L. helicina* by Lischka et al. (2010) and Lischka and Riebesell (2012). The steady decrease of ocean pH may lead to the elimination of *L. helicina* from the marine environment with ramifications impacting marine food-web dynamics and marine biogeochemistry (Comeau et al., 2010).

Throughout the past century there have been numerous studies investigating various aspects of *L. helicina*, although its life cycle remains poorly understood (Lalli and Gilmer, 1989; Hunt et al., 2008; Bednaršek et al., 2012). To date, there is no agreement on questions regarding **1**). the life cycle longevity, **2**.) the seasonal development of the population size-structure, and **3**.) the seasonal times of spawning. Using different methods in different ecological systems, life cycle studies of *L. helicina* have yielded varying, sometimes drastically different results.

2.1.2 *Limacina helicina*: Past Life Cycle Investigations

Currently there are four studies that have investigated the life cycle of *L. helicina* (Kobayashi, 1974; Fabry, 1989; Gannefors et al., 2005; Bednaršek et al., 2012). Appending to this list is a comprehensive literature review by Hunt et al. (2008) that compiled published and unpublished sources to assess knowledge gaps for *L. helicina* in the Southern Ocean. Supplementing this, are studies of *Limacina*

retroversa in the temperate waters of the Atlantic and Southern Ocean (Hsiao, 1939a,b; Redfield, 1939; Dadon and de Cidre, 1992). These studies cover the reproductive biology of *L. retroversa*. Studying *L. helicina* in the Central Arctic Ocean of the Canadian Basin, Kobayashi (1974) reported a life cycle of 1.5–2 years with three cohorts and two generations spawned during one life cycle. Bednaršek et al. (2012) proposed the possibility of some *L. helicina* having a life cycle exceeding three years in the Scotia Sea of the Southern Ocean. A one year life cycle (also hypothesized for other *Limacina*) is stated in Hunt et al. (2008); Gannefors et al. (2005), and Fabry (1989).

Kobayashi (1974) described *L. helicina* to display rapid growth throughout the fall/winter to reach sexual maturity. A major die-off occurs in the following spring after the mature adults produced the spring cohort (Kobayashi, 1974). Reaching maturity by summer, the spring cohort spawned the summer cohort (Kobayashi, 1974). Along with spring and summer as the times of peak spawning, Kobayashi (1974) also reported minor spawning during winter. In support of summer spawning, Weslawski et al. (1991) reported high abundances of small *L. helicina* during summer in the waters near Svalbard. Additional support of summer spawning is provided in Hunt et al. (2008), where a summer die-off of larger adults is reported.

Limacina helicina appears to show considerable size variation between regions, with individuals > 9 mm seen in the waters of the North Atlantic and the Scotia Sea, Southern Ocean (Gannefors et al., 2005; Bednaršek et al., 2012). Meanwhile the largest individual observed in the Central Arctic Ocean measures only 3.7 mm (Kobayashi, 1974). From Bednaršek et al. (2012) the smaller juveniles constitutes a large proportion of the population, although the size frequency data in Gannefors et al. (2005) suggests that this is seasonally variable.

2.1.3 Rivers Inlet: Historical Context

Located on the central coast (51° 2410" N to 52° 5215" N) of British Columbia, Canada, and measuring approximately 40 km long by 3 km wide, Rivers Inlet is an stratified estuarine fjord characterized by steep walls, a deep inner basin, and a deep sill at the mouth of the inlet. Situated near the north east upwelling area, the regional oceanography is influenced by both the southerly flowing California current and the northward Arctic Current (Mackas et al., 2001). Located at comparatively lower latitudes, the plankton community experiences a longer growing season and is subjected to reduced environmental extremes (e.g. warmer waters – compared to zooplankton in polar waters). Fed by numerous rivers throughout the inlet, discharge from Oweekeno Lake via the Wannock River is recognized to be the primary source of fresh water. Average returns of over 750,000 sockeye salmon over most of the twentieth century displayed high fluctuations in the 1970s, eventually dwindling to 3,500 in 1996 (McKinnell et al., 2001). Commercial fishing has been closed since then with a minor and sporadic recovery of the sockeye salmon. Various hypothesis have been put forward as to the cause of the precipitous decline of the sockeye salmon including 1.) marine and/or freshwater related causes and 2.) the plankton food supply of juvenile sockeye salmon in their early marine phase. The Rivers Inlet Ecosystem Study (RIES) conducted from 2008 to 2010 was designed to investigate the planktonic food webs of Rivers Inlet with an emphasis on plankton dynamics associated with the marine phase of juvenile sockeye salmon. *Limacina helicina* is a major dietary component of sockeye salmon in Rivers Inlet and the datasets collected during RIES provided an unprecedented opportunity to study its life cycle.

2.1.4 Goals and Aims

To describe the life cycle dynamics of *L. helicina*, high quality datasets of its size structure are required. Such a dataset should have high temporal resolution and span an entire life cycle. Ideally such a dataset should span several years, especially if the system in question is prone to fluctuations in physical and biological conditions (Fabry, 1989). Currently used in fisheries science, the size frequency method is well developed and consistent in detecting and documenting the occurrence and temporal dynamics of population cohorts (MacDonald and Pitcher, 1979). From the available literature there are numerous contradictions concerning **1**. life cycle longevities, **2**. the seasonal times of spawning and **3**. the seasonal development of the population size structure of *L. helicina*. It is possible that these inconsistencies have arisen from datasets of low temporal resolution collected in various geographical regions. It is our belief that the non-sequential sampling confined to a limited seasonal range may particularly mask many intricacies of *L. helicina* life cycle dynamics. Through the use of high temporal resolution data and the size frequency method, the aims of this chapter were three-fold.

1. Describe the inter-annual progression and development of the population size structure of *L. helicina* based on observational data.
2. Identify the seasonal date(s) of spawning.
3. Quantitatively determine the life cycle longevity

2.2 Methods

2.2.1 Study Area – Rivers Inlet

The hydrodynamics of RI are driven by salinity stratification, hence the large influence of riverine freshwater (Hodal, 2010). Tidal motion and wind-induced mixing during strong storm events also impact RI hydrodynamics (Hodal, 2010; Wolfe, 2010).

Eight stations were sampled as part of the RIES project, UBC 7, DFO 1, DFO 2, DFO 3, DFO 4, DFO 5, UBC 6, and UBC 8 (see Figure 1.6 in Hodal, 2010, for the spatial proximities of each station). Sampled along a defined transect, the location of each station was selected to emphasize major oceanographic features within the inlet (Hodal, 2010). Located at roughly the halfway point, DFO 2 (Figure 2.2) was the key station of interest and was considered the most representative station with respect to the zooplankton community structure. Accordingly, DFO 2 was the most comprehensively sampled station during the RIES project and the focal station of this study. Situated outside the inlet, UBC 7 best represented the hydrographic conditions on the B.C. shelf, while DFO 5, UBC 6 and UBC 8 was representative of the inner inlet.

2.2.2 Seawater Temperature, Fluorescence, Salinity

Environmental parameters at DFO 2 were collected as part of RIES during 2008, 2009, and 2010. Fort-nightly data was collected during 2008 and 2009, while monthly data was collected for 2010. The CTD (SBE-25, Sea-Bird Electronics Inc., with additional sensors measuring nutrients, oxygen, and fluorescence) was deployed to 300 m depth (maximum) or 10 m above the bottom for depths < 300 m. As RI features a shallow mixed layer, the measurements of sea water temperature and salinity were averaged over the top 30 m, while fluorescence

levels were integrated over the same depth. Seawater temperature was measured in °C, with salinity expressed in PSU. Raw fluorescence values were used as a proxy for chlorophyll-*a*, concentration.

2.2.3 Sample Collection and Selection

Zooplankton were sampled using a 0.50 m diameter bongo net (Aquatic Research Instruments) harnessed with General Oceanics flow meters to measure the volume filtered. Two nets, each of a differing mesh size (150 μm and 250 μm) were used simultaneously for sample collection. Only samples from the 150 μm net were processed (Table 2.1). Exceptions were made for the 2010–2011 winter-transition when both 150 μm and 250 μm net samples were processed.

Vertical hauls from 300 m to surface were conducted during each survey, with samples preserved in a 4 % buffered sea water formaldehyde solution.

Spatial Analysis

Stations DFO 1–5 were compared during three time periods in 2010 (Figure 2.2; Table 2.2) to determine whether *L. helicina* sampled at DFO 2 were representative of the population in RI. Zooplankton samples from September, 2010 were collected during the 2010-15 LaPerouse Zooplankton Monitoring Cruise coordinated by the Institute of Ocean Sciences aboard the C.C.G.S. John P. Tully. UBC 7 was excluded from this analysis due to its locality being outside the inlet. Due to their close proximity to DFO 5, UBC 6 and UBC 8 were also excluded (see Figure 2.2b in Hodal, 2010).

Zooplankton were sampled day and night in vertical tows from 300 m depth to surface (10 m from bottom if max depth was < 300 m) using 0.25 m^2 (mouth area) bongo nets with a 235 μm mesh-size. These samples were collected for the Department of Fisheries and Oceans Canada. A TSK flowmeter recorded

the volume filtered. Samples were preserved in a 4 % sea-water formaldehyde solution.

2.2.4 Sample Preparation and Enumeration

Processing was undertaken using a Leica microscope equipped with an ocular ruler. Ocular measurements were made to the nearest 0.1 μm from the tip of the aperture directly to the back of the shell (Figure 2.1).

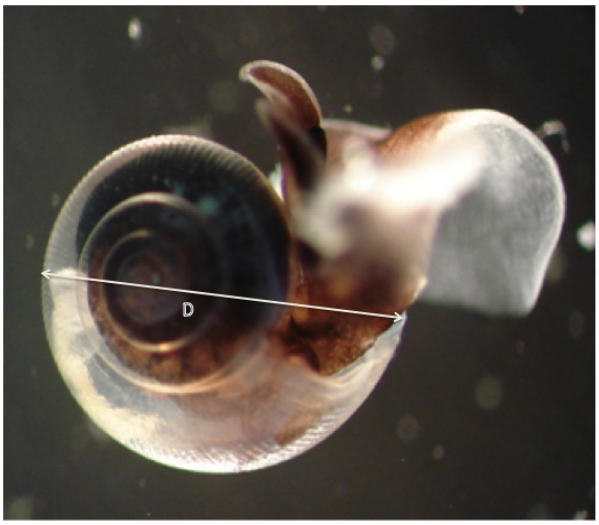

Figure 2.1: Photo of *L. helicina* with measurement of shell diameter (D)

Using No. 5 INOX tweezers from Fine Scientific Instruments, visibly large individuals (D $\geq$ 1.0 mm) were enumerated and measured from the entire sample. Visual inspection and removal of large individuals was necessary as the potential of excluding large individuals increases with a larger number of sample-splits. After inspection and the removal of large individuals, the sample was processed in its entirety or, when *L. helicina* were very abundant, split (1/2 to 1/64) to produce a manageable sub-sample. Whenever possible, a minimum of 128 indi-

viduals were measured, however, more or less were measured depending on the season. This was an attempt to ensure the data generated were representative.

2.2.5 Size Frequency Histograms and Identification of Cohorts

Size frequency histograms were constructed for each survey (Table 2.1). Discrete modal peaks seen in these histograms were deemed to indicate different population cohorts (e.g. age-classes) or distinct spawning events (MacDonald and Pitcher, 1979; Bednaršek et al., 2012). The ability to visually distinguish each cohort was of great importance when attempting to document the seasonal development of identified cohorts. For this reason, the size frequency histograms were not normalized. Due to the likelihood of strong overlap between cohorts, finite mixture distributions were fitted to each size frequency histogram. Functions from the R package `mixdist` were used to implement the fitting (MacDonald and contributions from Juan Du, 2011). By using an amalgamation of the EM and a Newton-type algorithm, the `mixdist` package computed the best fit to the observed data based on user-input of parameters (e.g. number of cohorts, mean size & standard deviation of each cohort, proportional abundance of each cohort, estimate of shape for the general distribution – Normal, Lognormal, Gamma, Weibull, Binomial, Exponential, and Poisson). Given the possibility of over parameterization (see Appendix B.5 for details concerning fitting finite mixture distributions), constraints were placed to reduce the number of parameters estimated (e.g. fitting the distributions were *aided* by the placement of constraints, not *forced*)

Cohorts can then be tracked from their time of recruitment into the population, to their likely times of die off (e.g. when they are no longer observed in the size frequency histograms).

2.2.6 Estimation of Growth and Life-Cycle Longevity

The seasonal growth of cohorts tracked was estimated by measuring the difference in the modal size (mean size) of the cohort(s) tracked between two dates of observation, then averaging that difference by the elapsed time between the two dates (in days)

$$G_c = \frac{m_j - m_i}{t_d} \tag{2.1}$$

$$t_d = t_j - t_i \tag{2.2}$$

$$LC = \frac{Date_{last} - Date_{first}}{365} \tag{2.3}$$

In Eq. 2.1, "m" is the modal size (in mm) of the cohort tracked and i and j are the observational dates at $t = i, j$, respectively, with t_d (Eq. 2.2) being the time difference in days, between t_i and t_j. Determination of the life-cycle longevity involved the tracking of cohorts from their dates of recruitment until their date of assumed die-off. The date of assumed die-off was deemed to be the date when the cohort was no longer detected in the corresponding size-frequency histogram. Life-cycle longevity ("LC") was calculated using Eq. 2.3 and expressed in years from the initial date of recruitment ($Date_{first}$) to the date of assumed die-off ($Date_{last}$). Expressed in days, the difference between $Date_{first}$ and $Date_{last}$ was averaged over the day duration of a year to estimate the life cycle longevity (in years) of *L. helicina*.

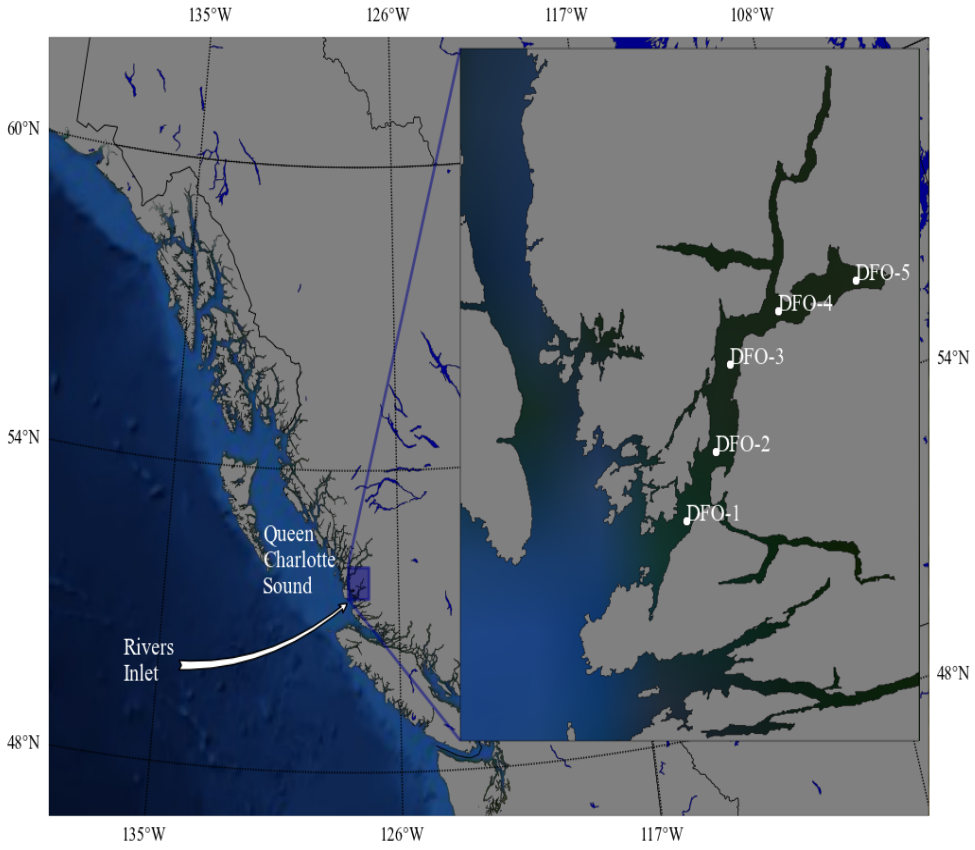

Figure 2.2: Lambert conformal conic projection of the British Columbia west coast and the northern tip of Washington State. Rivers Inlet is depicted in the zoomed inset of the mainland coast of BC. A NASA blue marble image is underlain as a general background of the region.

Table 2.1: Summary statistics of *L. helicina* size structure ordered by year and survey date. The sample from survey 9 of 2008 (collected on 22 July) was missing. The 2010W in the Year column indicates samples collected from the 2010–2011 winter transition, from October 25, 2010 to March 19, 2011. Note that one sample collected on November 22, 2010 was a combination of zooplankton sampled from both the 150 μm and 250 μm nets.

Year	**Date**	**Survey**	**Mean (mm)**	**Min (mm)**	**Max (mm)**	**Mesh (μm)**
2008	18 March	1	1.55	0.17	3.00	150
2008	31 March	2	1.75	0.17	3.00	150
2008	22 April	3	2.86	0.21	4.11	150
2008	9 May	4	0.87	0.13	5.50	150
2008	25 May	5	1.39	0.18	4.83	150
2008	8 June	6	0.51	0.12	3.45	150
2008	20 June	7	0.80	0.16	3.78	150
2008	8 July	8	0.98	0.16	3.35	150
2008	22 July	9	NA	NA	NA	150
2008	4 August	10	1.10	0.14	3.78	150
2008	22 September	11	0.51	0.18	2.65	150
2009	28 February	1	0.68	0.18	2.64	150
2009	17 March	2	0.99	0.22	2.43	150

Table 2.1 – continued on next page

Table 2.1 – continued from previous page

Year	Date	Survey	Mean (mm)	Min (mm)	Max (mm)	Mesh (μm)
2009	1 April	3	0.69	0.18	3.58	150
2009	15 April	4	0.49	0.12	3.63	150
2009	3 May	5	0.41	0.18	3.91	150
2009	20 May	6	0.57	0.13	4.42	150
2009	2 June	7	0.75	0.18	4.42	150
2009	18 June	8	0.64	0.17	2.82	150
2009	1 July	9	0.72	0.13	4.65	150
2009	17 July	10	0.66	0.13	4.42	150
2009	13 August	11	0.55	0.17	3.39	150
2010	19 March	1	0.62	0.21	2.74	150
2010	23 April	2	0.37	0.15	3.61	150
2010	17 May	3	1.04	0.16	5.30	150
2010	21 June	4	1.65	0.16	4.06	150
2010	20 July	5	1.11	0.16	3.56	150
2010W	25 October	1	0.72	0.20	2.03	150
2010W	8 November	2	0.63	0.29	2.43	150
2010W	8 November	3	0.63	0.39	2.11	250
2010W	22 November	4	0.64	0.44	2.36	250
2010W	22 November	5	0.69	0.19	2.54	150 & 250
2010W	18 January	6	0.73	0.23	1.84	150
2010W	8 February	7	0.84	0.51	2.10	150

Table 2.1 – continued on next page

Table 2.1 – continued from previous page

Year	Date	Survey	Mean (mm)	Min (mm)	Max (mm)	Mesh (μm)
2010W	19 March	8	0.50	0.21	0.56	150

Table 2.2: Dates of sample collection for DFO 1, DFO 2, DFO 3, DFO 4, DFO 5, for three time periods of 2010. Samples collected were used for analysis of the spatial variability in the population size structure of *L. helicina*. Samples for the early spring and early summer were collected using a 150 μm mesh net, while the Fall samples were collected using a 235 μm mesh net.

Season	Station	Date
Early Spring	DFO 1	18 March
Early Spring	DFO 2	19 March
Early Spring	DFO 3	19 March
Early Spring	DFO 4	19 March
Early Spring	DFO 5	19 March
Early Summer	DFO 1	17 May
Early Summer	DFO 2	17 May
Early Summer	DFO 3	18 May
Early Summer	DFO 4	18 May
Early Summer	DFO 5	18 May
Fall	DFO 1	11 September
Fall	DFO 2	11 September
Fall	DFO 3	11 September
Fall	DFO 4	11 September

Table 2.2 – continued on next page

Table 2.2 – continued from previous page

Season	Station	Date
Fall	DFO 5	11 September

2.3 Results

2.3.1 Environmental Parameters - Temperature, Salinity, Fluorescence

Temperature and salinity displayed opposite seasonal trends from spring to summer, during all years (Figure 2.3A). Temperature increased linearly from spring to summer while salinity showed a seasonal decrease. Exceptions were noted during July, 2008 when salinity displayed an increasing trend into September (Figure 2.3A). Although fluorescence values showed high variation throughout spring and summer of 2008, they were consistently higher during the summer, in 2009. Fluorescence in 2010 showed a decreasing trend from spring to summer (Figure 2.3B). Summer values were also consistently higher compared to the fall/winter period. The lower resolution sampling in 2010 may have masked potential variations between surveys, for temperature, salinity, and fluorescence.

2.3.2 *L. helicina* Abundance: Seasonal and Inter-annual Variation

Seasonal variations in abundance differed between years, although a general increase was observed from spring to summer (Figure 2.3B). Exceptions were seen in 2008 with peak abundances ($\geq$ 628 ind.m^{-3} max) occurring in late-spring (May 9). The 2009 and 2010 seasons exhibited peak abundances during the summer (Figure 2.3B). Highest abundances in 2009 and 2010 reaching $>$ 100 ind.m^{-3} were documented in August and late June, respectively (Figure 2.3B). Between survey variation in abundance was greatest in 2008 and lowest in 2009 (Figure 2.3B). Low sampling frequency in 2010 could be responsible for the low survey-to-survey variation.

Environmental Correlations

Seasonal abundances for each year were log-transformed and regressed against the environmental parameters. See the Tables in Appendix A.2 for the full statistical results. *Limacina helicina* abundance was significantly correlated with 30 m depth-averaged temperature in 2009 and 2010 (2009: $R^2 = 0.843$, $p < 0.01$, 2010: $R^2 = 0.961$, $p < 0.05$), and salinity in 2009 (2009: $R^2 = 0.721$, $p < 0.01$). There were no significant correlations found between abundance and depth-integrated fluorescence, for any year.

2.3.3 *L. helicina* Size Structure: Seasonal Development

The size-frequency histograms for 2008 and 2009 (Figure 2.4) showed seasonal growth to be continuous, although there appeared to be two major periods of growth during each year, in spring and summer. There was notable size development of the larger individuals during each major period of growth. Spring growth occurred from late February–mid March until late May–early June while summer growth was seen from June to late July–August, for both 2008 and 2009 seasons. Both periods showed steady growth of *L. helicina* to larger sizes, although the relative abundance of the larger individuals declined throughout each period of growth (Figure 2.4).

With the exception of surveys 1–3 from 2008 (Table 2.1; Figure 2.4), every survey throughout 2008 and 2009 displayed a prominent abundance of the 0.2–0.4 mm size-group. Shifting to the 0.40–0.60 mm size-group during the 2010-2011 winter-transition, a notable presence of the 0.2–0.4 mm size-group was not seen until the following spring (Figure A.1).

Despite fewer sampling through spring and summer, 2010, similar patterns of growth can be seen when compared to the size-frequency histograms from 2008 and 2009 (Figure 2.4). The static configuration of the size-frequency histograms

throughout the 2010-2011 winter transition indicated the cessation of growth in winter.

2.3.4 Spawning Activity

Spawning activity was identified by 1. a prominent abundance of the size-group ≤ 0.4 mm (known as immatures in catches) and 2. the relative abundance of the 0.2–0.4 mm size-group in the size-frequency histograms for each season (Figure 2.4).

Immatures consistently accounted for > 50 % (with maximum above 70 %) of the total abundance throughout May in 2008 and 2009 (Figure 2.4). In addition to immatures, prominence of the 0.2–0.4 mm size-group (relative to other size-groups) from May to August in 2008 and 2009, suggested continuous (e.g. protracted) spawning activity (Figure 2.4). Although the relative abundance of the 0.2–0.4 mm size-group suggested protracted spawning (throughout 2008 and 2009), the data indicated one period of peak spawning activity. The parallel peaks of total population abundance combined with the highest relative abundance of immatures, in 2008 (May 9), suggested that late spring was a time of peak spawning. In contrast, the peak population abundance was not seen until late summer (August 13) in 2009. Even so, there were noticeable differences in peak abundances between 2009 (~ 153 ind.m^{-3}) and 2008 (> 600 ind.m^{-3}). Based on the high contribution of immatures to the total abundance in late spring (late April–May) (Figure 2.5), it is possible the spring peak spawning was missed in 2009. Due to lower level sampling of 2010, direct comparisons to 2008 and 2009 cannot be made, although the population abundance was observed to increase from mid May to peak in late June. Based on the data, it is appeared protracted spawning occurred throughout the 2008 and 2009 seasons, however, it was evident that the late spring was a time of peak spawning (e.g.

followed by limited protracted spawning).

We found no indication of spawning activity during the 2010–2011 winter transition. Spawning likely began again in early-spring, 2011, with the re-establishment of the 0.2–0.4 mm size-fraction in the size frequency histogram in late-March (Figure A.1).

2.3.5 Estimate of Life-Cycle Longevity

Using finite mixture distributions, two cohorts were identified and tracked from May 9, 2008 to July 20, 2010 to determine the life cycle longevity of *L. helicina*. Cohort $\mathbf{C}_1$ was identified on 9 May, 2008 and tracked until its assumed to vanish on 4 August, 2009. Cohort $\mathbf{C}_2$ was identified on 3 May, 2009 and tracked until it was assumed to die-off on 20 July, 2010. Figure 2.7B depicts the growth cycle for each cohort and Table 2.3 lists the $\sim$ biweekly development of each cohort.

C_1 and C_2 exhibited slow initial growth (< 0.015 mm.day^{-1}) during the first two weeks, after which C_2 grew at a rate ~ 3 times faster than that of C_1. By 28–30 days into the respective growth-cycles, C_2 was roughly twice the size of C_1. It was not until early July when both cohorts were of similar size (Table 2.3). The growth-trajectories of C_1 and C_2 differed greatly after early–mid July, of 2008 and 2009, respectively. Peaking at 2.2 mm by early August 2008, C_1 exhibited a recession in shell-size by late-September prior to the fall–winter period. Meanwhile, during 2009 C_2 grew unabated and reached a modal size of 3.3 mm prior to entering the fall–winter period. Both cohorts were notably smaller in the following spring when compared to their respective sizes, from the previous summer. From the size-frequency histograms during the 2010–2011 winter-transition (Figure 2.4), it was likely the 2008–2009 and 2009–2010 winter-transitions also exhibited zero growth, of *L. helicina*. Rapid growth was observed the following spring when both cohorts likely reached sexual maturity

after a modal size of 3 mm was surpassed. The growth of C_1 appeared to level off from mid June–mid July, 2009, while the growth of C_2 showed no signs of tapering. From the data, C_2 was likely spawned by C_1 in late spring of 2009 (Figure 2.7B). Using Equation 2.3, C_1 was tracked for 461 days and C_2 for 443 days. This equated to life cycle longevities of 1.26 and 1.21 years, respectively.

A third cohort, $\mathbf{C_3}$, was identified on April 23, 2010, and was likely spawned by C_2 (orange line in Figure 2.7B). Tracked until July 20, 2010, the growth trajectory of C_3 resembled that of C_1 and C_2 post-recruitment, strengthening the growth cycles of C_1 and C_2 (Figure 2.7B). C_3 was not considered for estimates of life-cycle longevity as it was tracked for a limited time.

Table 2.3: The growth and development of C_1 and C_2 throughout their tracked life cycles. Growth rates are calculated using Eq. (1) and expressed in mm.day^{-1}. Note that the sample for 22 July, 2008 was not available, hence the NA under the **Modal Peak** and the **Growth** columns. C_1 was not observed in the size frequency histogram of 13 August, 2009 (Figure 2.4)) and assumed to have died off. C_2 was not seen in the size-frequency histograms of both 21 June and 20 July, 2010 and assumed to have died off on 20 July, 2010. (Figure 2.4)

Year	**Date**	**Day**	**Cohort**	**Modal Peak (mm)**	**Growth (mm.day^{-1})**
2008	09-May	1	C_1	0.229	NA
2008	25-May	14	C_1	0.300	0.004
2008	08-Jun	28	C_1	0.500	0.014
2008	22-Jun	42	C_1	0.945	0.031

Table 2.3– continued on next page

Table 2.3– continued from previous page

Year	Date	Day	Cohort	Modal Peak (mm)	Growth ($mm.day^{-1}$)
2008	08-Jul	58	C_1	1.900	0.059
2008	22-Jul	72	C_1	NA	NA
2008	04-Aug	85	C_1	2.200	0.011
2008	22-Sep	134	C_1	1.814	NA
2009	28-Feb	293	C_1	1.311	NA
2009	17-Mar	310	C_1	1.993	0.040
2009	01-Apr	325	C_1	2.860	0.057
2009	15-Apr	339	C_1	3.410	0.039
2009	03-May	357	C_1	3.690	0.015
2009	20-May	374	C_1	NA	NA
2009	02-Jun	387	C_1	3.900	0.007
2009	18-Jun	403	C_1	NA	NA
2009	01-Jul	416	C_1	4.580	0.023
2009	17-Jul	432	C_1	4.400	NA
2009	13-Aug	461	C_1	NA	NA
2009	03-May	1	C_2	0.200	NA
2009	20-May	17	C_2	0.361	0.009
2009	02-Jun	30	C_2	0.970	0.047
2009	18-Jun	46	C_2	1.530	0.035
2009	01-Jul	59	C_2	2.050	0.040
2009	17-Jul	75	C_2	3.040	0.062
2009	13-Aug	102	C_2	3.300	0.009
2010	19-Mar	320	C_2	2.680	NA

Table 2.3– continued on next page

Table 2.3– continued from previous page

Year	Date	Day	Cohort	Modal (mm)	Peak	Growth ($mm.day^{-1}$)
2010	23-Apr	355	C_2	3.130		0.013
2010	17-May	379	C_2	4.180		0.044
2010	21-Jun	414	C_2	NA		NA
2010	20-Jul	443	C_2	NA		NA

2.3.6 Rivers Inlet Spatial Analysis

The smaller size fractions displayed a dominant influence throughout the seasons at each station, while the larger individuals were sparsely distributed (Figure 2.6). During early spring individuals < 1.5 mm in size predominated with only a few larger individuals of > 3.0 mm also present. The size structure displayed bi-modality in early summer and fall with possible exceptions at DFO 1 and DFO 5 (Figure 2.6). For all stations, the principal modes discerned in early spring ranged from the 0.2–0.8 mm and 1–2 mm, and while the 0.2–0.8 mm mode was static in fall, the 1–2 mm mode present in summer appeared to shift to the 1.6–2.4 mm range in fall (Figure 2.6). Although there was no distinct mode seen for sizes above 2.0 mm, large specimens were recorded throughout for all seasons and stations in low numbers. From the data presented, we hypothesize the population size structure of *L. helicina* was broadly similar across the inlet, with spatial differences due to the patchiness of *L. helicina* and advective influences.

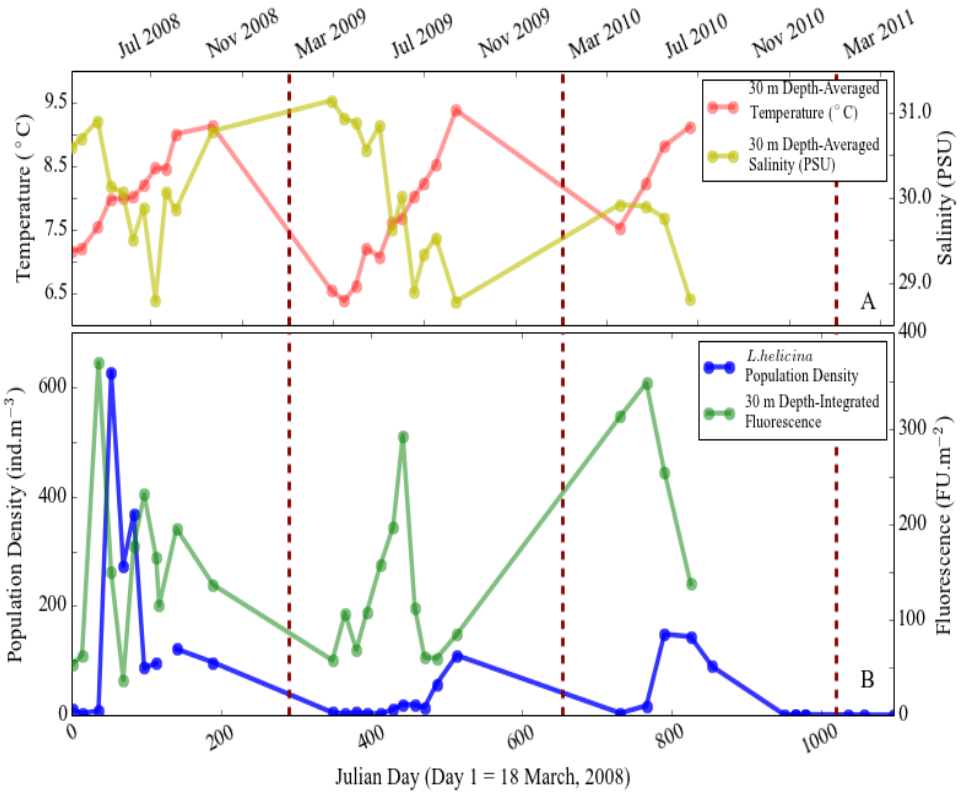

Figure 2.3: A: Seasonal and interannual variation of **30 m depth-averaged** temperature - red and salinity - yellow. Temperature is expressed in °C and salinity is expressed as PSU (Practical Salinity Units). B: Seasonal and interannual variation in *L. helicina density* (sampled from the top 300 m) and **30 m depth-integrated** fluorescence - green. Density is expressed in ind.m^{-3}. **Note** the X-axis is expressed in Gregorian dates on top and Julian Day at the bottom. January 1 is indicated by the dashed red lines (starting with January 1, 2009).

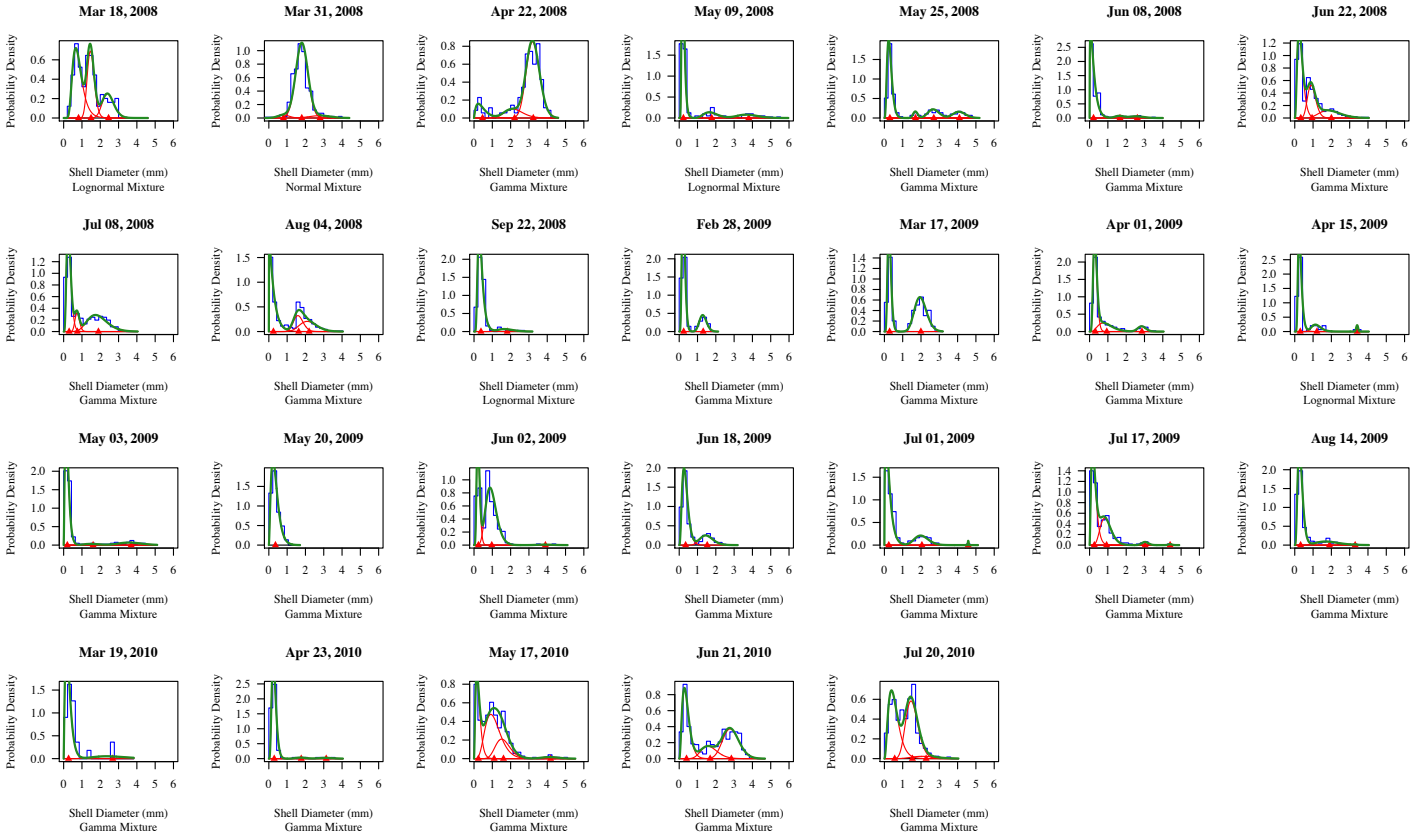

Figure 2.4: Finite mixture distributions were fitted to distinguish between different population cohorts at different times. The following subplots show the finite mixtures fitted to the size-frequency data for all fort-nightly samples collected from March 18, 2008 to August 14, 2009, and the monthly samples from March 19 to July 20, 2010. Cohort C_1 was likely recruited into the population on 9 May, 2008. C_2 was likely recruited on 3 May, 2009 (near bottom left subplot). It was probable that C_1 died-off on 13 August, 2009, while C_2 likely died off on 20 July, 2010.

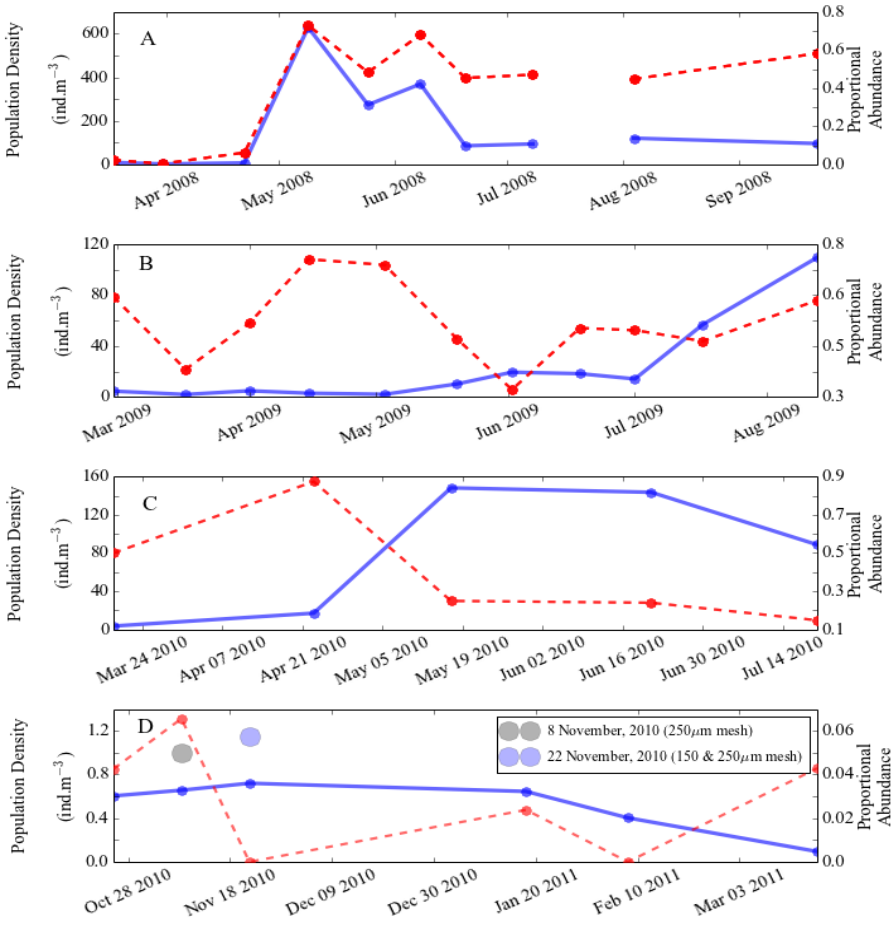

Figure 2.5: Seasonal population abundance of *L. helicina* for **A.** 2008, **B.** 2009, **C.** 2010, **D.** 2010-2011 winter-transition. **D**. The inter-annual population abundance of Figure 2.3B is broken into four different panels, one for each year of observation. Also included is the proportional abundance of the size-fraction < 0.40 mm (dashed red line). Note the different scaling of the Y-axis between panels. The **light grey and blue dots, respectively** indicate sampling on 8, 22 November with 250 μm and 150 & 250 μm mesh nets, respectively.

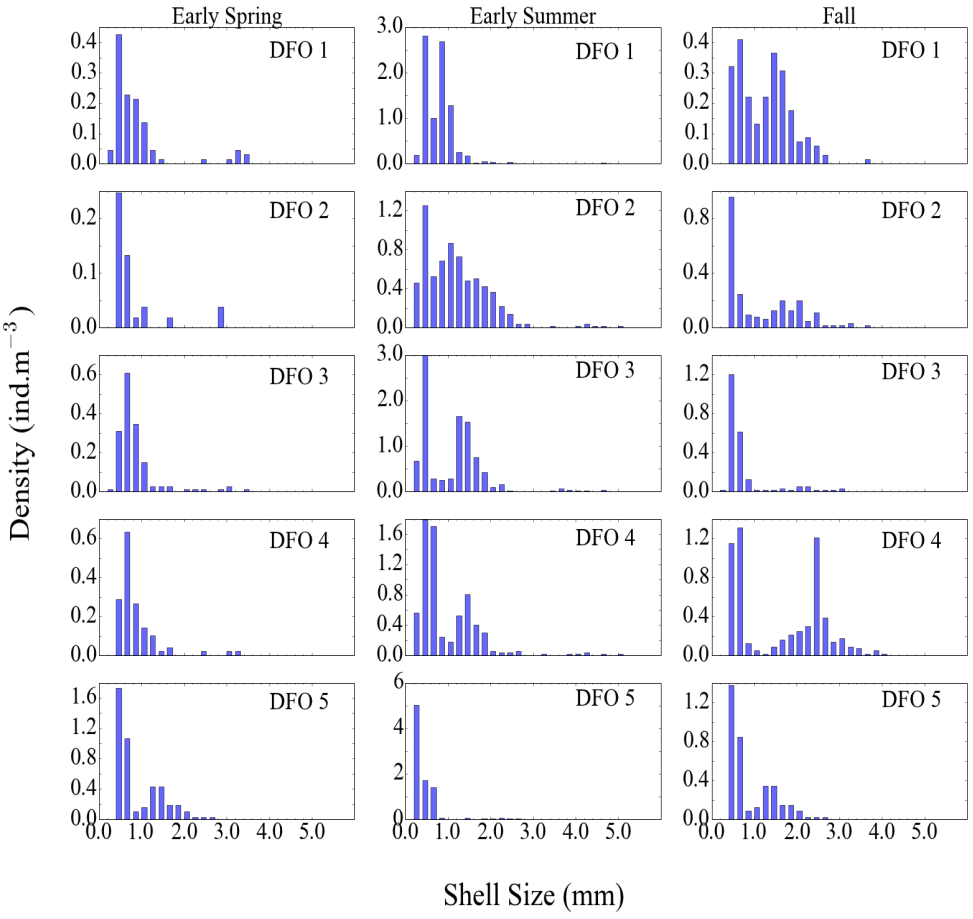

Figure 2.6: Histograms (0.2 mm bins) comparing the population size structure of *L. helicina* from stations DFO 1–5 during three seasonal time points in 2010, spring (19 March), summer (17–18 May), fall (11 September). Each column in the figure denotes the respective seasons while the stations are designated by row, with DFO-1 in row 1, and DFO-5 in row 5. All samples were collected with 150 μm mesh bongo nets with the exception of those during fall. Fall samples were collected with 236 μm mesh bongo nets. Note the different scaling in the y-axis for each histogram.

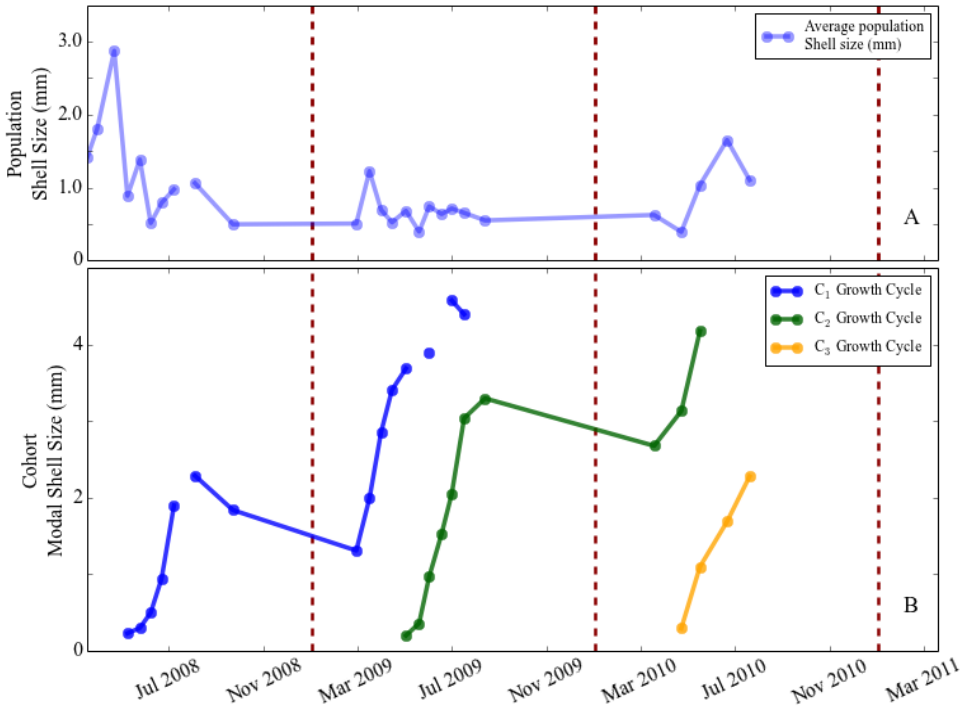

Figure 2.7: A: Seasonal and interannual distribution of the mean shell size of the population. B: Growth cycles of the two cohorts (C_1, C_2) tracked. The orange line denotes the third cohort (C_3) identified, and tracked for a limited time. January 1 is indicated by the dashed red lines (starting with January 1, 2009).

2.4 Discussion: Life-cycle re-evaluation

2.4.1 Seasonal Spawning and Recruitment

A strong influence of the smaller size-group (0.2–0.4 mm) from spring to fall combined with the high proportions of immatures indicates protracted spawning by *L. helicina* with a clear peak in spawning activity during the late spring. It appears that peak spawning is initiated in late spring and continues into the summer. The low contribution of the 0.2–0.4 mm size-group to the total abundance during the 2010–2011 winter-transition indicated the termination of spawning during the late fall–winter period.

Paranjape (1968) supports continuous spawning and interprets reproductive activity to extend over prolonged periods. Interpretations from Kobayashi (1974) describes reproductive activity to commence during spring and continue into the summer. Additionally, Dadon and de Cidre (1992) reports of spring and summer spawning events for *L. retroversa* of the Southern Argentine Sea.

Gannefors et al. (2005) found adult *L. helicina* in Kongsfjorden to be at differing stages of egg production during summer spawning. The zooplankton of Kongsfjorden are under strong influence from local hydrography, which can vary substantially between years (Hodal et al., 2012). *Limacina helicina* in Kongsfjorden are of Arctic origin and are most prevalent when Arctic waters are advected into the fjord (Willis et al., 2006). Thus, the interpretation of only summer spawning in Gannefors et al. (2005) may have been due to lower volumes of Arctic waters advected into the fjord, during spring. Alternatively, the observation of summer spawning in Gannefors et al. (2005) suggests the possibility of a late spring bloom delaying the spring peak spawning to summer.

Size of Spawning

Spawning size differed between C_1 and C_2, although both cohorts were larger than 3 mm during the time of the peak spawning. This differed considerably from the size of mature adults reported in Bednaršek et al. (2012) and Gannefors et al. (2005). Compared to zooplankton from temperate latitudes, zooplankton sampled from polar waters (e.g. Scotia Sea and Kongfjorden) are characterized by slow growth, delayed sexual maturity, and a larger size at sexual maturity (Clarke and Peck, 1991). The differences in spawning size between polar populations of *L. helicina* and this study could therefore be explained by latitudinal (*sensu* temperature and habitat) differences. Additional support for a smaller spawning size is provided by the gonadal analysis in Kobayashi (1974), where ova of differing sizes were observed in *L. helicina* at different stages of sexual maturity (Table 2 in Kobayashi, 1974). It is therefore likely that *L. helicina* is a pulsing spawner capable of releasing batches of matured ova, while developing ova continue its growth (Dadon and de Cidre, 1992). According to Table 2 in Kobayashi (1974), hermaphroditic organs are present in individuals reaching 0.7 mm in size, with little difference in increasingly larger individuals. It is probable that after spawning commences in spring when "some" of the fully matured ova are released, it continues as the remaining portions become mature, leading to protracted spawning.

2.4.2 Seasonal Growth and Environmental Correlations

The population size structures showed the continual growth of *L. helicina* throughout the 2008 and 2009 seasons, although there were two periods of enhanced growth (for larger individuals in particular). Larger individuals exhibited a notable increase in size from early–late spring, which we interpret as the parental cohort growing to sexual maturity. This was demonstrated by the rapid growth

of C_1 and C_2 in late spring of 2008 and 2009, respectively, culminating in the spawning peak. Of interest was the rapid development of C_2 during summer of 2009. Unlike C_1, C_2 was able to grow to $\geq$ 3 mm in size before overwintering. As it was likely that *L. helicina* in RI are able to spawn from a shell size of $\geq$ 3 mm, the rapid growth of C_2 from May–August of 2009 suggested the possibility of peak spawning in summer. The growth cycle of C_1 appeared to taper by mid-July, 2009, indicating C_1 was likely approaching senescence. In contrast, the growth of C_2 did not taper. Although we were unable to track C_2 for the remainder of the 2010 season, the growth trajectory of C_2 suggested the life cycle of C_2 to be potentially longer compared to C_1. Both C_1 and C_2 over-wintered and matured sexually in spring, of the following year.

The dependence of *L. helicina* on food quantity and most likely, quality is well documented (Lalli and Gilmer, 1989; Gilmer and Harbison, 1991; Hunt et al., 2008; Seibel et al., 2012). Although linear regressions indicated an non-significant relationship between seasonal abundance and 30 m depth-integrated fluorescence (for all years), it is possible that the data used here was too coarse to resolve the connection between these parameters (e.g. *Limacina* responses to temporal changes in chlorophyll may be occurring at finer time scales).

We found no evidence of winter growth, although Kobayashi (1974) argued winter was a time of a notable growth in the Arctic. A cessation of growth in winter was supported by Lischka and Riebesell (2012). Our results also clearly indicated a decrease in shell size prior to over-wintering, suggesting higher mortality of the larger demographic during the fall–winter. It appears that *L. helicina* halts its growth during the winter till resources are sufficient, and conditions become optimal in early spring the following year.

2.4.3 Rivers Inlet Spatial Analysis

Broadly, *L. helicina* displayed a similar size structure across the inlet. The spatial differences in size structure that were observed were likely due to the inherent patchiness of *L. helicina*. However, advective influences may also have played a role. The fresh water run-off from the Wannock River may have carried away certain size-groups at the DFO 5 towards the inlet mouth. This may account for a general lack of individuals > 2 mm in size at DFO 5. Incidentally, DFO 4 displayed presence of individuals ranging from 1.4–4 mm in size across seasons. Additionally, spatial differences in chlorophyll concentrations and the timing of the spring bloom may have influenced the size-structure of *L. helicina* across the inlet.

2.4.4 Potential Sampling Errors

Despite bi-weekly sampling, there is the possibility that some short term variability was not identified. This is especially true when attempting to track the growth and size progression of the identified cohorts. Numerous surveys for each year showed no apparent change in the overall shape of the population size distribution suggesting that the population of *L. helicina* is stable between surveys. However, greater seasonal changes may have been observed if zooplankton samples were collected more frequently (e.g. using data of higher temporal resolution).

In this chapter, we have shown that *L. helicina* displays peak spawning activity during the spring, when the population reaches sexual maturity. Spawning was observed at a size of 3 mm and larger. Protracted spawning commences after spring-spawning and continues into and throughout the summer. We found no evidence of spawning during the late fall–winter period. Continuous size-development was seen in the size-frequency histograms throughout the seasons

(for all years), although the relative abundance of the larger demographic decreased with increases in size. By tracking two cohorts for over 400 days, we were able to estimate a life-cycle longevity of 1.2 years, although it appears possible for *L. helicina* to live up to 1.5 years. From the data, it seems the life cycle of *L. helicina* in the temperate North East Pacific resembles that of *Limacina retroversa* in the Southern Argentine Sea (Dadon and de Cidre, 1992). This is substantially shorter than the 3 year life history proposed by (Bednaršek et al., 2012). It is possible that the differences between the *L. helicina* life histories observed in our study and Bednaršek et al. (2012) can be explained by genetic differences (Hunt et al., 2010). This chapter has also shown the importance of temporal resolution in resolving the seasonal and inter-annual dynamics of *L. helicina* in Rivers Inlet. Even though an non-significant relationship was found between seasonal abundance and fluorescence, perhaps higher resolution data in addition to a lag analysis is needed for clear relations to be seen, especially if slight changes in environmental conditions (e.g. chlorophyll, temperature, and salinity) can stimulate and drive population responses (e.g. increasing population abundance, growth/maturation, and/or spawning). Based on the results of Chapter 2, it appears that higher resolution zooplankton sampling (e.g. collected daily) is needed in order to determine the factors driving the seasonal dynamics observed, for *L. helicina* in Rivers Inlet.

Chapter 3

Seasonal Growth and Mortality – Spring *vs.* Summer

3.1 Introduction

Despite narrowing the knowledge gaps regarding the life cycle of *L. helicina*, the results from Chapter 2 showed that life-cycle dynamics can potentially vary at finer time scales. Specifically, difficulties were encountered in resolving seasonal spawning (e.g. possibility of more than one period of peak spawning) events in Chapter 2. Clearly, higher resolution data should be used to fully resolve the *L. helicina* life cycle in RI. Use of higher resolution data may also provide an opportunity to accurately estimate mortality rates which are fundamental for the construction of predictive models for the *L. helicina* population dynamics.

Growth rates of three species of Limacinidae and one Cavoliniidae from Barbados were determined by Wells (1976) from census data. An average growth rate of 0.12 mm.month^{-1} was reported with no significant differences between small and large *Limacina* (Wells, 1976). Nevertheless, it was documented that the growth rates of *Limacina* species diminished once the adult

stage was reached (Wells, 1976). Other studies have also investigated *Limacina* growth rates, but without common units (e.g. grams of carbon), the studies are generally not comparable (Gannefors et al., 2005; Bednaršek et al., 2012).

In order to construct robust models predicting zooplankton abundance, accurate estimates of both seasonal growth and mortality are needed (Ohman and Wood, 1995; Gentleman et al., 2012). Currently, the literature abounds with studies investigating zooplankton growth rates (e.g. production) with little attention to mortality estimates (Ohman and Wood, 1995). Moreover, the large number of non-standardized methods within the literature ultimately leads to incomparable results (Aksnes et al., 1997). While the large majority of growth-rate experiments can be performed on-ship and/or nearby on-shore laboratories to produce fairly robust estimates, lab-based mortality experiments are not representative of natural populations as many factors influencing mortality (e.g. parasitism, predation, advection) cannot be incorporated into the experiment (Harris, 2000). This clearly called for more research focusing on mortality rate measurements on natural populations using high resolution time series data (Aksnes et al., 1997). Bednaršek et al. (2012) quantified mortality rates for *L. helicina* in the Southern Ocean, however, the large spatial extent of the study was restricted to summer months only (Wiens, 1989).

As part of the RIES (Rivers Inlet Ecosystem Study) sampling protocol (*www.riversinlet.eos.ubc.ca*), a Daily Station was established to investigate the timing of the spring bloom in RI and its drivers. This provided an unprecedented opportunity to capture the seasonal dynamics and assess accurately the mortality rates of *L. helicina*, using daily resolved observations for over 100 days.

Two methods, *horizontal* and *vertical*, of estimating mortality rates have been implemented in many studies throughout the past decades (Ohman and

Wood, 1995; Gentleman et al., 2012). Horizontal methods (*aka* cohort methods) can be applied to a sampling time series to monitor temporal changes experienced by individual cohorts (Aksnes and Ohman, 1996; Aksnes et al., 1997; Gentleman et al., 2012). Based on recruitment, stage-duration, and mortality, the vertical method approximates the number of individuals observed for a development stage at a point in time (Aksnes et al., 1997). Although time series data are not required, the vertical method is tied to more restrictive assumptions than the horizontal method (Gentleman et al., 2012). Each method is bound by their respective list of assumptions which if not met, can yield potentially biased estimates (Gentleman et al., 2012). For example, an assumption of a negligible advection may introduce a substantial bias, impacting horizontal methods (Aksnes and Ohman, 1996; Aksnes et al., 1997; Gentleman et al., 2012). If advection is a factor influencing the seasonal distribution of zooplankton, the real temporal changes in a population may be masked by the advection (immigration *vs.* emigration) of potentially different sub-populations (Aksnes and Ohman, 1996). The use of coarse time resolution data may also significantly affect the outcome of horizontal methods (Gentleman et al., 2012). If however, the time series is of sufficient resolution, then the horizontal method may yield vital information if the population is homogeneously distributed in the system considered. From the spatial analysis of Chapter 2 (Section 2.3.6), it would appear that *L. helicina* exhibits a broadly similar size-distribution within RI, with differences in density depending on location.

3.2 Goals

Despite criticisms of the horizontal method, there have been only few studies in the literature to utilize a dataset of > 100 days (Gentleman et al., 2012). We believe the horizontal estimation method combined with daily data for more

than 100 days will offset much of the current criticisms, as well as provide robust and accurate estimates of seasonal growth and mortality.

The aims of this chapter are as follows:

1. To provide a high resolution analysis of the seasonal cycle of recruitment.
2. To document the seasonal development of *L. helicina* by providing daily rates of growth in shell-size in spring and summer.
3. To provide a first-approximation of the seasonal mortality of *L. helicina* of the coastal North East Pacific, by estimating instantaneous mortality as well as documenting its seasonal changes, from spring to summer.

3.3 Methods

3.3.1 Study Area & Sample Collection

Established in the proximity of Dawsons Landing (51°57'40" N, 127°58'60" W), the nearby dock was the ideal location for the sampling of zooplankton and other physical parameters (fluorescence). The hydrodynamics of RI and other physical factors (wind) are detailed in Hodal (2010) and Wolfe (2010), respectively.

Zooplankton samples were collected each day after dusk from March 22 to July 7, 2010, using a ring net (0.30 m diameter, 80 μm mesh-size) supplied by Aquatic Instrument Supply Company, from the deepest section (25–30 m depth) of the dock. Sample handling followed the same protocol outlined in Chapter 2 (Section 2.2.3). *Limacina helicina* individuals were measured and enumerated in the entire sample under a Leica microscope equipped with an ocular ruler. Measurements were made to the nearest 0.01 μm from the tip of the shell aperture directly to the back of the shell (Figure 2.1). Every confirmed individual was considered for size-frequency enumeration unless there was sufficient physical damage preventing correct measurements. In these cases, the individuals were only considered for abundance estimates.

3.3.2 Daily Fluorescence

An autonomous ECO-Fl fluorometer (WetLabs) was moored on the dock at Dawsons Landing to measure daily fluorescence. Fluorescence measurements were collected from 5 m depth at 2 hour intervals. Daily average values were converted to chlorophyll using Equations 3.1 and 3.2. Data were available from January 1 to July 20, 2010 with a gap of missing data from February 13 to March 31, hence only data from April 1 to July 7, 2010 was used for analysis.

$$Chl = SF * (Op - DC) \tag{3.1}$$

$$SF = \frac{x}{Op - DC} \tag{3.2}$$

Op in Equation 3.1 indicates the signal output from the fluorometer and x in Equation 3.2 is the concentration of the solution used during instrument standardization. SF (Equation 3.2) is the scale factor and DC is the Dark Counts (signal output of the fluorometer in clean water with black tape over detector). A DC of 105 was used, with an SF of 0.0077 μg.l^{-1}.count^{-1}. Chlorophyll was expressed in μg.chl-a.l^{-1}.

3.3.3 Size-Frequency Histograms & Identification of Cohorts

Measurements from each sample (Table B.1 in Appendix B) were binned into 0.02 mm size-bins to distinguish the smallest changes in the population size structure on a daily basis (see the size frequency histograms in Appendix B). Population cohorts were identified following the protocol from Chapter 2 (Section 2.2.5). Once identified, finite mixture distributions (MacDonald and contributions from Juan Du, 2011) were fitted to the size-frequency histograms. This was followed by iterative trials of parameter estimates until the best fit to the biological data was found. It is important to be aware of the temporal progression of each cohort identified as certain sequences of parameter estimates will likely yield rates that could be biased. So as to limit the extent of personal bias in the construction of finite mixture distributions, parameter constraints were not included unless necessary, such that the temporal progression of each pa-

rameter (mean shell size and the standard deviation for each cohort identified) was biologically appropriate (see Section B.5 for details on placing constraints). Each cohort was named after their probable dates of being spawned, with **c** prefixed to the abbreviated date. (e.g. **cApr01** signifies a cohort recruited on April 1, 2010).

3.3.4 Spawning Events

Spawning events were identified by an increase in the abundance (ind.m^{-3}) of the population and the size-group $\leq$ 0.15 mm. Dates of probable spawning would then be recognized by periods displaying a combination of an increase in both total population abundance and the density (ind.m^{-3}) of the size-group $\leq$ 0.15 mm. Daily estimates for the total population abundance was based on *L. helicina* processed for size frequency enumerations, as well as those considered for abundance estimates. Only *L. helicina* processed for size frequency enumerations were considered for density estimates of the size-group $\leq$ 0.15 mm.

3.3.5 Shell Size Growth and Mortality

The daily growth rate of the population was calculated from averaging the daily growth rates of each cohort tracked, during the period from March 22 to July 7, 2010. The daily cohort growth was calculated using Equations 2.1 and 2.2 from Chapter 2.

Cohort densities were estimated by using a combination of the proportional abundance of each cohort tracked and the total population abundance. The proportional abundance of each population cohort was one of the parameters obtained from fitting the finite mixture distributions (along with the modal shell size and standard deviation of each cohort). The temporal densities of

each cohort tracked was estimated by multiplying the proportional abundance of each cohort by the total population abundance (ind.m^{-3}) for each day.

The daily density of each cohort was log-transformed and regressed against the duration each cohort was tracked. Regression lines were super-imposed for each cohort on Figure 3.4, where the slope was an indication of either increasing (positive slope) or decreasing (negative slope) density for each cohort. A negative slope was indicative of the mortality experienced by each cohort, with the daily mortality rate given by the slope value.

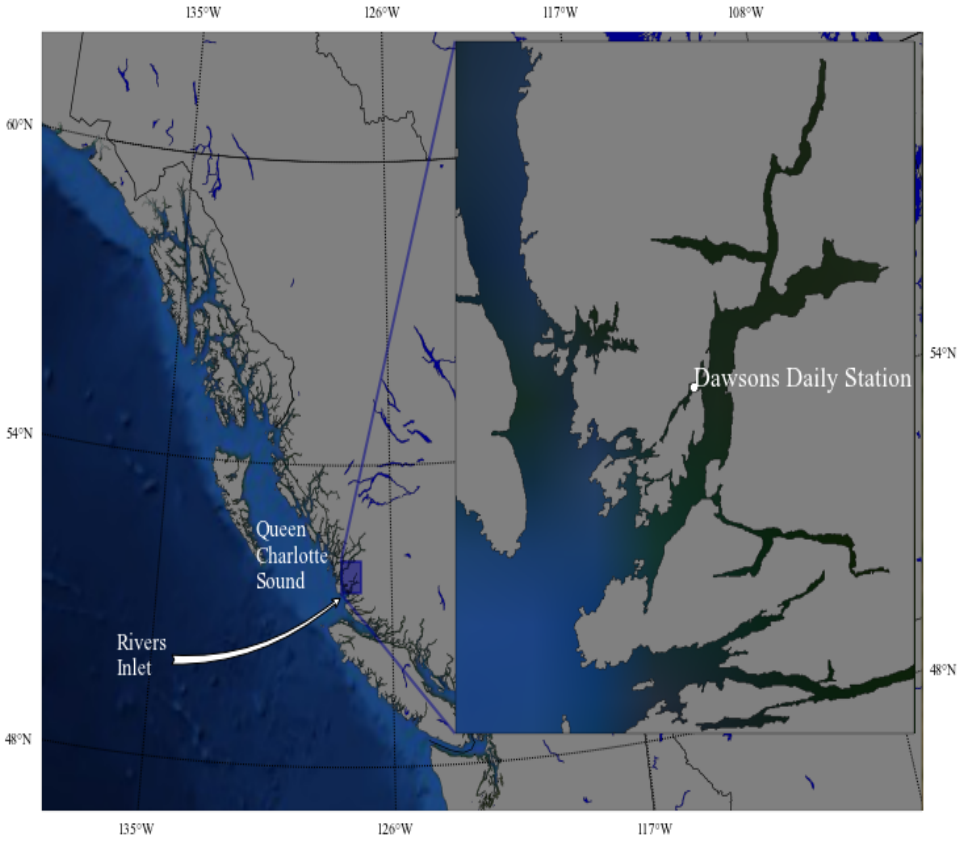

Figure 3.1: The British Columbia west coast. Rivers Inlet is depicted in the zoomed inset of the mainland coast of B.C. The location of the Dawsons Daily station is indicated within the zoomed inset.

3.4 Results

3.4.1 Daily Chlorophyll

Large differences were seen in daily chlorophyll from January to July, 2010. While a small peak was observed in early January, chlorophyll values were relatively low throughout the month when compared to the values recorded from April 1 onwards (Figure 3.2A). Chlorophyll (chl-*a*) levels although variable from spring to summer showed increased daily fluctuations during the summer months. High Chl-*a* levels (> 16 μg.l^{-1}) were observed throughout April with lower values (< 8 μg.l^{-1}) recorded late in the month. Lower values were maintained throughout May with sporadic peaks (Figure 3.2A). Early summer (late May to early June) displayed high chl-*a* concentrations (> 20 μg.l^{-1}) before subsiding as the season progressed to minimal values (< 5 μg.l^{-1}) in late June (Figure 3.2A). Chl-*a* levels increased to maximum values of $>$ 60–70 μg.l^{-1} in mid July.

Based on the higher chlorophyll values sustained throughout April, the 2010 season had likely experienced a prolonged bloom that was initiated early in the season (Figure 3.2A).

3.4.2 Daily Population Abundance

A strong seasonal cycle was observed, with marked contrasts between spring and summer (Figure 3.2B). Mean population abundances in spring (late March to April) were relatively low compared to those during summer, with May, June and July displaying means in excess of 1000 ind.m^{-3} (Figure 3.2B). Increasing in late April and continuing throughout early to mid May, pteropods reached maximum densities (> 4300 ind.m^{-3}) on May 20 before declining for the remainder of the month (Figure 3.2B). An increasing trend was also noticeable

from early to late June, with peak abundances of > 4700 ind.m^{-3} observed on June 30 which rapidly declined in July (Figure 3.2B).

3.4.3 Daily Population Size-Structure

During late spring the *L. helicina* population was represented largely by small individuals with only a few samples showing individuals ≥ 0.5 mm, in late March and early April (Figure 3.3). As the seasons progressed the range in pteropod size expanded and a bi-modal distribution was observed in the size-frequency histograms during summer months (see the size-frequency histograms in Appendix B). A reversion to a uni-modal size structure was however evident during July.

The largest individuals (≥ 3 mm in size) was observed on June 22, while the smallest (< 0.1 mm) recorded on June 13.

With few exceptions, the majority of individuals measured were ≤ 1 mm (Figure 3.3). Two individuals, each ≥ 2.5 mm, were sampled on June 6 and 20. Overall however, smaller size-groups (≤ 0.5 mm) dominated the pteropod population throughout the observation period. This was confirmed by a smaller mean shell size (see the lowess smoother in Figure 3.3). Additionally, there were few larger individuals early in the season when compared to the population size-structures in 2008 and 2009, from Chapter 2.

3.4.4 Spawning Events

From the daily densities of the size-group ≤ 0.15 mm, spawning likely occurred continuously (Figure 3.2C). Mean densities of ≤ 0.15 mm individuals increased from < 1 ind.m^{-3} in March to > 30 ind.m^{-3} by June (Figure 3.2C). Daily variations in the density of this size-group was low in late March and April, with increasing variation in May and June.

Based on the seasonal peaks in total population abundance in late May and late June, the late spring and summer appear to be the two periods of peak spawning. The spring spawning period (late April to late May) featured a slow but steady increase in the size-group ≤ 0.15 mm, with densities peaking at > 19 ind.m^{-3} on May 11 (Figure 3.2C). The summer spawning period (early June to early July) showed peak abundances exceeding 110 ind.m^{-3} on June 26, and was characterized by considerable daily variation (Figure 3.2C). Reaching peak densities on June 26, the summer peak of the size-group ≤ 0.15 mm paralleled the increase in total population abundance during the same time period, suggesting late June as a time of peak spawning. This was not reflected during late spring as the peak in total population abundance was not matched by a similar peak for the size-group ≤ 0.15 mm.

Identification of Cohorts

Table B.2 in Appendix B contains the statistical results and constraints placed, for the finite mixture distributions fitted. See Appendix B.5 for the finite mixture distribution figures, for each month.

3.4.5 Cohorts Identified and Tracked

Twenty-four individual cohorts (Figure 3.2D) were identified (7 in April, 8 in May, and 9 in June) and tracked for variable lengths of time (up to 34 days – see the life table data in Appendix B.7). Their daily growth trajectories are plotted in Figure 3.2D. Transparency was added to the growth trajectory for each cohort tracked, revealing that the growth trajectories of many cohorts were merging together at different times (shown by the colour boldness - more bold means more cohorts were merging together), and was interpreted as merged cohorts (e.g. ≥ 2 cohorts combining together) for the overlapping periods. Consequently, the

growth trajectories became progressively more unrealistic (e.g. too much overlap and insufficient number of individuals measured) once a size of 0.5 mm to 1 mm was reached. Accordingly, only the size-group < 0.5 mm was considered for daily estimates of seasonal growth and mortality.

3.4.6 Seasonal Growth

Limacina growth rates were highly variable throughout the season with a general decreasing trend observed throughout April. This was followed by generally increasing trends observed in early May (May 1–13), and from late May to mid June (May 26 to June 16) (Figure 3.2E). When the data points from May 27, June 3, and June 10 were removed, linear regressions showed a significant increase in growth rates ($R^2 \geq 0.65$, $p < 0.01$) (Table B.4 in Appendix B) during these two time periods (May 1–13 and May 26 to June 3). Growth rates ranged from 0.0005 mm.day^{-1} to 0.08 mm.day^{-1}, with an average of 0.03 mm.day^{-1} estimated for the time span between April 1 to July 7, 2010.

Environmental Correlation

There was no significant correlation ($R^2 < 0.009$, $p > 0.05$) between short term growth rates and chl-*a* concentration, for both May 1–13 and May 26 to June 16 time intervals.

3.4.7 Daily Mortality

For each cohort tracked, the range of R^2 value from 0.002 to 0.610 indicated high daily variability. The majority of cohorts tracked showed a temporal increase in density, while comparatively few cohorts displayed a temporal decrease. Two periods of short term mortality were observed (e.g. decreasing regression lines). Cohorts cMay16 and cMay20 showed a significant decrease in density from May

16 to June 4 (cMay16: $p < 0.05$; cMay20: $p < 0.01$), and cJun15 and cJun18 showed a significant decrease in density from June 29 to July 6 (cJun15: $R^2 = 0.83$, $p < 0.05$; cJun18: $R^2 = 0.82$; $p < 0.01$, although the entire time period that cJun15 and cJun18 was tracked, was found to be insignificant) (Figure 3.4). An average mortality rate of $0.14.day^{-1}$ was estimated for the cohorts cMay16 and cMay20, while an average rate of $155.1.day^{-1}$ was estimated for cJun15 and cJun18, for the period from June 29 to July 6.

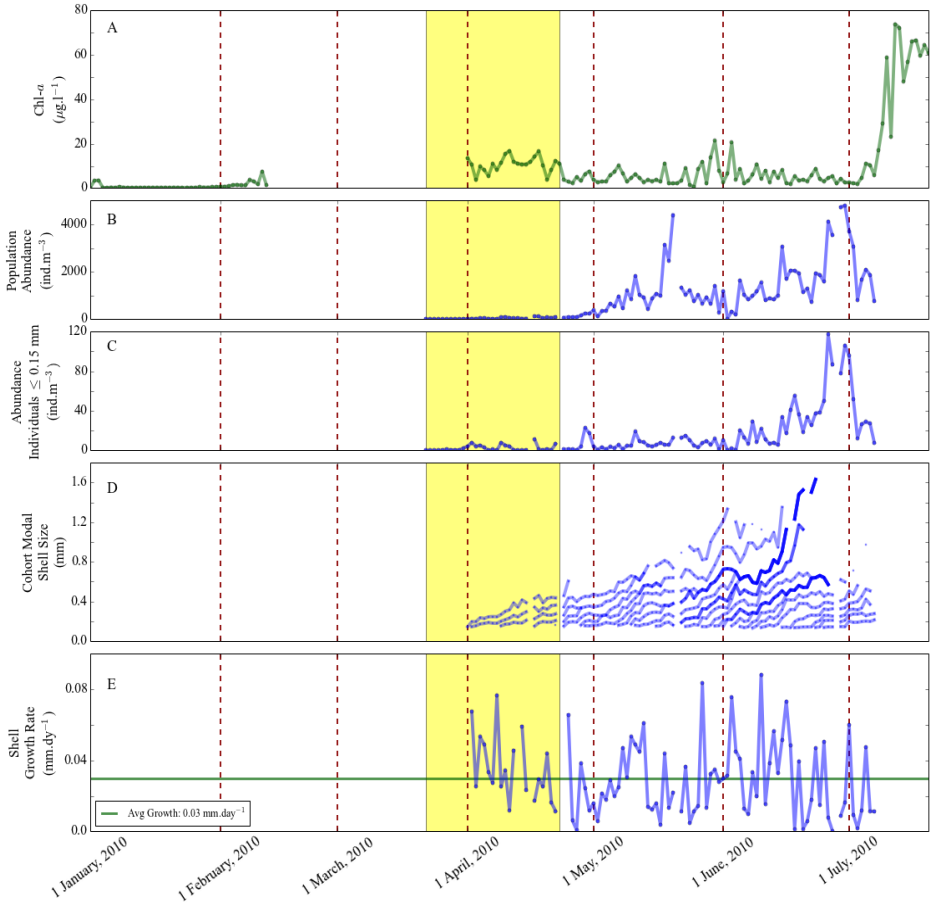

Figure 3.2: Composite 5 x 1 panel figure. Panel **A** depicts the daily variation in fluorescence from 1 January to 20 July, 2010. A data gap exists between mid-February to late-March. Panel **B** portrays the daily variation in the population of *L. helicina* observed from 22 March, 2010 to 7 July, 2010. Panel **C** portrays the daily variation in abundance of the size-fraction ≤ 0.15 mm in shell size. Panel **D** displays the daily development in shell size of each cohort identified and tracked, from 1 April, 2010 to 7 July, 2010. Note that there is transparency added such that the bold colours depicts the times when ≥ 2 components had combined together to grow as one component. Panel **E** portrays the daily growth in shell size of the population of *L. helicina*. These are the average values of the daily growth in shell size of each component tracked, in panel **D**. The dashed red lines marks the first day of each month, starting on 1 April. The shaded yellow region in each panel was the likely duration of the bloom experienced in 2010.

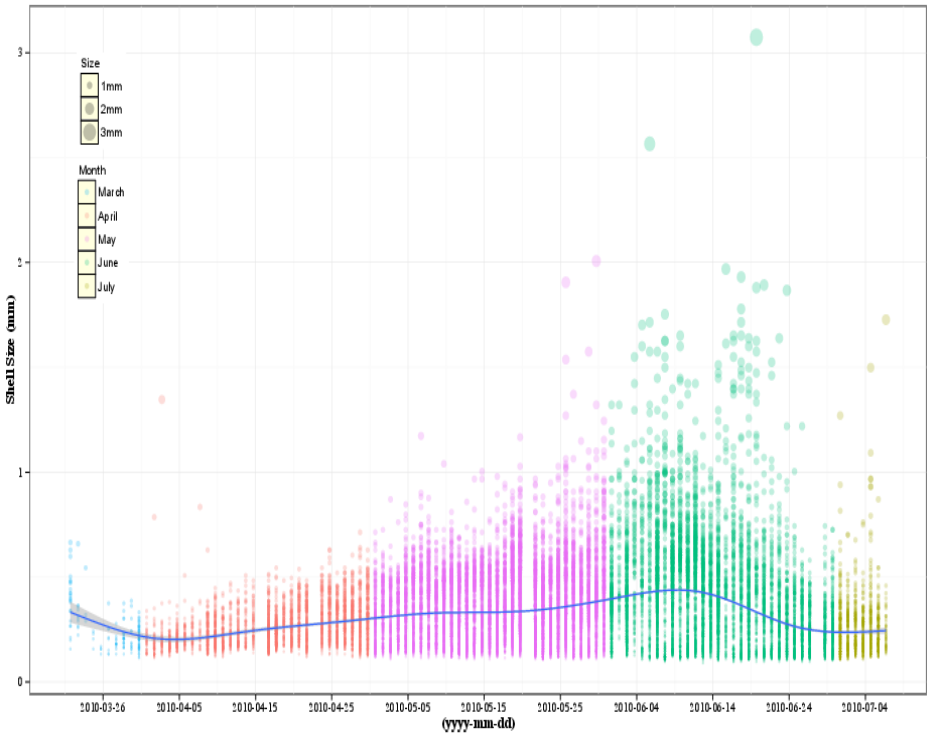

Figure 3.3: Scatterplot of the daily population size structure of *L. helicina*. The data points are colour coordinated with the months of observation; **blue** - March, **red** - April, **purple** - May, **green** - June, **yellow** - July. There is transparency added to show the proportional presence of certain size-fractions in the population, hence the bolder the colour, the more measurements were recorded for the specific shell size. The size of the data point reflects the shell size of the individual measured. A blue loess smoother shows the seasonal trend in the development of the size structure.

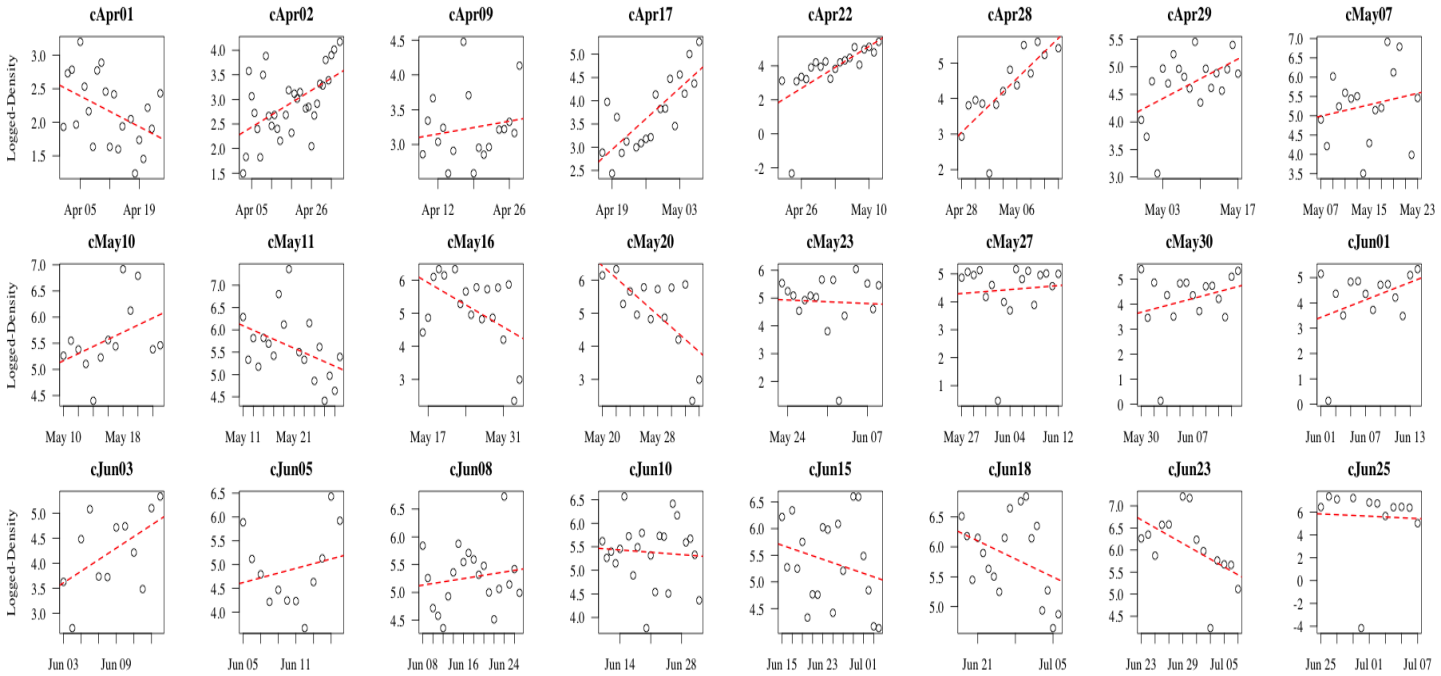

Figure 3.4: Composite figure of the log-transformed daily density of each cohort identified and tracked. Linear regressions are fitted against the respective time periods for each cohort tracked (indicated by the dashed red line). All cohorts are indicated by their abbreviated name (e.g. "cApr01"–cohort recruited on April 1). Significant mortality was identifid for cMay16 ($p < 0.05$) and cMay20 ($p < 0.01$) in late spring. Significant mortality was also observed for the period of June 29 to July 6, for cJun15 ($p < 0.05$) and cJun18 ($p < 0.01$). Note the limited number of cohorts (8) showing a decrease in density.

3.5 Discussion

3.5.1 Spawning, Cohorts, and Size-Structure Development: Comparison to Chapter 2 and Relevant Literature

Based on the results of Chapter 2, *L. helicina* was hypothesized to spawn continuously. A main spawning event occurred in late spring and this was followed by protracted spawning throughout summer. The smaller size-groups generally had a high proportional abundance ($> 40\%$ of the population) in all years of observation, supporting the occurrence of continuous daily spawning. However, it was apparent from the seasonal differences observed between years that the time resolution of Chapter 2 may have been too coarse to determine the seasonal patterns in the life cycle of *L. helicina*. Evidence from the daily data clearly showed that spawning was occurring at a high frequency, and protracted spawning appeared to be the norm.

The literature (Kobayashi, 1974; Dadon and de Cidre, 1992) indicated that the reproductive cycle of *L. helicina* involves a period of enhanced spawning activity followed by a prolonged period of reduced activity. Building from the life cycle study of Chapter 2, the identification of a peak spawning event in summer, from the daily data pointed to the possibility for the newly spawned summer cohort to overwinter *with* the spring cohort (e.g. C_1 and C_2 identified in Chapter 2). Both the C_1 and C_2 cohorts (spring cohorts) were observed to successfully overwinter and it is assumed the same is true for the summer cohort. Dadon and de Cidre (1992) observed the summer cohort of *L. retroversa* to grow at slower rates compared to the spring cohort, due to reduced food availability in summer. Considering *L. helicina* in this study, it may be possible for the slower growing summer cohort to "catch-up" (in terms of shell size) to the remnants of the newly spawned spring spring cohort after summer spawning, although the

new spring cohort is likely approaching senescence (lower relative abundance of larger individuals). Although the summer cohort may be growing *slower* (when compared to the newly spawned spring cohort, possibly during a spring bloom), their growth rates are likely equivalent if not faster than those of the newly spawned spring cohort still remaining after summer peak spawning. This allows the summer cohort to "catch-up" to the spring cohort (e.g. larger individuals of the spring cohort are fully mature and most have already all spawned, hence slower growth rates or no further growth). Maturing by late April to early May of the next year, it is probable that spring spawning was initiated by either the summer cohort, or a combination of both the spring and summer cohorts from the previous year. As significant relations were found between the seasonal distribution of *L. helicina* and 30 m depth-averaged temperature in Chapter 2, it is probable that spring spawning may be partly triggered by slight increases in sea water temperature. The increase in total population abundance during early May (from daily data) provided an indication of spring spawning. Spawning sizes of > 3 mm was identified in Chapter 2, and although the largest individual (> 3 mm) from the daily data was observed on June 21 (e.g. almost 2 months after initiation of spring spawning), the absence of larger individuals throughout May could be a result of either advection, mortality (e.g. predation), or the patchy distribution of *L. helicina*. Detection of these larger individuals in late June may attest to the 1.2–1.5 year life cycle longevity, estimated in Chapter 2. Indeed, if the spring and summer cohorts are *both* able to overwinter then the smaller shell sizes observed in the following spring (from Chapter 2) may be explained (e.g. a larger proportion of smaller summer cohort individuals to individuals of the larger spring cohort). Dadon and de Cidre (1992) postulated the ability of the spring cohort (*L. retroversa*) to grow to sexual maturity by summer, to spawn the summer cohort. Summer is asserted in Gannefors et al.

(2005) and Bednaršek et al. (2012) as a time of enhanced spawning activity, with which we are in agreement. Based on an average growth rate of 0.03 mm.day^{-1}, individuals spawned (assumed shell size of 0.15 mm at spawn) on May 1 (e.g. spring cohort) are able to reach the respective sizes of 1.98 mm, 2.58 mm, and 3 mm by June 30, July 20, and August 3, respectively. With the highest population abundance recorded at the end of June, it is probable that the spring cohort initiated spawning early in the month and at a smaller size. Shell sizes of 1–1.2 mm characterized the spring cohort between late May and early June. From this, it is apparent that *L. helicina* in Rivers Inlet may become capable of spawning once a shell size of $\geq$ 1.00 mm is reached. This is credible given that *L. helicina* is able to develop mature ova from a shell size of $\geq$ 0.70 mm (Kobayashi, 1974). Based on the continually high proportion of smaller individuals after July, from Chapter 2, it would appear that *L. helicina* exhibits reduced spawning activity after peak spawning in summer. The May peak in population abundance (from daily data) was not matched by a parallel peak in the smaller size-groups ($\leq$ 0.15 mm), and it is possible that the spring spawning event was missed. Spatial analysis from Chapter 2 showed that *L. helicina*, although exhibiting broadly similar size-structures across the inlet, do exhibit spatial differences in density (between size-groups). Due to the surface waters at Dawsons Landing always being a state of flux, it is very unlikely the same water mass was sampled. Consequently, there is high potential for patches of *L. helicina* to be advected out of the system, to be replaced by other patches (or portions thereof) from different areas.

High frequency spawning combined with the substantial overlap between cohorts (see the finite mixture distributions in Appendix B) makes it highly unlikely every newly spawned "cohort" was distinct. Instead, the newly spawned cohorts during spring and summer can be considered additive portions (e.g. re-

cruits), and only those contributing to the overall recruitment for the year are considered "true" cohorts. The remaining recruits likely succumb to various forms of mortality (most likely predation). Wootton et al. (2008) proposed an increase in ocean pH from CO_2 uptake by photosynthesis, which is heightened during bloom conditions, to increase the $CaCO_3$ saturation state. Although the short term increase in $CaCO_3$ saturation state is very minimal (e.g. suggesting that there is no real benefit), there is the possibility that any beneficial changes in environmental conditions may assist developing cohorts (Wootton et al., 2008).

The population size structure was generally uni-modal throughout late March and April. A multi-modal size structure characterized the population by mid May, which we interpret as a developing spring cohort. Multi-modality continued into late June, with the smallest size-groups displaying the strongest signals from early–late June (see the finite mixture figures for June in Appendix B). Disappearing by early July when the size structure became more uni-modal, the general absence of the larger individuals ($\geq$ 1 mm) likely signified at least partial die-off of the spring cohort, after summer spawning. A summer mortality of newly spawned recruits may account for a large decrease in the pteropod abundance observed in early July. However, as sampling had terminated early in the month, the absence of the larger individuals could also be interpreted as an sampling artifact (e.g. patchiness).

3.5.2 Caveats to Estimating Daily Growth

Short term trends of significant growth were detected prior to the spring and summer periods of increased spawning. Individual growth rates declines or ceases entirely during the final stages of sexual maturation when energy is dedicated towards reproduction (Lalli and Gilmer, 1989). In this light, the declining

growth rates during mid May in Rivers Inlet may have been an indication that the overwintering cohort had reached sexual maturity. Similarly, the spring cohort reaching sexual maturity may account for the rapidly declining growth rates in late June. Estimations of daily growth rates were complicated by numerous recruits of the summer cohort merging together throughout June (for up to 10 days or more), and recruits exhibiting high short term variations in growth rates. Because these recruits were indistinguishable, the average growth rates calculated could overestimate values for larger individuals.

Environmental Correlation

The non-significant relation between seasonal growth rates and chlorophyll-*a* may have been related to the fact that fluorescence values were measured at 5 m depth. If the fluorescence values measured from 5 m depth were not representative of full water column integrated chlorophyll concentrations, then relationships between seasonal growth rates and chlorophyll-*a* concentrations may be obscured. However, it is most likely that *L. helicina* may have exhibited a delayed response to temporal increases in chlorophyll-*a*. If so, then the heightened chlorophyll-*a* concentrations observed through most of April and late May/early June may have been the driving force responsible for the peak population abundances seen, in mid May and late June, respectively. The termination of zooplankton sampling in early July was unfortunate given the very large increase in chlorophyll-*a* by mid July.

3.5.3 Estimating Daily Mortality and Problems Encountered

Observations of numerous recruits exhibiting temporal increases in density (instead of a decrease) complicated the estimates of seasonal mortality for *L. helicina*. Based on the highly variable spatial density distribution for each recruit

cohort, the variability (large increases on day followed by large decreases the next) in individual cohort density observed at the daily station may be primarily explained by the advection of different patches of *L. helicina* into the sampling location. Therefore, for example, large decreases in density could be attributed to both mortality and *L. helicina* that are advected away from the daily station. It appears that although we were sampling the same population of *L. helicina* in Rivers Inlet, our initial assumption about low spatial density variability could be an oversimplification. Clearly, following an eulerian approach, temporal decreases in cohort density cannot be solely attributed to mortality. Mortality may have been further complicated by high-frequency spawning events (e.g. spring and summer peak spawning) and the possibility of cohorts merging together at differing times.

Despite the above caveats, there were short-term periods of significant mortality. The significant declines shown by the recruits cMay16 and cMay20 from May 16 to June 3, as well as cJun15 and cJun18 from June 29 to July 6 were coincident with a high decrease in total population abundance (after the spring and summer spawning events). Assuming an exponential decrease in mortality with increasing shell size, a mortality rate of $0.14.\text{day}^{-1}$ in late spring translates to a daily mortality of 13 %, which does not appear to match the large decrease in total abundance. A mortality rate of $155.1.\text{day}^{-1}$ for the period of June 29 to July 6, equates to a daily mortality of 100 % which appears to match the large decline in both total population abundance and the density of the size-group $\leq$ 0.15 mm after the summer spawning. Based on this, it appeared that the smallest size-groups experienced the highest mortality after peak spawning in summer. This is in agreement with literature studies of copepod egg-mortality (Peterson and Kimmerer, 1994; McLaren, 1997). Investigating the influence of egg-mortality on the recruitment of *Temora longicronis*, Peterson and Kim-

merer (1994) found high mortalities in spring (162.5 day^{-1}) and summer (21.57 day^{-1}) (Table 2 in Peterson and Kimmerer, 1994). The high mortality observed in spring was hypothesized to be caused by cannibalism (Peterson and Kimmerer, 1994). As *L. helicina* are also known to feed on younger *L. helicina* (e.g. small individuals trapped in the feeding web), it may be likely that the high mortality in late June was partly due to cannibalism (Lalli and Gilmer, 1989).

3.5.4 Potential Sampling Errors

Only 30 m Sampled...

A sampling depth of 30 m considerably limited the representative sampling of the larger size-groups (compared to 300 m in Chapter 2). This could have resulted in a bias and forced inferential interpretations for seasonal rates of growth and mortality. Even though the larger size-groups formed only a small component of the population, the accurate estimate of growth and mortality rates for the larger individuals are still required if size-dependent growth and mortality are to be resolved (Bednaršek et al., 2012).

Influence of Advection

The spatial analysis from Chapter 2 put forward the hypothesis that the *L. helicina* is broadly similar across the inlet. However, the density-differences between stations for varying size-groups, pointed to the patchiness of *L. helicina*. Highlighted in our attempts to track numerous population recruits, it is evident that advection could have a large impact on the temporal distribution of *L. helicina*. Because RI hydrodynamics is largely influenced by freshwater input and hence, highly seasonal (e.g. the rate of surface-freshwater input can change from 100 $m^{-3}.s^{-1}$ from winter-spring, to $\sim$ 1000 $m^{-3}.s^{-1}$ in the summer, Hodal,

2010), the temporal size distribution of *L. helicina* across the inlet would likely varied seasonally as well. Since only 3 dates were considered for spatial analysis in Chapter 2, more work is needed to determine the influence of advection on the size-specific distribution of *L. helicina* in RI (e.g. high resolution vertical-distribution studies throughout the seasons).

Potential Limitations with the Mixdist Statistical Package

In periods of continuous spawning, there is the possibility of the new recruits merging together to grow in synchrony for varying lengths of time. While doing so, it is also possible that certain proportions of the merged group can break away at different times to grow at faster or slower rates than the merged group. If each new recruit cohort is indistinguishable from one another, the growth rate dynamics that each will experience is masked by the presence of the others.

The `mixdist` statistical package appears to be unsuitable for the tracking of the numerous recruits of *L. helicina*. Because there were many newly spawned recruits merging together for a lengthy period ($\geq$ 10 days), there is still uncertainty concerning the growth rates estimated. We suggest that `mixdist` is inadequate for the study of animals exhibiting protracted spawning such as *L. helicina*, and propose that the most efficient method of estimating growth rate is to successfully culture *L. helicina* in experimental aquaria, for extended periods.

Size Frequency Method...

For studies of *L. helicina*, shell size may not be an adequate proxy of age. The seasonal growth of *L. helicina* as well as other *Limacina* spp. is said to be dependent upon environmental conditions (Dadon and de Cidre, 1992; Hunt et al., 2008). Accordingly, problems can arise when two individuals of similar size are at different stages of sexual maturation, due to environmental influence (Dadon and de Cidre, 1992). Nonetheless, the size frequency method may be the only

viable option to study the seasonal dynamics of *L. helicina*, efficiently. According to Aksnes et al. (1997), a physical and quantifiable character is required for the study of natural populations with time series data. Furthermore, because there have been no studies of the development stages nor stage duration times of *L. helicina* in the literature, the use of shell size as a proxy of age appears to be the only option (Aksnes et al., 1997).

Using high temporal resolution data, and building from the results of Chapter 2, this chapter has revealed many facets of *L. helicina* seasonal dynamics. Namely, we have confirmed the phenomenon of protracted spawning hypothesized in Chapter 2. In addition to the spring peak spawning period identified in Chapter 2, the daily data also showed increased spawning during summer. With the initiation of spring spawning (in mid-May), spawning was continuous and identified every 2–4 days leading to the 2nd peak in summer (late-June). By tracking numerous recruits through the period of April 1 to July 7, 2010, an average population growth rate (in terms of shell size) of 0.03 mm.day^{-1} was estimated. Short-term periods of significant growth were identified for the periods of May 1–13 and May 26 to June 16. This was indicative of the sexual maturation of *L. helicina* prior to the spring and summer periods of peak spawning. Based on an average growth rate of 0.03 mm.day^{-1}, it was evident that the recruits spawned in spring are able to grow to a size of up to 3 mm (becoming sexually mature) by August (assuming May 1 as time of spawn and an initial shell size of 0.15 mm). Our attempt to estimate the seasonal mortality of *L. helicina* was greatly undermined by a combination of advective influences, patchy distributions, and the likelihood of merged recruits. However, significant mortality did appear to occur during certain periods, coincident with the days after spring and summer peak spawning (e.g. late-May and late-June). This would suggest that the smallest size-groups experienced the highest mortality

after being spawned. Due to the caveats in our estimates of daily growth and mortality rates, they should be interpreted as very generalized and approximate estimates.

The results from this chapter also highlighted the importance of advection. Clearly, the assumption of a negligible advection must be considered with great caution when studying the seasonal dynamics of *L. helicina*. With this said, it seems the most effective method to study *L. helicina* (i.e. to avoid problems associated with advection and patchiness) is to successfully culture them in laboratory aquaria. There is already headway being made in this respect (see the review of pteropod culture techniques in Howes et al., 2014). Culturing pteropods may be the most effective method in the identification and tracking of the newly spawned recruits. Because they are already accustomed to the culture conditions (when spawned), any temporal changes observed in the individuals (e.g. growth rate, life cycle longevity) should be physiologically mediated (e.g. not biased by culture conditions), and representative of natural populations (Howes et al., 2014). However, estimating the natural mortality of *L. helicina* still presents additional challenges (e.g. cannot be representatively estimated via. culture). A possible solution may be to identify and track water parcels (a lagrangian approach) by using temperature and salinity signatures. This way, it may be possible to continually sample the same population of *L. helicina* over a prolonged period.

Chapter 4

Life Cycle of *L. helicina*: A Conceptual Model and General Conclusions

Despite various studies investigating the life cycle of *L. helicina*, there is a lack of consensus regarding fundamental aspects of its life history. Previous studies have suggested that the life cycle of *L. helicina* ranges from 1.5–2 years in the Central Arctic Ocean, Canadian Basin to over 3 years for *L. helicina* of the Scotia Sea, Southern Ocean. Studying the life cycle of *L. helicina* in the subarctic Pacific and Atlantic, respectively, Fabry (1989) and Gannefors et al. (2005) were in agreement with an annual life cycle. Dadon and de Cidre (1992) postulated a 1–1.5 year life cycle but for *L. retroversa*, a species with a similar reproductive biology to *L. helicina*.

This thesis used datasets of high temporal resolution combined with the size frequency method to examine the life cycle of *L. helicina*. Population cohorts were identified and tracked using the `mixdist` statistical package. In Chapter 2, two cohorts were identified and tracked for > 400 days. From this, a life cycle longevity of 1.2–1.5 years was estimated, with 1.5 years being the likely maximum. Both cohorts were observed to successfully overwinter, although both

exhibited a reduced shell size in the following spring. Observations from Lischka and Riebesell (2012) provides evidence of *L. helicina* successfully overwintering. Additionally, there was no growth or spawning activity during the winter period (Lischka and Riebesell, 2012). Based on the seasonal abundances, late spring was hypothesized as a time of peak spawning activity. From the size-frequency histograms, prominent growth was observed in spring and summer with evident development of the population size structure. The dominant influence of the smallest size-groups throughout the seasons for all years, suggested that *L. helicina* is capable of protracted spawning. Utilizing higher resolution data, the results of Chapter 3 indeed confirmed that *L. helicina* is capable of protracted spawning, with the newly spawned recruits identified every 2–4 days. Spring and summer was affirmed as the times of peak spawning activity. With the identification of increased summer spawning as well as a summer cohort, there is a high probability that *both* the summer cohort and the spring cohort are overwintering together. Overwinter survival may be achieved by a combination of reduced metabolic activity, and migration to deeper depths (Maas et al., 2012). Significant growth ($\text{mm}_{shell\ growth}.\text{day}^{-1}$) was found for the periods prior to both the spring and summer spawning events, although this was not related to chlorophyll-*a* concentrations at 5 m depth. However, the daily distribution of *L. helicina* pointed to the possibility of a delayed response to seasonal periods of high chlorophyll-*a*, which may have obscured any evident relation between chlorophyll-*a* and seasonal growth. Although only short-term growth was significant, the average seasonal growth rate showed that the spring cohort is capable of growing to maturity by summer (like *L. retroversa*). This indicated a potentially much smaller spawning size when compared to the literature, and the spawning sizes ($\geq$ 3 mm) from Chapter 2. Attempts were made in Chapter 3 to accurately estimate instantaneous mortality. Difficulties were encountered

as it became clear that we were not sampling the same population from day to day. Additionally, many newly spawned recruit cohorts were likely merging during spring and summer spawning, which considerably biased the parameters (modal shell size and proportional abundance for each cohort) produced from fitting finite mixture distributions. Consequently, the estimates of daily growth (in terms of shell size) and mortality rates should be regarded as first approximates. The potential merging of cohorts pointed to the inability of `mixdist` to distinguish between merged population recruits, suggesting that this statistical package may be unsuitable for the study of *L. helicina*. Although many recruits showed temporal increases in density, significant decreases were identified for two recruits during mid–late May (after peak spawning in late spring). Additionally, significant decreases in late June (short term), coincided with sharp declines in total population abundance. However, as it was highly unlikely that the same population was continuously sampled, periods of significant decline in density could not be attributed solely to mortality. Even so, the high mortality observed from late June to early July suggested that the smallest size-groups of *L. helicina* experienced the highest mortality after peak spawning in summer.

4.1 A Conceptual Model

Integrating the results from Chapters 2 and 3, the life cycle of *L. helicina* can be described by the conceptual model in Figure 4.1. At Year_{t-1}, the cohort spawned in spring is able to utilize resources from the spring bloom to grow to a shell size corresponding to sexual maturity by summer. Summer spawning is initiated once sexual maturity is reached, and is likely triggered by increasing sea water temperature. Despite the majority of the spring cohort dying off after synchronized spawning, there is still a small proportion that continues to survive (and possible grow) into the summer and fall months (thin arrows in Figure 4.1).

As this happens, any adult individuals that have yet to release their eggs do so throughout the late summer and early fall, resulting in low levels protracted spawning (e.g. small scale spawning events–unsynchronized). Utilizing the remaining resources from the fall bloom, the summer cohort may be able to grow at comparatively faster rates, to reach a shell size nearly equivalent to that of the spring cohort, which is likely experiencing some mortality towards summers end. This may explain the high overlap between cohorts throughout the seasons, and between years. Entering the winter, both the spring and summer cohorts are able to survive into the next year, possibly by migrating to deeper depths and experiencing reduced metabolic rates (Maas et al., 2012). During the late fall/winter period, the *Limacina* exhibits no shell growth and all reproductive activity ceases. With the comparatively lower food availability during winter, as well as the likelihood of increased predation, the overwintering spring cohort experiences comparatively higher mortality (e.g. from senescence and/or predation), resulting in a larger ratio of smaller summer cohort individuals (Year_{t-1}) to larger spring cohort individuals (Year_{t-1}) in the following spring. Becoming more active in the spring of Year_t, limited spawning activity by portions of the summer cohort (already at shell sizes of potential spawning) may be triggered by slight increases in sea water temperature during spring. When environmental conditions become more optimal in late spring (e.g. warmer sea water temperatures and increased food availability from the spring bloom), the overwintered summer cohort experiences rapid growth and with the full maturation of the summer cohort (from Year_{t-1}), begins the spring period of peak spawning. It is also possible for the small portion of the spring born cohort from Year_{t-1} to contribute to the spring spawning event in Year_t, however, the majority of the spawning is from the overwintered summer cohort from Year_{t-1}. Depending on the environmental conditions during the summer/fall period of Year_{t-1} and the

winter conditions transitioning into Year_t, there is a possibility that the summer cohort overwinters by itself, *with* the still present spring cohort, or not at all (e.g., only the spring cohort overwinters).

Based on this model, the survival of the population to Year_{t+1} depends on the recruitment of the summer cohort (and potentially the spring cohort), and its survival through winter. In turn, this will depend on the timing of the spring spawning period and also, the magnitude of the spring bloom. In the case of a delayed spring bloom, there may be a delayed spring spawning such that the summer cohort will be spawned later in the season, meaning they may have insufficient time to grow before the onset of winter. Similarly, if the bloom magnitude is insufficient to allow the effective growth of the spring cohort, it may result in delayed summer spawning or reduced recruitment during summer spawning. This means the summer cohort will enter the fall–winter period at a smaller size and in reduced numbers, thereby decreasing the summer cohorts likelihood of successfully overwintering. Given that the majority of the spring cohort likely dies off after peak spawning, the reduced probability of the summer cohort successfully surviving the winter suggests a low survivorship of the *L. helicina* population into the next year. If winter survival is successful, the smaller adults from the summer cohort may require longer periods to reach maturity in the next year. Again, this may lead to delayed spring spawning. Interestingly, depending on the bloom timing, there could be various proportions of the cohort(s) (spring and summer) overwintering to the next year (e.g. a delayed bloom could mean a higher proportion of the spring cohort overwintering, whereas an earlier bloom may infer a lower proportion). This may have implications to recruitment in the following year (e.g. higher proportion of spring cohorts may mean lower recruitment in the following spring as the majority of the spring cohort have either already spawned in the previous summer, or

have died off). Regardless, the possibility of two cohorts overwintering may dramatically increase the stability of the population dynamics.

4.2 General Conclusions

By investigating the inter-annual and seasonal dynamics of the *L. helicina* population in Chapters 2 and 3, respectively, we have shown that 1.) the normal seasonal cycle of recruitment is characterized by continuous spawning activity outside winter months, 2.) although continuous, these periods are punctuated by short term episodes of very intense reproductive output during the late spring and summer, and 3.) reproductive activity terminates during the late fall and winter periods, and commences again in the following spring. Accordingly, we propose that spring and summer are the two primary periods of spawning activity, with low level but continuous spawning outside these times, with the exception of winter. The spring and summer cohorts result from these two periods of intense spawning. Assuming uniform growth, it is plausible that 4.) the spring cohort reaches sexual maturity by summer, and subsequently spawns the summer cohort. Finally, we have also shown that 5.) it is possible that both the spring and summer cohorts overwinter into the following year, which may explain the high overlap between cohorts in the size-frequency histograms.

In our attempt to estimate the daily growth and mortality rates of *L. helicina*, we've discovered potentially significant obstacles hindering estimate derivation. Most notably, the influence of advection combined with the inherently patchy distribution of *L. helicina* created great difficulty during our eulerian sampling. Consequently, the estimates likely represent underestimates with high uncertainty. Regarding estimates of growth rates, the most viable option (currently) would appear to be the successful culturing of *Limacina* in experimental aquaria. If this can be accomplished, the newly spawned can be effectively mon-

itored through time to obtain accurate estimates of growth in shell size, biomass, etc. However, recent literature has only begun to address the potential benefits and challenges of culturing *Limacina*. For representative estimates of mortality, it is crucial to temporally sample the same group of specimens through time. As experimental aquaria does not simulate the natural environment (e.g. zooplankton community). A feasible course of action is to track parcels of water during a lagrangian study Since Rivers Inlet is highly stratified, the vertical distribution of *L. helicina* in the inlet should be investigated.

Due to the unprecedented rates of change in seawater chemistry and temperature, it is crucial to gain an mechanistic understanding of the forces driving the seasonal and inter-annual changes observed in the *L. helicina* population. Predictive models can then be constructed and optimized to better understand the synergistic effects of increasing temperature and acidity, as well as other parameters, on *L. helicina* populations over time. Once optimized, it is hoped the knowledge gained from these models will provide effective methods of monitoring and predicting the physical and biological changes occurring in the marine environment, into the future.

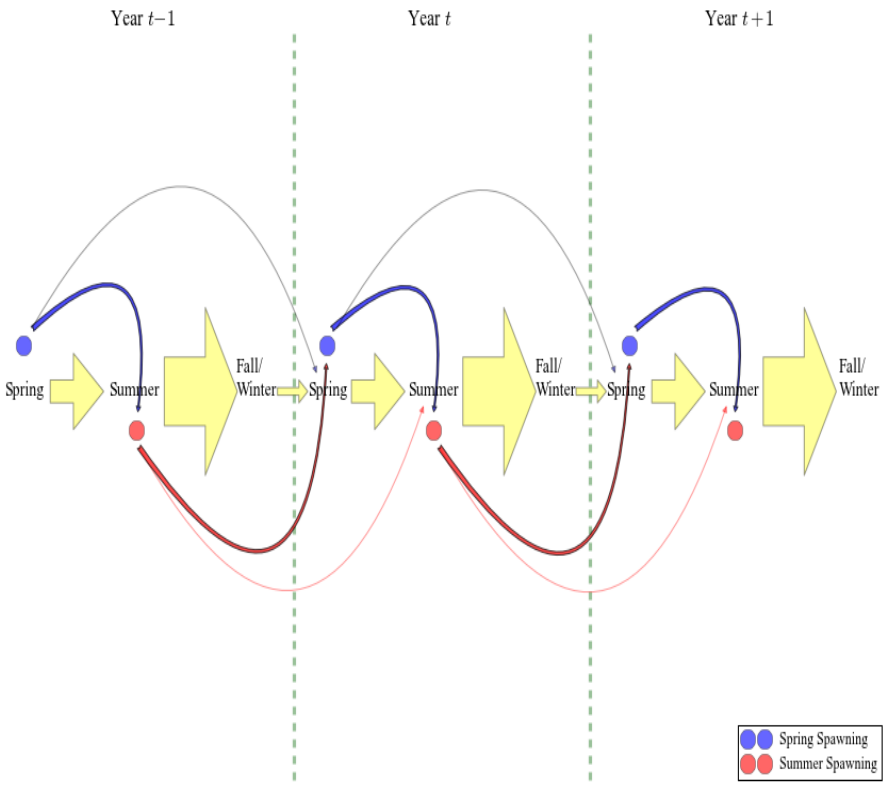

Figure 4.1: Conceptual model depicting the life-cycle of *L. helicina*. The **blue & red dots** marks the spring and summer spawning events, respectively. The **yellow arrows** mark the population abundance passing from one season to the next. Larger arrows indicate a higher abundance. **Blue arrows** indicate the growth cycle of the spring cohort, while the **red arrows** marks the growth cycle of the summer cohort. The **thin blue and red lines**, indicates the potential life-cycle longevity of the spring and summer cohorts, respectively. Note the overlap of cohorts throughout and between years.

Bibliography

Aksnes, D. L., Miller, C. B., Ohman, M. D., and Wood, S. N. (1997). Estimation techniques used in studies of copepod population dynamicsa review of underlying assumptions. *Sarsia*, 82(4):279–296.

Aksnes, D. L. and Ohman, M. D. (1996). A vertical life table approach to zooplankton mortality estimation. *Limnology and Oceanography*, 41(7):1461–1469.

Bednaršek, N., Tarling, G., Fielding, S., and Bakker, D. (2012). Population dynamics and biogeochemical significance of *Limacina helicina antarctica* in the scotia sea (southern ocean). *Deep Sea Research Part II: Topical Studies in Oceanography*, 59:105–116.

Bernard, K. and Froneman, P. (2009). The sub-antarctic euthecosome pteropod, *Limacina retroversa*: Distribution patterns and trophic role. *Deep Sea Research Part I: Oceanographic Research Papers*, 56(4):582–598.

Clarke, A. and Peck, L. S. (1991). The physiology of polar marine zooplankton. *Polar research*, 10(2):355–370.

Comeau, S., Gorsky, G., Alliouane, S., and Gattuso, J.-P. (2010). Larvae of the pteropod *Cavolinia inflexa* exposed to aragonite undersaturation are viable but shell-less. *Marine biology*, 157(10):2341–2345.

Comeau, S., Gorsky, G., Jeffree, R., Teyssie, J., Gattuso, J., et al. (2009). Impact of ocean acidification on a key arctic pelagic mollusc (*Limacina helicina*). *Biogeosciences*, 6(9):1877–1882.

Conover, R. and Paranjape, M. (1977). Comments on the use of a deep tank in planktological research. *Helgoländer Wissenschaftliche Meeresuntersuchungen*, 30(1-4):105–117.

Dadon, J. R. and de Cidre, L. L. (1992). The reproductive cycle of the thecosomatous pteropod *Limacina retroversa* in the western south atlantic. *Marine Biology*, 114(3):439–442.

Dixson, D. L., Munday, P. L., and Jones, G. P. (2010). Ocean acidification disrupts the innate ability of fish to detect predator olfactory cues. *Ecology Letters*, 13(1):68–75.

Doney, S. C., Fabry, V. J., Feely, R. A., and Kleypas, J. A. (2009). Ocean acidification: the other co2 problem. *Marine Science*, 1.

Du, J. (2002). Combined algorithms for fitting finite mixture distributions. Master's thesis, McMaster.

Fabry, V. J. (1989). Aragonite production by pteropod molluscs in the subarctic pacific. *Deep Sea Research Part A. Oceanographic Research Papers*, 36(11):1735–1751.

Fabry, V. J., Seibel, B. A., Feely, R. A., and Orr, J. C. (2008). Impacts of ocean acidification on marine fauna and ecosystem processes. *ICES Journal of Marine Science: Journal du Conseil*, 65(3):414–432.

Gannefors, C., Böer, M., Kattner, G., Graeve, M., Eiane, K., Gulliksen, B., Hop, H., and Falk-Petersen, S. (2005). The arctic sea butterfly *Limacina helicina*: lipids and life strategy. *Marine Biology*, 147(1):169–177.

Gentleman, W., Pepin, P., and Doucette, S. (2012). Estimating mortality: Clarifying assumptions and sources of uncertainty in vertical methods. *Journal of Marine Systems*.

Gilmer, R. and Harbison, G. (1986). Morphology and field behavior of pteropod molluscs: feeding methods in the families cavoliniidae, limacinidae and peraclididae (gastropoda: Thecosomata). *Marine Biology*, 91(1):47–57.

Gilmer, R. and Harbison, G. (1991). Diet of *limacina helicina* (gastropoda: Thecosomata) in arctic waters in midsummer. *Marine ecology progress series. Oldendorf*, 77(2):125–134.

Harris, R. (2000). *ICES zooplankton methodology manual*. Academic Press, San Diego,.

Hlavac, M. (2013). *stargazer: LaTeX code for well-formatted regression and summary statistics tables*. Harvard University, Cambridge, USA. R package version 3.0.1.

Hodal, H., Falk-Petersen, S., Hop, H., Kristiansen, S., and Reigstad, M. (2012). Spring bloom dynamics in kongsfjorden, svalbard: nutrients, phytoplankton, protozoans and primary production. *Polar biology*, 35(2):191–203.

Hodal, M. (2010). Net physical transports, residence times, and new production for rivers inlet, british columbia. Master's thesis, University of British Columbia.

Howes, E. L., Bednaršek, N., Büdenbender, J., Comeau, S., Doubleday, A., Gallager, S. M., Hopcroft, R. R., Lischka, S., Maas, A. E., Bijma, J., et al. (2014). Sink and swim: a status review of thecosome pteropod culture techniques. *Journal of Plankton Research*, 36(2):299–315.

Hsiao, S. C. (1939a). The reproduction of *Limacina retroversa* (flem.). *The Biological Bulletin*, 76(2):280–303.

Hsiao, S. C. (1939b). The reproductive system and spermatogenesis of *Limacina (Spiratella) retroversa* (flem.). *Biological Bulletin*, pages 7–25.

Hunt, B., Pakhomov, E., Hosie, G., Siegel, V., Ward, P., and Bernard, K. (2008). Pteropods in southern ocean ecosystems. *Progress in Oceanography*, 78(3):193–221.

Hunt, B., Strugnell, J., Bednarsek, N., Linse, K., Nelson, R. J., Pakhomov, E., Seibel, B., Steinke, D., and Würzberg, L. (2010). Poles apart: the bipolar pteropod species *Limacina helicina* is genetically distinct between the arctic and antarctic oceans. *PloS one*, 5(3):e9835.

Kobayashi, H. (1974). Growth cycle and related vertical distribution of the thecosomatous pteropod *Spiratella ("Limacina") helicina* in the central arctic ocean. *Marine Biology*, P26:295–301.

Lalli, C. and Gilmer, R. (1989). *Pelagic Snails: The Biology of Holoplanktonic Gastropod Mollusks*. Stanford University Press.

Lalli, C. M. and Wells, F. E. (1978). Reproduction in the genus *Limacina* (opisthobranchia: Thecosomata). *Journal of Zoology*, 186(1):95–108.

Lischka, S., Büdenbender, J., Boxhammer, T., and Riebesell, U. (2010). Impact of ocean acidification and elevated temperatures on early juveniles of the polar shelled pteropod *Limacina helicina*: mortality, shell degradation, and shell growth. *Biogeosciences discussions*, 7(6):8177–8214.

Lischka, S. and Riebesell, U. (2012). Synergistic effects of ocean acidification and warming on overwintering pteropods in the arctic. *Global Change Biology*.

Maas, A. E., Elder, L. E., Dierssen, H. M., and Seibel, B. A. (2011). Metabolic response of antarctic pteropods (mollusca: Gastropoda) to food deprivation and regional productivity. *Marine Ecology Progress Series*, 441:129–139.

Maas, A. E., Wishner, K. F., and Seibel, B. A. (2012). Metabolic suppression in thecosomatous pteropods as an effect of low temperature and hypoxia in the eastern tropical north pacific. *Marine biology*, 159(9):1955–1967.

MacDonald, P. and contributions from Juan Du (2011). *mixdist: Finite Mixture Distribution Models*. R package version 0.5-4.

MacDonald, P. and Pitcher, T. (1979). Age-groups from size-frequency data: A versatile and efficient method of analyzing distribution mixtures. *Journal of Fisheries Research Board Canada*, 36(8):987–1001.

MacDonald, P. M. (2011). Personal communications.

Mackas, D., Thomson, R. E., and Galbraith, M. (2001). Changes in the zooplankton community of the british columbia continental margin, 1985-1999, and their covariation with oceanographic conditions. *Canadian Journal of Fisheries and Aquatic Sciences*, 58(4):685–702.

McKinnell, S., Wood, C., Rutherford, D., Hyatt, K., and Welch, D. (2001). The demise of owikeno lake sockeye salmon. *North American Journal of Fisheries Management*, 21(4):774–791.

McLaren, I. (1997). Modeling biases in estimating production from copepod cohorts. *Limnology and oceanography*, 42(3):584–589.

Morton, J. (1954). The biology of *Limacina retroversa*. *J. mar. biol. Ass. UK*, 33:297–312.

Mucci, A. (1981). *The solubility of calcite and aragonite and the composition of calcite overgrowths in seawater and related solutions*. PhD thesis, University of Miami.

Ohman, M. D. and Wood, S. N. (1995). The inevitability of mortality. *ICES Journal of Marine Science: Journal du Conseil*, 52(3-4):517–522.

Paranjape, M. A. (1968). The egg mass and veligers of *Limacina helicina* phipps. *The Veliger*, 10(4):322–326.

Peterson, W. T. and Kimmerer, W. J. (1994). Processes controlling recruitment of the marine calanoid copepod temora zortgicoks in long island sound: Egg production, egg mortality, and cohort survival rates. *Limnol. Oceanogr*, 39(7):1594–1605.

R Core Team (2013). *R: A Language and Environment for Statistical Computing*. R Foundation for Statistical Computing, Vienna, Austria.

Redfield, A. C. (1939). The history of a population of *Limacina retroversa* during its drift across the gulf of maine. *The Biological Bulletin*, 76(1):26–47.

Seibel, B. A., Maas, A. E., and Dierssen, H. M. (2012). Energetic plasticity underlies a variable response to ocean acidification in the pteropod, *Limacina helicina antarctica*. *PLoS One*, 7(4):e30464.

Tommasi, D., Hunt, B., Pakhomov, E., and Mackas, D. L. (2013). Mesozooplankton community seasonal succession and its drivers: Insights from a british columbia, canada, fjord. *Journal of Marine Systems*.

Wells, F. E. (1976). Growth rates of four species of euthecosomatous pteropods occurring off barbados, west indes. *The Nautilus (Philadelphia)*, 90:114–116.

Weslawski, J., Kwasniewski, S., and Wiktor, J. (1991). Winter in a svalbard fjord ecosystem. *Arctic*, pages 115–123.

Wiens, J. A. (1989). Spatial scaling in ecology. *Functional ecology*, 3(4):385–397.

Willis, K., Cottier, F., Kwasniewski, S., Wold, A., and Falk-Petersen, S. (2006). The influence of advection on zooplankton community composition in an arctic fjord (kongsfjorden, svalbard). *Journal of Marine Systems*, 61(1):39–54.

Wolfe, M. A. (2010). Impact of wind and river flow on the timing of the rivers inlet spring phytoplankton bloom. Master's thesis, The University of British Columbia.

Wootton, J. T., Pfister, C. A., and Forester, J. D. (2008). Dynamic patterns and ecological impacts of declining ocean ph in a high-resolution multi-year dataset. *Proceedings of the National Academy of Sciences*, 105(48):18848–18853.

Yamamoto-Kawai, M., McLaughlin, F. A., Carmack, E. C., Nishino, S., and Shimada, K. (2009). Aragonite undersaturation in the arctic ocean: effects of ocean acidification and sea ice melt. *Science*, 326(5956):1098–1100.

Appendices

Appendix A

Chapter 2: Supplementary Data

A.1 2010–2011 Winter-Transition

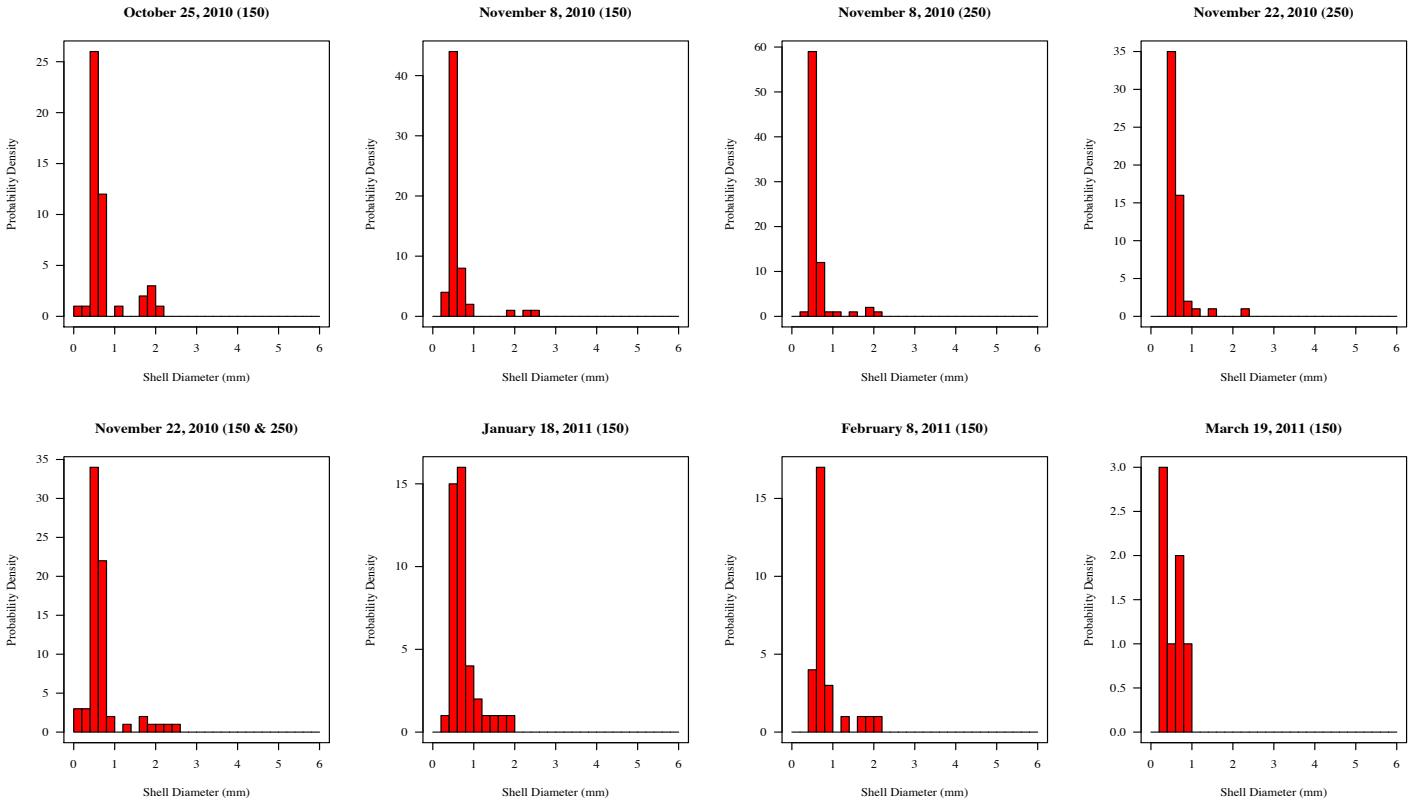

Figure A.1: A composite 2x4 set of histograms displaying the change in the population size-structure of *L. helicina* throughout the 2010–2011 winter-transition. Note the shift of the 0.2–0.4 mm size-bin to the 0.4–0.6 mm size-bin during the winter months. The mesh size of the net used for sampling is indicated in brackets for each sampling date. Due to precarious weather conditions, the samples from the 150 μm and 250 μm nets had to be combined on November 22, 2010.

A.2 Seasonal Correlations - Physical Parameters & Population Abundance

Table A.1: Linear regressions testing the correlation between the environmental parameters - 30 m depth-averaged temperature, 30 m depth-averaged salinity (PSU), 30 m depth-integrated fluorescence (m^{-2}) - and *L. helicina* logged-abundance ($ind.m^{-3}$) for the 2008 season (18 March to 22 September).

	Dependent variable:		
	Log-Abundance (2008)		
	(1)	(2)	(3)
30 m Depth-Avg Temperature	1.543*		
	(0.756)		
30 m Depth-Avg Salinity		−1.514*	
		(0.786)	
30 m Depth-Integrated Fluorescence			−0.001
			(0.006)
Constant	−8.257	49.788*	4.338***
	(6.117)	(23.676)	(1.161)
Observations	10	10	10
R^2	0.342	0.317	0.003
Adjusted R^2	0.260	0.232	−0.122
Residual Std. Error (df = 8)	1.520	1.549	1.872
F statistic (df = 1; 8)	4.163*	3.712*	0.023
Note:			*p<0.1; **p<0.05; ***p<0.01

Table A.2: Linear regressions testing the correlation between the environmental parameters - 30 m depth-averaged temperature, 30 m depth-averaged salinity (PSU), 30 m depth-integrated fluorescence (FU) - and *L. helicina* logged-abundance (ind.m^{-3}) for the 2009 Season (28 February to 13 August).

	Dependent variable:		
	Log-Abundance (2009)		
	(1)	(2)	(3)
30 m Depth-Avg Temperature	1.297***		
	(0.187)		
30 m Depth-Avg Salinity		−1.284***	
		(0.266)	
30 m Depth-Integrated Fluorescence			−0.001
			(0.006)
Constant	−7.517***	40.887***	2.376**
	(1.422)	(7.997)	(0.827)
Observations	11	11	11
R^2	0.843	0.721	0.001
Adjusted R^2	0.825	0.690	−0.110
Residual Std. Error (df = 9)	0.548	0.729	1.381
F statistic (df = 1; 9)	48.280***	23.304***	0.012
Note:			*p<0.1; **p<0.05; ***p<0.01

Table A.3: Linear regressions testing the correlation between the environmental parameters - 30 m depth-averaged temperature, 30 m depth-averaged salinity (PSU), 30 m depth-integrated fluorescence (FU) - and *L. helicina* logged-abundance (ind.m^{-3}) for the 2010 season (19 March to 20 July).

	Dependent variable:		
	Log-Abundance (2010)		
	(1)	(2)	(3)
30 m Depth-Avg Temperature	2.535**		
	(0.361)		
30 m Depth-Avg Salinity		−2.156	
		(1.869)	
30 m Depth-Integrated Fluorescence			−0.014
			(0.010)
Constant	−17.810**	67.332	7.285
	(3.043)	(55.319)	(2.625)
Observations	4	4	4
R^2	0.961	0.400	0.529
Adjusted R^2	0.942	0.099	0.294
Residual Std. Error (df = 2)	0.437	1.716	1.520
F statistic (df = 1; 2)	49.390**	1.331	2.248
Note:			*p<0.1; **p<0.05; ***p<0.01

Table A.4: Linear regressions testing the correlation between the environmental parameters - 30 m depth-averaged temperature, 30 m depth-averaged salinity (PSU), 30 m depth-integrated fluorescence (FU) - and *L. helicina* logged-abundance (ind.m^{-3}) for the 2009 Season (28 February to 13 August).

	Dependent variable:
	Log-Abundance (28 February - 2 June, 2009)
30 m Depth-Integrated Fluorescence	0.007*
	(0.003)
Constant	0.571
	(0.516)
Observations	7
R^2	0.491
Adjusted R^2	0.390
Residual Std. Error	0.651($df = 5$)
F statistic	4.831*($df = 1; 5$)
Note:	*p<0.1; **p<0.05; ***p<0.01

Appendix B

Chapter 3: Supplementary Data

B.1 Daily Data Sampling Dates

Table B.1 presents the dates of zooplankton sample collection at the Daily Station located at Dawsons Landing, Rivers Inlet from 22 March to 7 July, 2010. The statistcal results of all size-frequency enumerations of *L. helicina* individuals processed (max., mean, min.) for each sample, is also presented. **Note** the missing samples for 16, 23 April, 21 May, and 28 June.

Table B.1: Daily dates of sample collection at Dawsons Daily Station. Also presented is the summary statistics of the shell size structure for each sample on their respective dates of sampling. An 80 μm mesh net (30 cm diameter) was used. **Note** the lack of summary statistics for the shell size enumerations, for dates of missing samples (indicated by blank lines).

Year	**Month**	**Day**	**Mesh (μm)**	**Depth (m)**	**Max. (mm)**	**Mean (mm)**	**Min. (mm)**
2010	March	22	80	30	0.66	0.40	0.16
2010	March	23	80	30	0.66	0.34	0.22
2010	March	24	80	25	0.54	0.38	0.29
2010	March	25	80	28	0.24	0.21	0.16
2010	March	26	80	27	0.17	0.15	0.13
2010	March	27	80	29	0.37	0.21	0.13
2010	March	28	80	28	0.28	0.19	0.13
2010	March	29	80	29	0.37	0.22	0.13

Continued on next page

Table B.1 – continued from previous page

Year	Month	Day	Mesh (μm)	Depth (m)	Max. (mm)	Mean (mm)	Min. (mm)
2010	March	30	80	28	0.39	0.22	0.14
2010	March	31	80	29	0.33	0.21	0.11
2010	April	1	80	29	0.34	0.19	0.13
2010	April	2	80	30	0.79	0.19	0.11
2010	April	3	80	29	1.35	0.22	0.13
2010	April	4	80	28	0.38	0.18	0.12
2010	April	5	80	30	0.36	0.21	0.15
2010	April	6	80	30	0.51	0.22	0.15
2010	April	7	80	30	0.35	0.22	0.13
2010	April	8	80	30	0.83	0.25	0.15
2010	April	9	80	30	0.63	0.22	0.13
2010	April	10	80	30	0.45	0.23	0.12
2010	April	11	80	30	0.42	0.21	0.12
2010	April	12	80	30	0.47	0.24	0.14
2010	April	13	80	30	0.44	0.23	0.15
2010	April	14	80	30	0.51	0.26	0.16
2010	April	15	80	30	0.48	0.27	0.14
2010	April	16	80	30			
2010	April	17	80	30	0.51	0.24	0.13
2010	April	18	80	30	0.54	0.24	0.15
2010	April	19	80	30	0.48	0.28	0.15
2010	April	20	80	30	0.50	0.25	0.15
2010	April	21	80	30	0.54	0.30	0.13
2010	April	22	80	30	0.48	0.26	0.12
2010	April	23	80	30			
2010	April	24	80	30	0.54	0.29	0.13
2010	April	25	80	30	0.63	0.30	0.13
2010	April	26	80	30	0.52	0.28	0.13
2010	April	27	80	30	0.54	0.30	0.13
2010	April	28	80	30	0.60	0.30	0.12
2010	April	29	80	30	0.71	0.27	0.11
2010	April	30	80	30	0.63	0.29	0.12
2010	May	1	80	30	0.71	0.28	0.12
2010	May	2	80	30	0.73	0.32	0.12
2010	May	3	80	30	0.87	0.28	0.11
2010	May	4	80	30	0.76	0.31	0.13
2010	May	5	80	30	0.85	0.34	0.12
2010	May	6	80	30	0.69	0.34	0.12
2010	May	7	80	30	1.17	0.35	0.11
2010	May	8	80	30	0.88	0.37	0.11
2010	May	9	80	30	0.73	0.31	0.12
2010	May	10	80	30	1.04	0.34	0.12

Continued on next page

Table B.1 – continued from previous page

Year	Month	Day	Mesh (μm)	Depth (m)	Max. (mm)	Mean (mm)	Min. (mm)
2010	May	11	80	30	0.81	0.33	0.12
2010	May	12	80	30	0.69	0.31	0.11
2010	May	13	80	30	0.86	0.30	0.11
2010	May	14	80	30	0.97	0.32	0.11
2010	May	15	80	30	1.00	0.33	0.12
2010	May	16	80	30	0.77	0.32	0.12
2010	May	17	80	30	0.98	0.31	0.12
2010	May	18	80	30	0.94	0.36	0.11
2010	May	19	80	30	0.91	0.38	0.12
2010	May	20	80	30	1.17	0.38	0.12
2010	May	21	80	30			
2010	May	22	80	30	0.97	0.32	0.11
2010	May	23	80	30	0.88	0.32	0.11
2010	May	24	80	30	0.95	0.32	0.11
2010	May	25	80	30	1.02	0.36	0.12
2010	May	26	80	30	1.91	0.38	0.11
2010	May	27	80	30	1.37	0.36	0.11
2010	May	28	80	30	1.15	0.34	0.11
2010	May	29	80	30	1.57	0.37	0.11
2010	May	30	80	30	2.01	0.37	0.11
2010	May	30	80	30	1.24	0.41	0.12
2010	June	1	80	30	1.32	0.36	0.11
2010	June	2	80	30	1.32	0.52	0.21
2010	June	3	80	30	1.11	0.38	0.12
2010	June	4	80	30	1.55	0.54	0.13
2010	June	5	80	30	1.70	0.56	0.11
2010	June	6	80	30	2.57	0.49	0.10
2010	June	7	80	30	1.57	0.43	0.11
2010	June	8	80	30	1.75	0.48	0.10
2010	June	9	80	30	1.40	0.43	0.12
2010	June	10	80	30	1.65	0.52	0.10
2010	June	11	80	30	1.42	0.40	0.11
2010	June	12	80	30	1.42	0.47	0.12
2010	June	13	80	30	1.17	0.37	0.10
2010	June	14	80	30	1.01	0.37	0.11
2010	June	15	80	30	1.51	0.37	0.10
2010	June	16	80	30	1.97	0.41	0.11
2010	June	17	80	30	1.65	0.45	0.10
2010	June	18	80	30	1.93	0.37	0.10

Continued on next page

Table B.1 – continued from previous page

Year	Month	Day	Mesh (μm)	Depth (m)	Max. (mm)	Mean (mm)	Min. (mm)
2010	June	19	80	30	1.64	0.35	0.11
2010	June	20	80	30	3.07	0.47	0.10
2010	June	21	80	30	1.89	0.32	0.10
2010	June	22	80	30	1.52	0.29	0.11
2010	June	23	80	30	1.64	0.29	0.10
2010	June	24	80	30	1.87	0.29	0.10
2010	June	25	80	30	1.00	0.24	0.11
2010	June	26	80	30	1.22	0.25	0.10
2010	June	27	80	30	0.58	0.23	0.10
2010	June	28	80				
2010	June	29	80	30	0.74	0.23	0.10
2010	June	30	80	30	0.73	0.24	0.10
2010	July	1	80	30	1.27	0.24	0.11
2010	July	2	80	30	0.70	0.23	0.11
2010	July	3	80	30	0.68	0.23	0.12
2010	July	4	80	30	0.76	0.23	0.11
2010	July	5	80	30	1.50	0.28	0.12
2010	July	6	80	30	0.87	0.23	0.12
2010	July	7	80	30	1.72	0.25	0.13

B.2 Size-Frequency Histograms - March, April, May, June, July

Presented are the size-frequency histograms of the population structure of *L. helicina* individuals processed for each day of sample collection, in Table B.1. The histograms are presented according to the month of observation and arranged column-wise. **Note** the missing samples on 16, 23 April, 21 May, and 28 June. For these dates, there is no histogram presented. The size-frequency histograms are binned into 0.02mm size-bins and the overall shape of the histogram, for each day, will depend on the number of size-frequency enumerations made. Consequently, the histograms for dates of low population abundance will show no definitive shape, whereas dates with high population abundances will. Finite mixture distributions were created and modified, to fit these histograms.

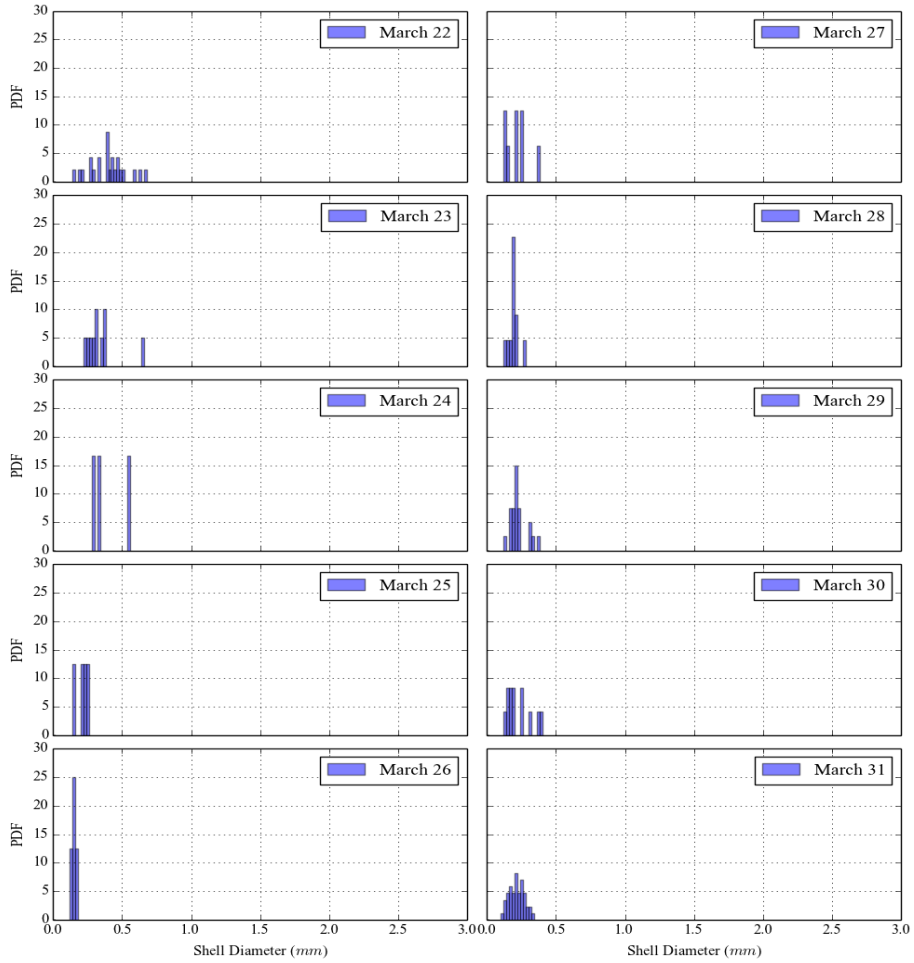

Figure B.1: Size-frequency histograms of the population size structure of *L. helicina* for samples collected from 22–31 March, 2010.

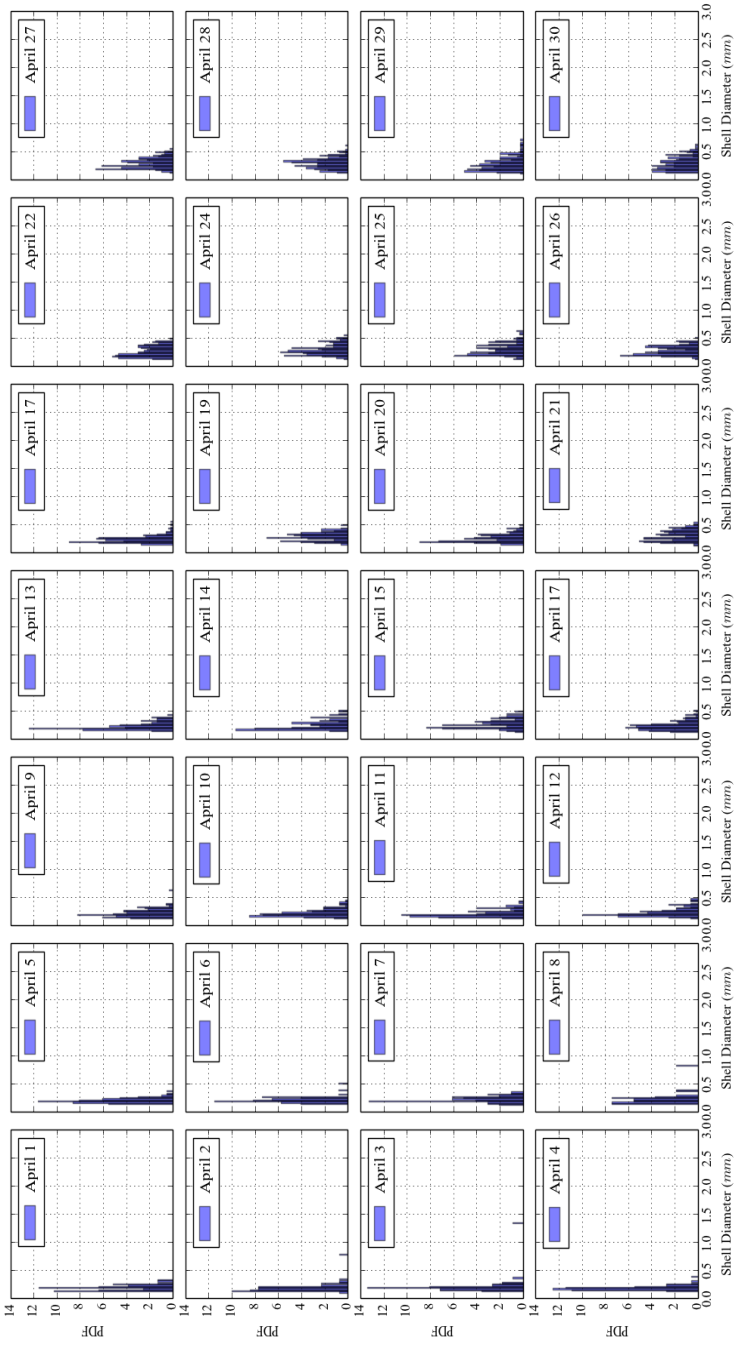

Figure B.2: Size-frequency histograms of the population size structure of *L. helicina* for samples collected from 1–15, 17–22, 24–30 Apri, 2010. **Note** the missing samples for 16, 23 April.

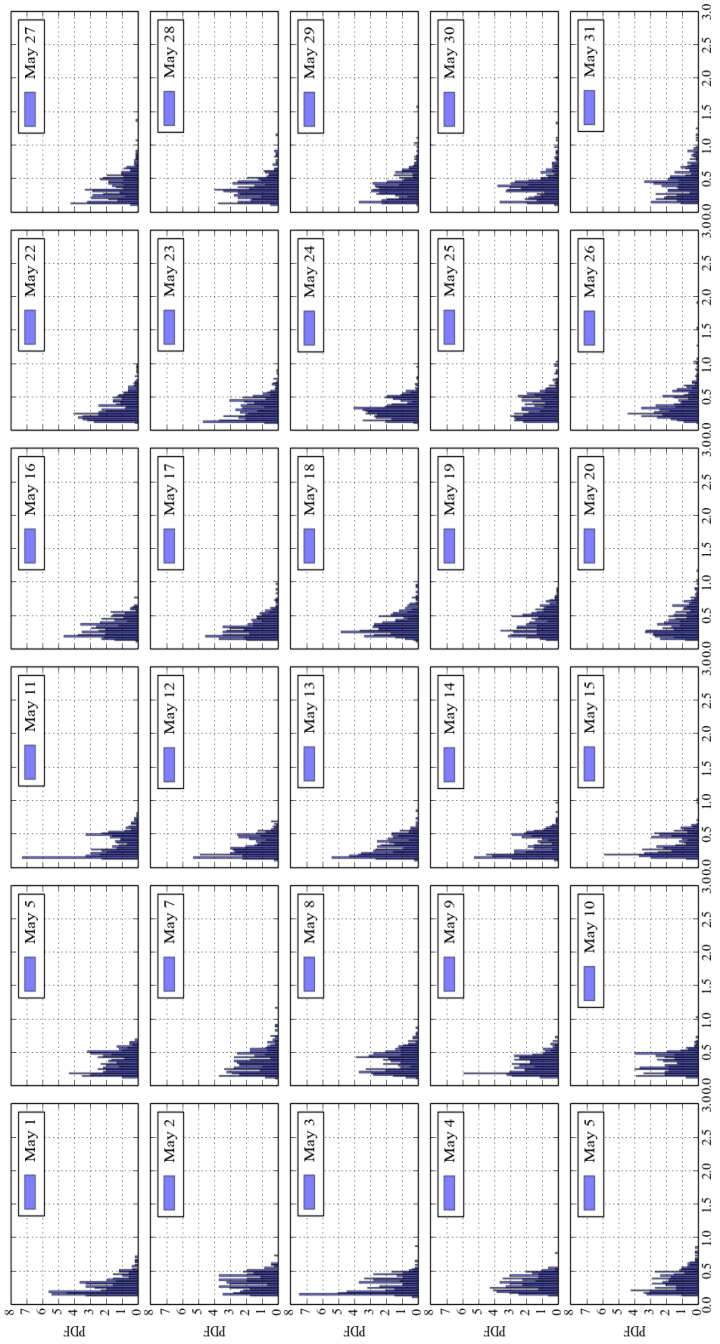

Figure B.3: Size-frequency histograms of the population size structure of *L. helicina* for samples collected from 1–20, 22–31 May, 2010. **Note** the missing sample for 21 May.

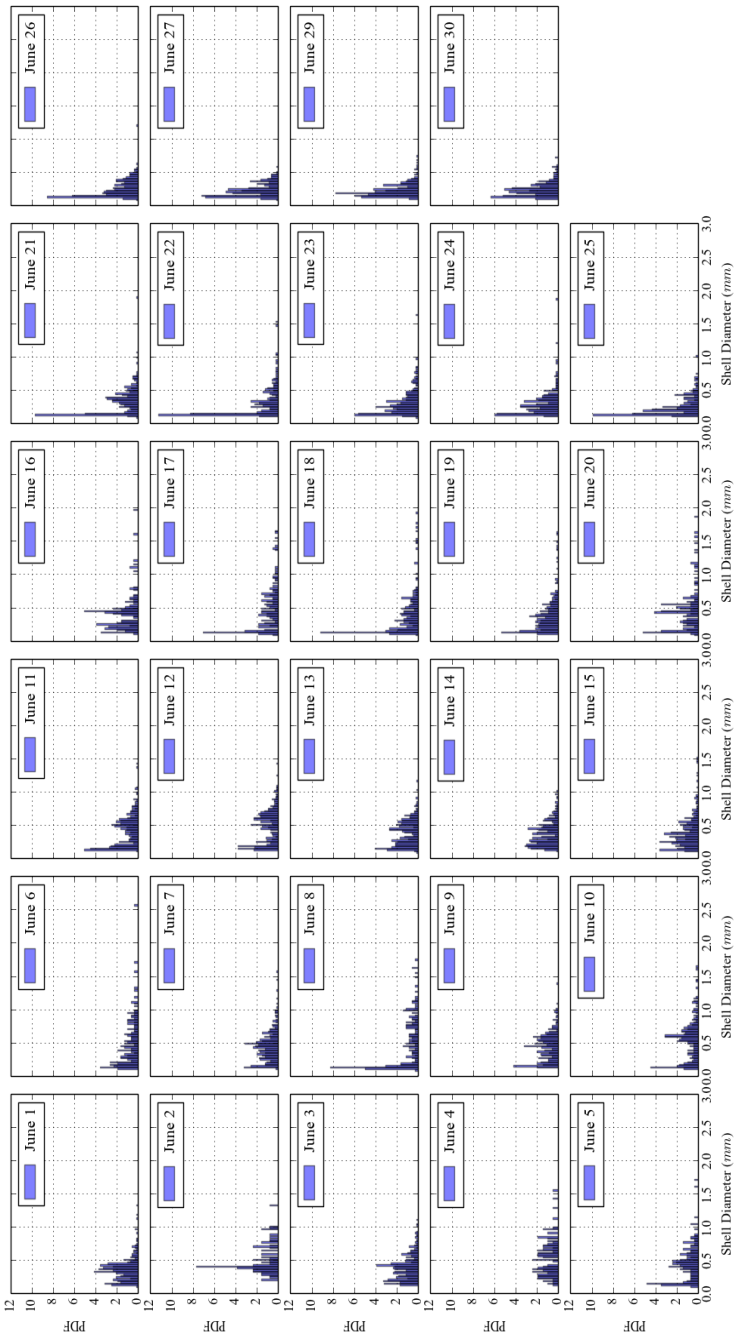

Figure B.4: Size-frequency histograms of the population size structure of *L. helicina* for samples collected from 1–27, 29–30 June, 2010. **Note** the missing sample for 28 June.

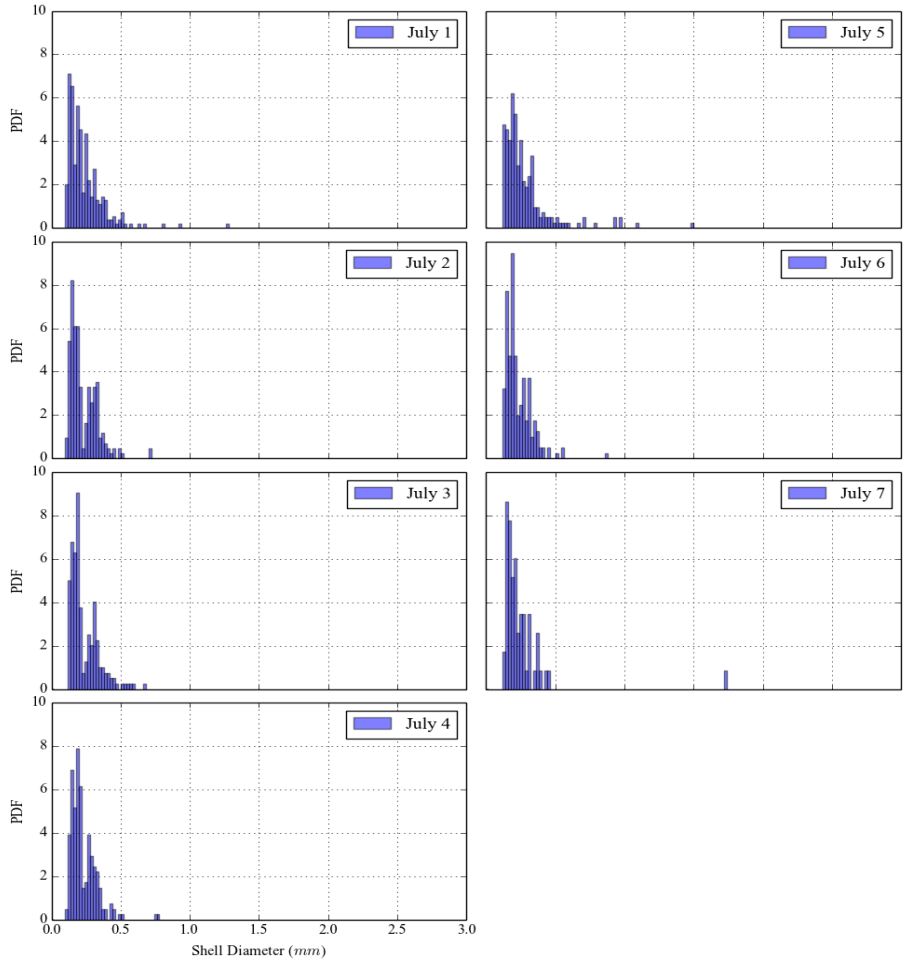

Figure B.5: Size-frequency histograms of the population size-structure of *L. helicina* for samples collected from 1–7 July, 2010.

B.3 Finite Mixture Distributions – Daily Data

B.4 What Are Finite Mixture Distributions

Finite mixture distributions were fitted onto the size frequency histograms (Appendix B.2) using the `mixdist` package (MacDonald and contributions from Juan Du, 2011) written for the `R` statistical programming environment (R Core Team, 2013). Utilizing maximum likelihood as well as the EM algorithm, `mixdist` fits finite mixture distributions onto grouped and/or conditional data. A "mixture distribution" results from a heterogeneous population of differ-

ent age-classes where the overall distribution is composed of a finite number of overlapping component distributions (normal, lognormal, gamma, exponential, Weibull, binomial, negative binomial, Poisson distributions), with each component possessing component parameters (mixing proportions, means and standard deviations of each component distribution) (MacDonald and contributions from Juan Du, 2011). The primary function `mix` finds sets of overlapping component distributions that gives the best fit to the grouped and conditional data. Each component possesses a different probability density, although the component densities do not necessarily have to belong to the same parametric family (Du, 2002). Despite this non-requirement, it appears that the current version of `mixdist` assumes all component densities belong to the same parametric family (MacDonald and contributions from Juan Du, 2011), although dialogue with Peter MacDonald disclosed future upgrades to the package (MacDonald, 2011).

B.5 Fitting Finite Mixtures

Fitting finite mixture distributions begins with parameter estimation for each components of the mixture model (Du, 2002). When the data is complete (no missing data), population components are easily identified and the proportional abundance is estimated by counting the number of observations for each component Du (2002). For incomplete data, entire components and/or various portions of component(s) are not observed, thus complicating the maximum likelihood estimates (Du, 2002). Given this issue, there are cases of over-parameterization (Du, 2002) if constraints are not implemented (MacDonald and Pitcher, 1979). Bearing in mind that census data is almost always incomplete, given the restrictions to sampling protocols, the estimation of all component parameters is often not possible, especially when components have high overlap (MacDonald and Pitcher, 1979; Du, 2002). Thus, to avoid this problem it is best to reduce the number of parameters estimated (Du, 2002). Although this may not be reasonable given the observed data, Du (2002); MacDonald and Pitcher (1979) assume constraints (fixed proportions, means, and standard deviations) in order to reduce the number of parameters estimated. Of course by assigning constraints, one introduces bias into the parameter estimates however, constraints may have to be assigned for incomplete data, with judgement of constraints based on the observed data (Du, 2002; MacDonald, 2011). Essentially, the passing of parameter constraints is based on the expert knowledge of the user (MacDonald, 2011).

Concerning the census data collected for *L. helicina*, the identification of likely components (or different age-classes) was based on the appearance of distinct modal peaks in the size-frequency histograms of the population size-structure. In cases when the size-frequency histograms lacked distinct modal peaks (daily data), the previous date of observation was used as a reference to judge the most likely course of development through time t. Since a comparatively high resolution time-series was used for both Chapter 2 and Chapter 3,

the appropriateness of applied constraints was validated over the entire time series.

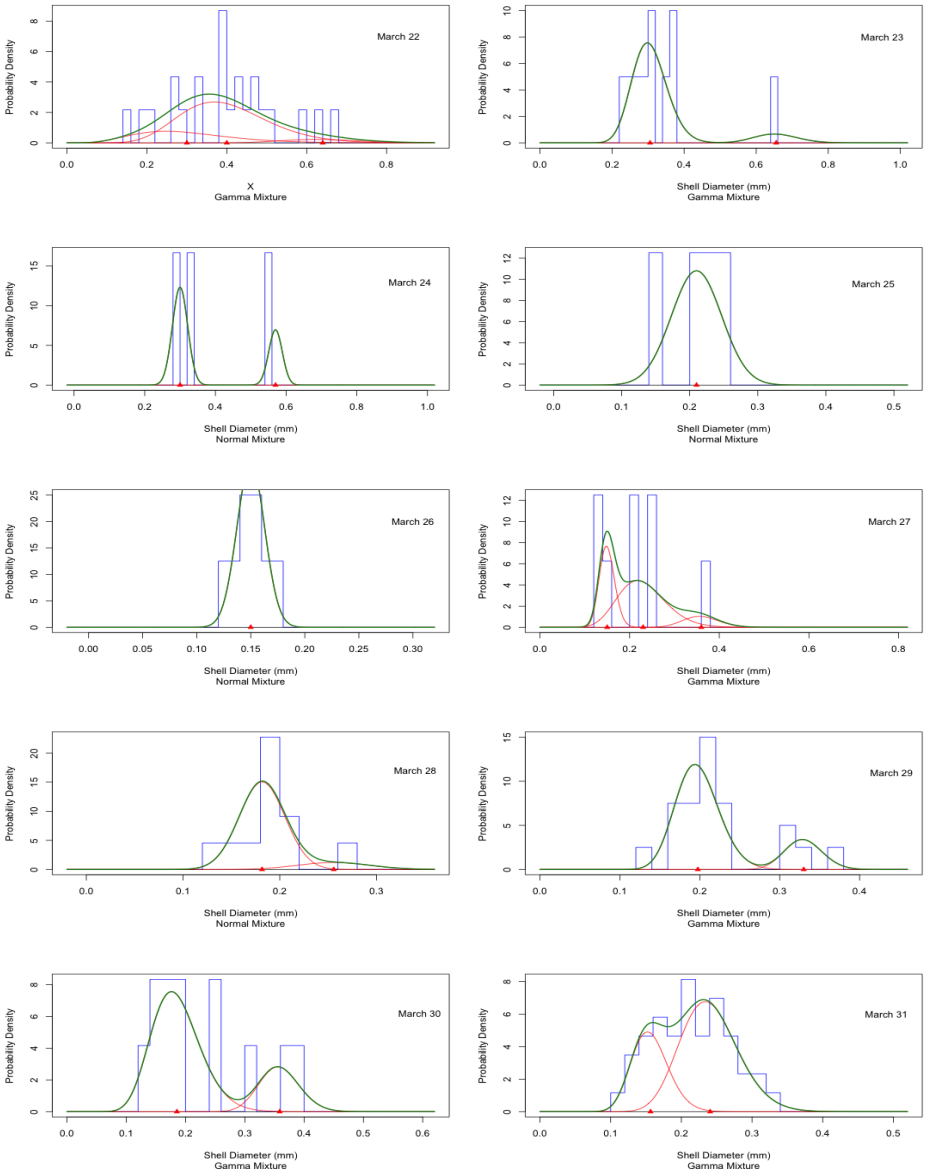

Figure B.6: Finite mixture distributions fitted to the size-frequency histograms from samples collected from 22–31 March, 2010.

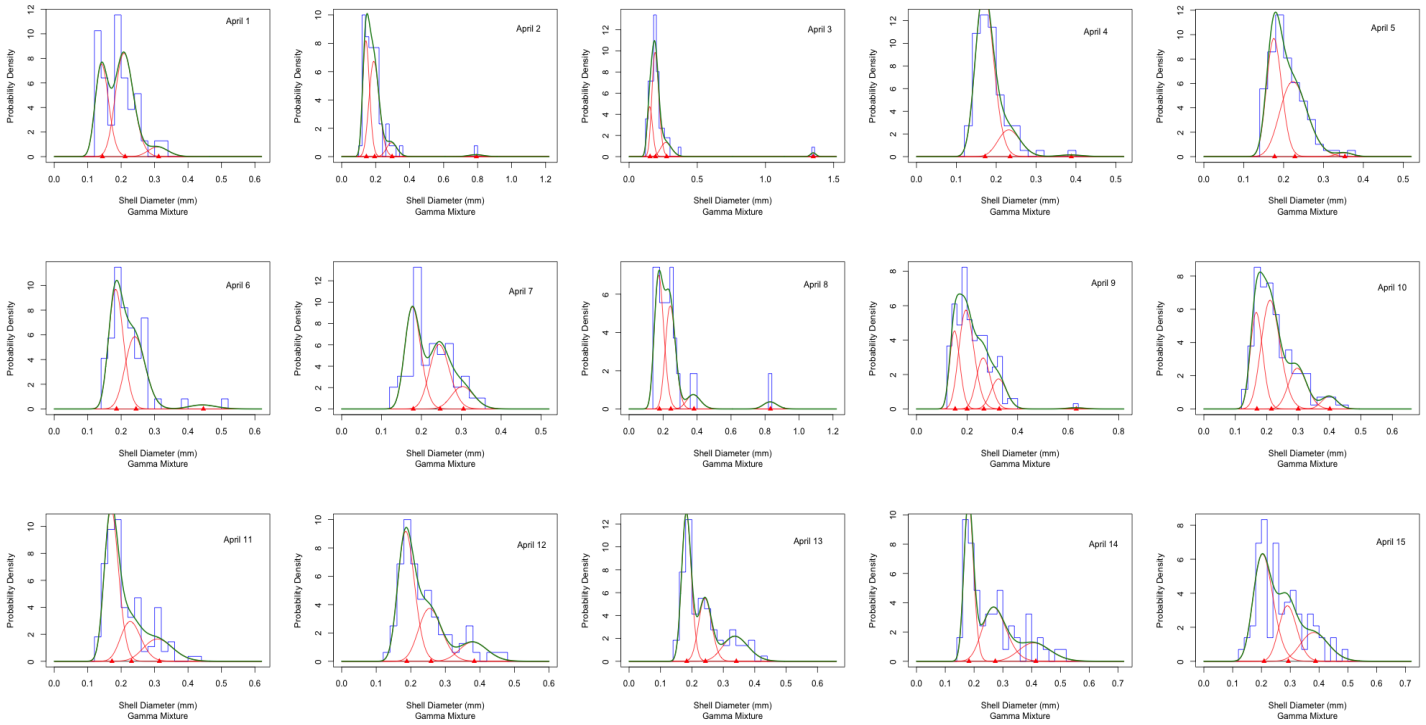

Figure B.7: Finite mixture distributions fitted to the size-frequency histograms of samples collected from 1–30 April, 2010. **Note** the two missing samples on 16 and 23 April.

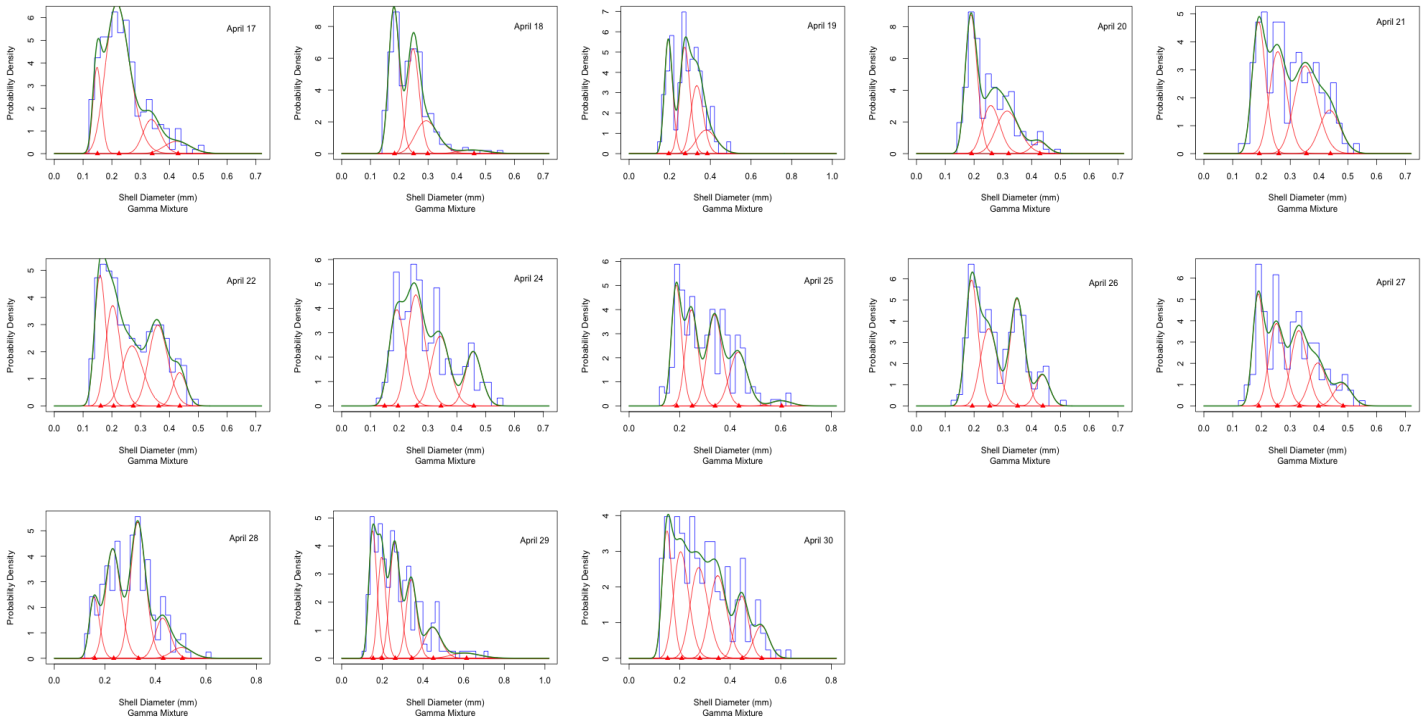

Figure B.8: Finite mixture distributions fitted to the size-frequency histograms of samples collected from 17–22 and 23–30 April, 2010. **Note** the missing samples on 16 and 23 April.

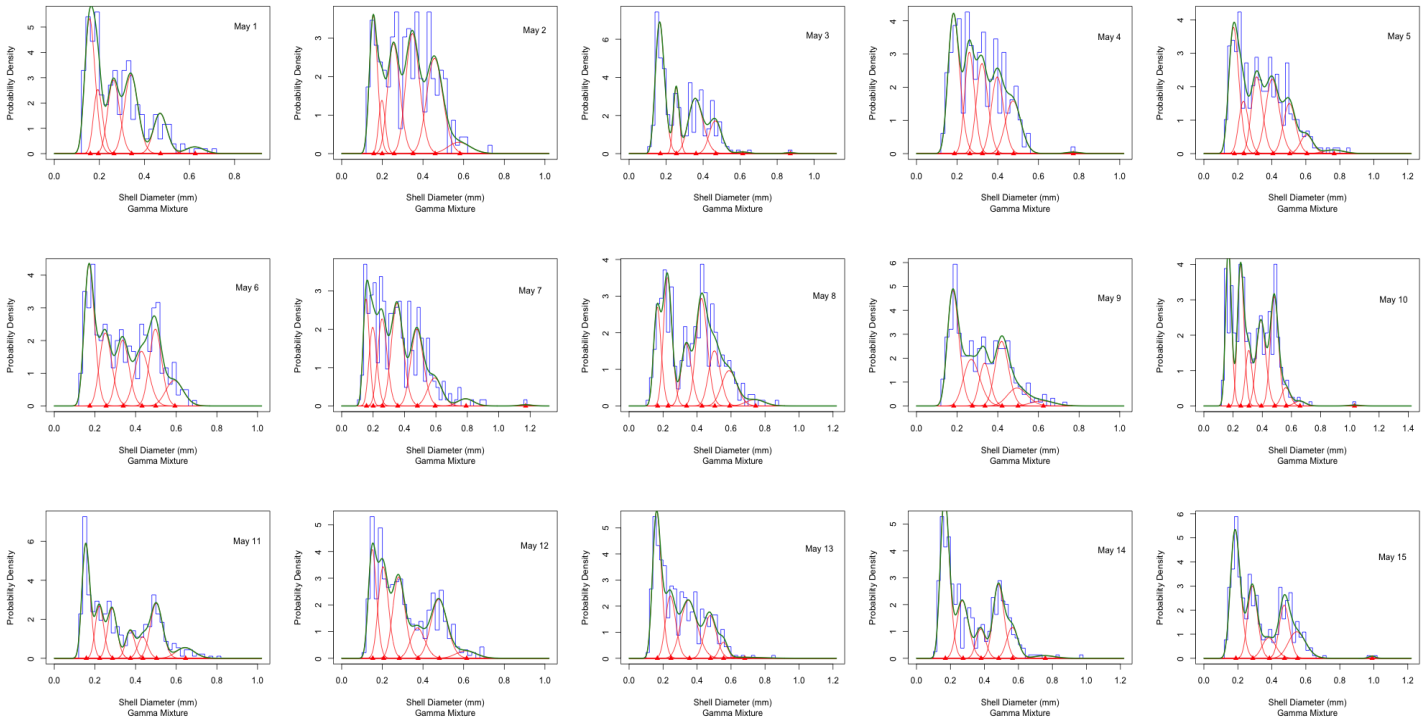

Figure B.9: Finite mixture distributions fitted to the size-frequency histograms of samples collected from 1–15 May, 2010.

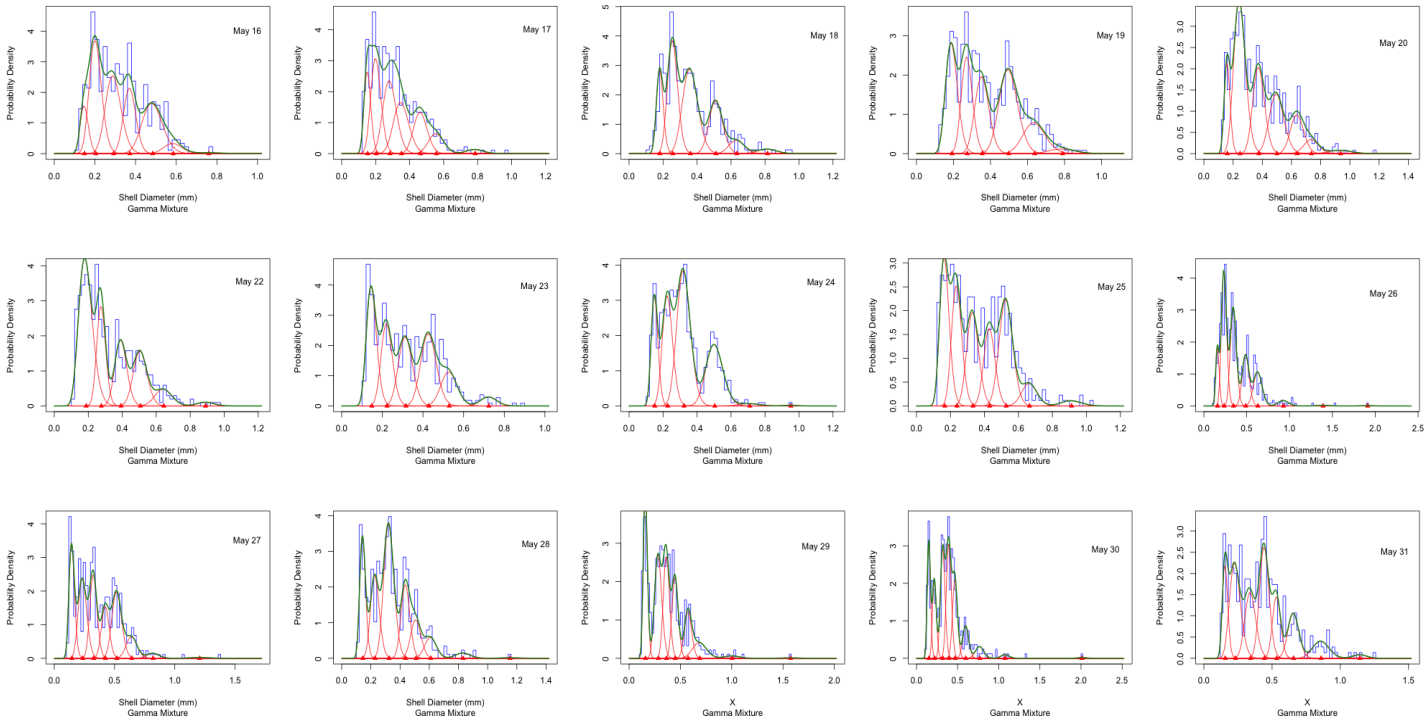

Figure B.10: Finite mixture distributions fitted to the size-frequency histograms of samples collected from 16–20, 22–31 May, 2010. **Note** the missing sample for 21 May.

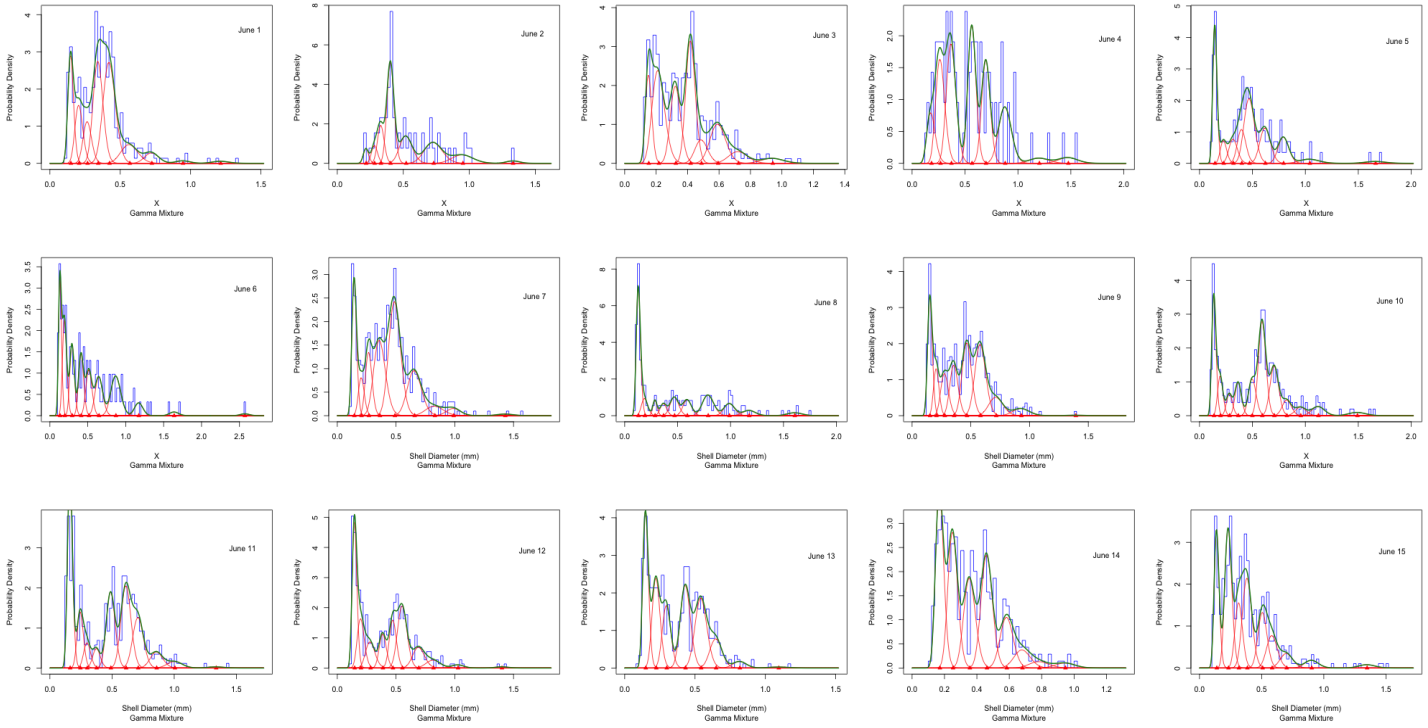

Figure B.11: Finite mixture distributions fitted to the size-frequency histograms of samples collected from 1–16 June, 2010.

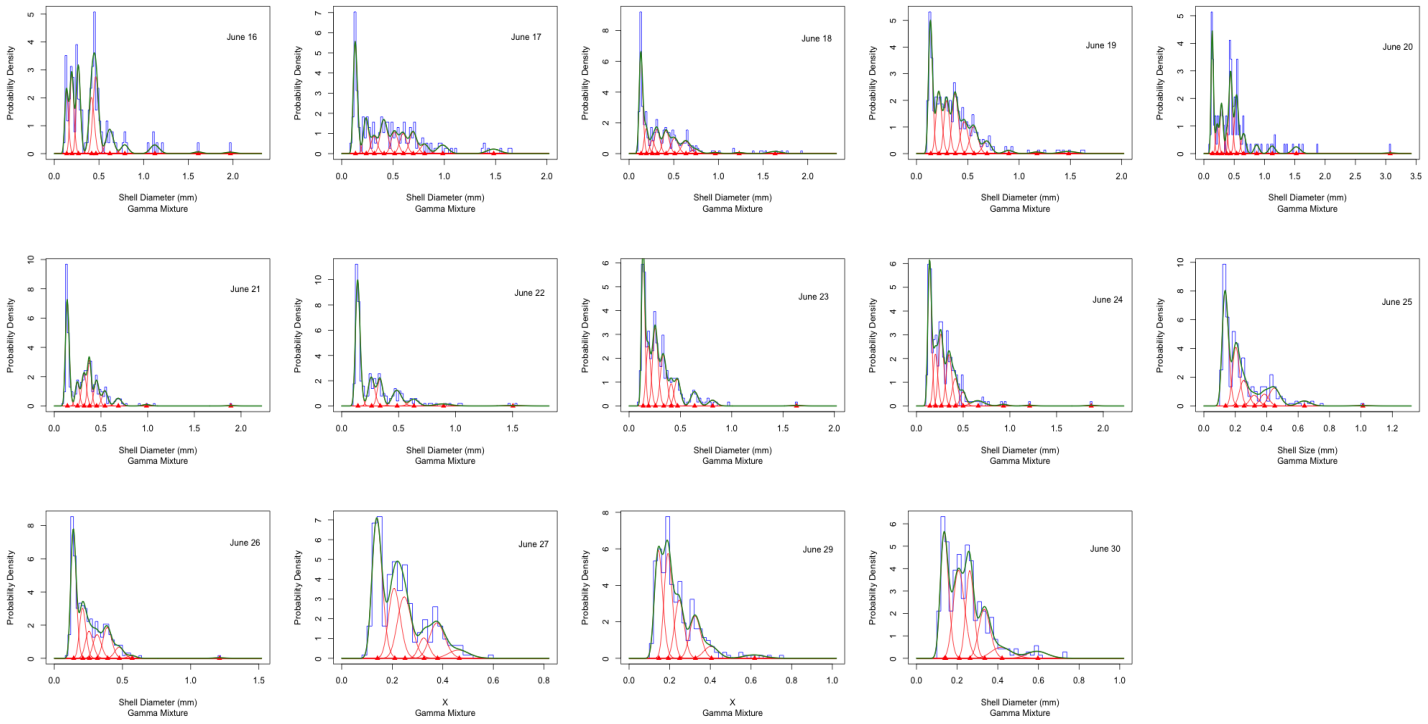

Figure B.12: Finite mixture distributions fitted to the size-frequency histograms of samples collected from 17–27, 29–30 June, 2010. **Note** the missing sample for 28 June.

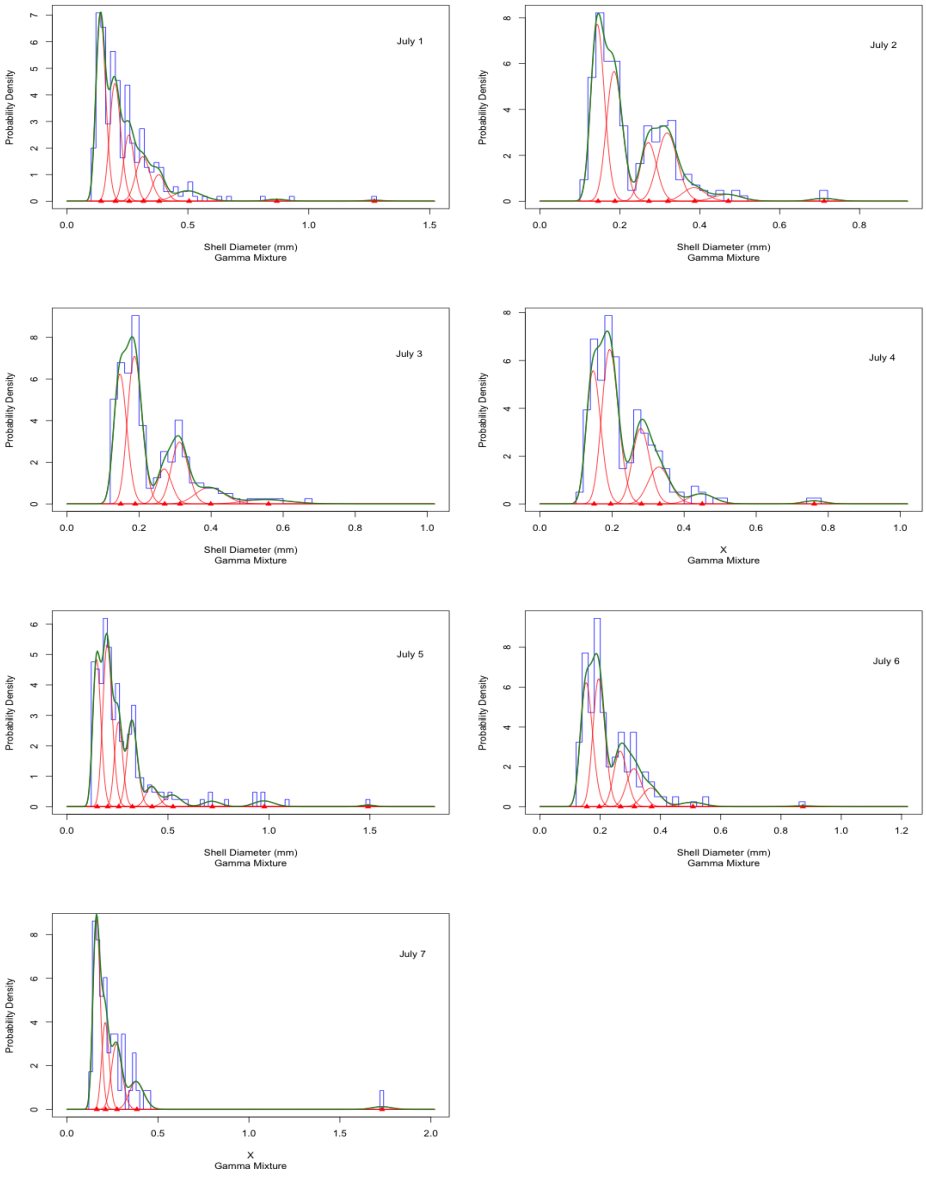

Figure B.13: Finite mixture distributions fitted to the size-frequency histograms of samples collected from 1–7 July, 2010.

B.6 Finite Mixture Distributions – Statistical Output

The statistical output of the finite mixture distributions fitted, are provided in the following table. Each finite mixture distribution contains the initial parameter estimates for each component within the overall distribution (propotion, mean and standard deviation) as well as the overall distribution (also the same for each component density), and any constraints applied to the mixture model. In the interest of space, only the ANOVA results and any constraints applied to the mixture model are presented in Table B.2.

For the majority of dates sampled, only the standard deviation was constrained with `SFX` (Specific Sigmas Fixed, Du, 2002). On certain occassions, the constraint `MFX` (Specific Means Fixed, Du, 2002) was implemented as there were so few size-frequency measurements made that the data was too "incomplete" for accurate parameter estimates (MacDonald, 2011). In these situations, a combination of both `MFX` and `SFX` was used, after considering biological relevance (Du, 2002).

Table B.2: The ANOVA statistial results, signifiance, and constraints applied to the finite mixture model fitted for each day of observation in the Dawsons Daily time-series. **DF** – degrees of freedom, χ^2 – the statistical result returned from the Maximum Likelihood Method, **con***pi* – component proportions constraints, **con**μ – component mean modal size constraints, **con**σ – component standard deviation constrains. **NONE** signifies no constraints, **MFX** – specific means constrained, **SFX** – specific sigmas constrained. **Note** the significance codes: '***' – 0, '**' – 0.001, '*' – 0.01, '.' – 0.05. **Note** the missing dates for 16, 23 April, 21 May, and 28 June, indicated by **NA**.

Month	**Day**	**ANOVA Table:**		**Signif.**	**Constraints:**		
		DF	χ^2	Pr($>\chi^2$)	**con-***pi*:	**con-**μ	**con-**σ
March	22	40	30.026	0.8745	NONE	MFX	SFX
March	23	35	11.321	1	NONE	NONE	SFX
March	24	15	6.1844	0.9765	NONE	MFX	NONE
March	25	14	5.272	0.9817	NONE	NONE	NONE
March	26	4	0.3486	0.9929	NONE	NONE	NONE
March	27	21	15.621	0.7906	NONE	MFX	SFX
March	28	9	7.6023	0.5747	NONE	NONE	SFX
March	29	11	12.601	0.3202	NONE	NONE	NONE
March	30	18	13.769	0.744	NONE	NONE	NONE
March	31	14	2.9729	0.9991	NONE	NONE	NONE
April	1	12	13.326	0.3458	NONE	NONE	SFX
April	2	26	16.344	0.9276	NONE	NONE	SFX
April	3	19	12.076	0.8824	NONE	NONE	SFX
April	4	14	8.4987	0.8618	NONE	NONE	SFX
April	5	8	6.1058	0.6354	NONE	NONE	NONE

Continued on next page

Table B.2 – continued from previous page

Month	**Day**	**ANOVA Table: DF**	χ^2	$\Pr(>\chi^2)$	**Signif.**	**Constraints:** **con-pi:**	**con-μ**	**con-σ**
April	6	18	19.539	0.3593		NONE	NONE	SFX
April	7	11	13.003	0.2932		NONe	NONE	SFX
April	8	32	11.236	0.9997		NONE	NONE	SFX
April	9	21	18.893	0.592		NONE	NONE	SFX
April	10	10	7.645	0.6635		NONE	NONE	SFX
April	11	14	26.171	0.02462	*	NONE	NONE	SFX
April	12	16	8.6914	0.9256		NONE	NONE	SFX
April	13	12	7.3204	0.8357		NONE	NONE	NONE
April	14	19	16.572	0.6188		NONE	NONE	NONE
April	15	18	20.721	0.2937		NONE	NONE	NONE
April	16	NA	NA	NA		NA	NA	NA
April	17	19	20.008	0.3941		NONE	MFX	NONE
April	18	17	12.766	0.7517		NONE	NONE	SFX
April	19	17	11.081	0.8523		NONE	NONE	SFX
April	20	12	17.474	0.1326		NONE	NONE	SFX
April	21	15	16.767	0.333		NONE	NONE	SFX
April	22	13	7.093	0.8681		NONE	NONE	SFX
April	23	NA	NA	NA		NA	NA	NA
April	24	15	21.645	0.1175		NONE	NONE	SFX
April	25	23	47.005	0.002238	**	NONE	NONE	SFX
April	26	11	16.824	0.1132		NONE	NONE	SFX
April	27	16	30.009	0.01796	*	NONE	NONE	SFX
April	28	20	27.138	0.1314		NONE	NONE	SFX
April	29	29	27.796	0.5289		NONE	NONE	SFX

Continued on next page

Table B.2 – continued from previous page

Month	**Day**	**ANOVA Table: DF**	χ^2	$\Pr(>\chi^2)$	**Signif.**	**Constraints:** **con-*pi*:**	**con-μ**	**con-σ**
April	30	17	36.043	0.004527	**	NONE	NONE	SFX
May	1	23	35.812	0.04311	*	NONE	NONE	SFX
May	2	24	423.776	0.0081	**	NONE	NONE	SFX
May	3	26	38.249	0.05742	.	NONE	NONE	SFX
May	4	27	30.313	0.3003		NONE	NONE	SFX
May	5	31	29.401	0.5483		NONE	NONE	SFX
May	6	22	25.023	0.296		NONE	NONE	SFX
May	7	42	67.996	0.006758	**	NONE	NONE	SFX
May	8	30	38.875	0.1286		NONE	NONE	SFX
May	9	21	25.35	0.2323		NONE	NONE	NONE
May	10	31	46.208	0.03877	*	NONE	NONE	SFX
May	11	24	52.986	0.000581	***	NONE	NONE	SFX
May	12	25	47.028	0.004866	**	NONE	NONE	SFX
May	13	36	52.796	0.03506	*	NONE	NONE	SFX
May	14	34	65.755	0.0008729	***	NONE	NONE	SFX
May	15	25	39.565	0.03231	*	NONE	NONE	SFX
May	16	31	61.193	0.0009742	***	NONE	NONE	SFX
May	17	31	56.748	0.003199	**	NONE	NONE	SFX
May	18	34	59.576	0.004301	**	NONE	NONE	SFX
May	19	35	63.031	0.002529	**	NONE	NONE	SFX
May	20	42	75.644	0.001115	**	NONE	NONE	SFX
May	21	NA	NA	NA	NA	NA	NA	NA
May	22	38	58.777	0.01685	*	NONE	NONE	SFX
May	23	29	91.153	2.42E-08	***	NONE	NONE	SFX

Continued on next page

Table B.2 – continued from previous page

Month	**Day**	**ANOVA Table: DF**	χ^2	$\Pr(>\chi^2)$	**Signif.**	**Constraints:** **con-*pi*:**	**con-μ**	**con-σ**
May	24	38	36.953	0.5177		NONE	NONE	SFX
May	25	40	64.854	0.007726	**	NONE	NONE	SFX
May	26	76	110.59	0.005896	**	NONE	NONE	SFX
May	27	54	84.783	0.004717	**	NONE	NONE	SFX
May	28	48	72.76	0.01207	*	NONE	NONE	SFX
May	29	64	72.776	0.2115		NONE	NONE	SFX
May	30	57	90.605	0.003064	**	NONE	NONE	SFX
May	31	46	76.275	0.003319	**	NONE	NONE	SFX
June	1	49	59.154	0.1518		NONE	NONE	SFX
June	2	53	38.706	0.9294		NONE	NONE	SFX
June	3	40	66.041	0.005907	**	NONE	NONE	SFX
June	4	71	63.833	0.7145		NONE	NONE	SFX
June	5	79	37.324	1		NONE	NONE	SFX
June	6	87	58.145	0.9926		NONE	NONE	SFX
June	7	62	81.507	0.04903	*	NONE	NONE	SFX
June	8	70	69.361	0.4991		NONE	NONE	SFX
June	9	59	81.794	0.02643	*	NONE	NONE	SFX
June	10	64	57.755	0.6955		NONE	NONE	SFX
June	11	53	88.465	0.001615	**	NONE	NONE	SFX
June	12	56	59.808	0.3392		NONE	NONE	SFX
June	13	46	54.472	0.1833		NONE	NONE	SFX
June	14	38	58.126	0.01935	*	NONE	NONE	SFX
June	15	58	98.97	0.0006467	***	NONE	NONE	SFX
June	16	80	45.058	0.9994		NONE	NONE	SFX

Continued on next page

Table B.2 – continued from previous page

Month	**Day**	**ANOVA Table: DF**	χ^2	$\Pr(>\chi^2)$	**Signif.**	**Constraints:** **con-pi:**	**con-μ**	**con-σ**
June	17	60	73.784	0.1088		NONE	NONE	SFX
June	18	70	97.68	0.01611	*	NONE	NONE	SFX
June	19	65	53.94	0.8344		NONE	NONE	SFX
June	20	97	103.49	0.3073		NONE	NONE	SFX
June	21	49	53.5	0.3056		NONE	NONE	SFX
June	22	66	62.327	0.6055		NONE	NONE	SFX
June	23	41	34.881	0.7383		NONE	NONE	SFX
June	24	62	43.058	0.968		NONE	NONE	SFX
June	25	37	62.632	0.005307	**	NONE	NONE	SFX
June	26	28	20.164	0.8584		NONE	NONE	SFX
June	27	17	30.885	0.02062	*	NONE	NONE	SFX
June	28	NA	NA	NA	NA	NA	NA	NA
June	29	26	36.826	0.07749	.	NONE	NONE	SFX
June	30	23	42.703	0.007509	**	NONE	NONE	SFX
July	1	49	59.154	0.1518		NONE	NONE	SFX
July	2	53	38.706	0.9294		NONE	NONE	SFX
July	3	40	66.041	0.005907	**	NONE	NONE	SFX
July	4	71	63.833	0.7145		NONE	NONE	SFX
July	5	79	37.324	1		NONE	NONE	SFX
July	6	87	58.145	0.9926		NONE	NONE	SFX
July	7	62	81.507	0.04903	*	NONE	NONE	SFX

B.7 Life Tables for Cohorts Tracked

From the finite mixture distributions fitted (Appendix B.3), numerous population components were identified and tracked, from their likely date of recruitment into the population to the last date that they were observed within the size-frequency histograms and subsequently assumed to have either died off of possibly merged together with another component. Each component is identified with the "c" prefixed to the abbreviated date of the most likely date the component was recruited into the population. For example "cApr01" signifies the component that was likely recruited into the population on 1 April.

Because it was most probable that many components were possibly merging together to grow as a single component for variable lengths of time only to separate at a later time, the daily changes in shell size and abundance for the larger size fractions were very unrealistic. Due to this, only the 0–0.5 mm size-fraction was considered as the daily rates of shell-size growth was fairly consistent with the results from Chapter 2.

Table B.3: The seasonal development of the modal shell size (mm) for every recruit cohort tracked. Also included is the daily variation in abundance (Ind.m^{-3}) of component as well as its daily estimate of its growth (mm) in shell size. **Note** that the dates of observation in the **Dates** column is expressed as "mm/dd/yy", and **Size (mm)** refers to the modal shell size for each component tracked. **NA** in the **Growth** column signifies either no observations, or times of no perceived growth in shell size. **NA** in the **Size** and **Abundance** columns signifies no observations for those dates.

Cohort	**Size Fraction**	**Date**	**Size (mm)**	**Abundance (Ind.m^{-3})**	**Growth (mm.day^{-1})**
cApr01	0 to 0.5mm	04/01/10	0.1441	6.8984	NA
cApr01	0 to 0.5mm	04/02/10	0.1937	15.352	0.0496
cApr01	0 to 0.5mm	04/03/10	0.1943	16.1977	6.00E-04
cApr01	0 to 0.5mm	04/04/10	0.2348	7.147	0.0405
cApr01	0 to 0.5mm	04/05/10	0.2283	24.5423	NA
cApr01	0 to 0.5mm	04/06/10	0.2445	12.5892	0.0162
cApr01	0 to 0.5mm	04/07/10	0.247	8.7086	0.0025
cApr01	0 to 0.5mm	04/08/10	0.2456	5.1246	NA
cApr01	0 to 0.5mm	04/09/10	0.2667	16.0081	0.0211
cApr01	0 to 0.5mm	04/10/10	0.3003	17.9858	0.0336
cApr01	0 to 0.5mm	04/11/10	0.3144	11.6811	0.0141
cApr01	0 to 0.5mm	04/12/10	0.3837	5.123	0.0693
cApr01	0 to 0.5mm	04/13/10	0.3414	11.2259	NA
cApr01	0 to 0.5mm	04/14/10	0.4146	4.9498	0.0732
cApr01	0 to 0.5mm	04/15/10	0.3878	6.9603	NA

Continued on next page

Table B.3 – continued from previous page

Cohort	Size Fraction	Date	Size (mm)	Abundance (Ind.m^{-3})	Growth (mm.day^{-1})
cApr01	0 to 0.5mm	04/16/10	NA	NA	NA
cApr01	0 to 0.5mm	04/17/10	0.43	7.7563	0.0211
cApr01	0 to 0.5mm	04/18/10	0.4599	3.4479	0.0299
cApr01	0 to 0.5mm	04/19/10	0.385	5.6777	NA
cApr01	0 to 0.5mm	04/20/10	0.4287	4.2813	0.0437
cApr01	0 to 0.5mm	04/21/10	0.4396	9.1887	0.0109
cApr01	0 to 0.5mm	04/22/10	0.4363	6.7107	NA
cApr01	0 to 0.5mm	04/23/10	NA	NA	NA
cApr01	0 to 0.5mm	04/24/10	0.4588	11.3875	NA
cApr02	0 to 0.5mm	04/02/10	0.1453	4.4537	NA
cApr02	0 to 0.5mm	04/03/10	0.1538	6.2291	0.0085
cApr02	0 to 0.5mm	04/04/10	0.1722	35.7462	0.0184
cApr02	0 to 0.5mm	04/05/10	0.1775	21.412	0.0053
cApr02	0 to 0.5mm	04/06/10	0.1861	15.2353	0.0086
cApr02	0 to 0.5mm	04/07/10	0.1796	11.0007	NA
cApr02	0 to 0.5mm	04/08/10	0.1788	6.1829	NA
cApr02	0 to 0.5mm	04/09/10	0.2003	33.0411	0.0215
cApr02	0 to 0.5mm	04/10/10	0.215	48.5465	0.0147
cApr02	0 to 0.5mm	04/11/10	0.231	14.3427	0.016
cApr02	0 to 0.5mm	04/12/10	0.2587	11.7324	0.0277
cApr02	0 to 0.5mm	04/13/10	0.2431	14.6235	NA
cApr02	0 to 0.5mm	04/14/10	0.2736	11.0428	0.0305
cApr02	0 to 0.5mm	04/15/10	0.2934	8.6546	0.0198
cApr02	0 to 0.5mm	04/16/10	NA	NA	NA
cApr02	0 to 0.5mm	04/17/10	0.34	14.6416	0.0233

Continued on next page

Table B.3 – continued from previous page

Cohort	Size Fraction	Date	Size (mm)	Abundance (Ind.m^{-3})	Growth (mm.day^{-1})
cApr02	0 to 0.5mm	04/18/10	0.2987	24.2295	NA
cApr02	0 to 0.5mm	04/19/10	0.3359	10.1752	0.0372
cApr02	0 to 0.5mm	04/20/10	0.3199	22.573	NA
cApr02	0 to 0.5mm	04/21/10	0.3562	20.3883	0.0363
cApr02	0 to 0.5mm	04/22/10	0.3628	23.2981	0.0066
cApr02	0 to 0.5mm	04/23/10	NA	NA	NA
cApr02	0 to 0.5mm	04/24/10	0.3449	16.6977	NA
cApr02	0 to 0.5mm	04/25/10	0.4343	17.2336	0.0894
cApr02	0 to 0.5mm	04/26/10	0.439	7.7459	0.0047
cApr02	0 to 0.5mm	04/27/10	0.398	14.4788	NA
cApr02	0 to 0.5mm	04/28/10	0.4307	18.3966	0.0327
cApr02	0 to 0.5mm	04/29/10	0.4507	27.619	0.02
cApr02	0 to 0.5mm	04/30/10	0.4474	26.6309	NA
cApr02	0 to 0.5mm	05/01/10	0.4715	44.7813	0.0241
cApr02	0 to 0.5mm	05/02/10	0.4599	29.6462	NA
cApr02	0 to 0.5mm	05/03/10	0.468	49.373	0.0081
cApr02	0 to 0.5mm	05/04/10	0.4777	55.3083	0.0097
cApr02	0 to 0.5mm	05/05/10	NA	NA	NA
cApr02	0 to 0.5mm	05/06/10	0.4992	64.7789	0.0107
cApr09	0 to 0.5mm	04/09/10	0.153	17.4426	NA
cApr09	0 to 0.5mm	04/10/10	0.1689	28.2732	0.0159
cApr09	0 to 0.5mm	04/11/10	0.1726	39.0586	0.0037
cApr09	0 to 0.5mm	04/12/10	0.1885	20.8694	0.0159
cApr09	0 to 0.5mm	04/13/10	0.1835	25.5514	NA
cApr09	0 to 0.5mm	04/14/10	0.1823	13.2443	NA

Continued on next page

Table B.3 – continued from previous page

Cohort	Size Fraction	Date	Size (mm)	Abundance (Ind.m^{-3})	Growth (mm.day^{-1})
cApr09	0 to 0.5mm	04/15/10	0.2091	18.338	0.0268
cApr09	0 to 0.5mm	04/16/10	NA	NA	NA
cApr09	0 to 0.5mm	04/17/10	0.225	87.868	0.0079
cApr09	0 to 0.5mm	04/18/10	0.2497	40.7468	0.0247
cApr09	0 to 0.5mm	04/19/10	0.2762	13.2736	0.0265
cApr09	0 to 0.5mm	04/20/10	0.2616	19.1604	NA
cApr09	0 to 0.5mm	04/21/10	0.2691	17.3462	NA
cApr09	0 to 0.5mm	04/22/10	0.2746	19.3442	0.0145
cApr09	0 to 0.5mm	04/23/10	NA	NA	NA
cApr09	0 to 0.5mm	04/24/10	0.261	24.8679	NA
cApr09	0 to 0.5mm	04/25/10	0.3403	25.0483	0.0793
cApr09	0 to 0.5mm	04/26/10	0.3511	27.7882	0.0108
cApr09	0 to 0.5mm	04/27/10	0.332	23.6773	NA
cApr09	0 to 0.5mm	04/28/10	0.3331	62.3996	0.0011
cApr17	0 to 0.5mm	04/17/10	0.15	17.897	NA
cApr17	0 to 0.5mm	04/18/10	0.1836	53.2406	0.0336
cApr17	0 to 0.5mm	04/19/10	0.1952	11.4283	0.0116
cApr17	0 to 0.5mm	04/20/10	0.1914	38.396	NA
cApr17	0 to 0.5mm	04/21/10	0.1927	17.7527	0.0013
cApr17	0 to 0.5mm	04/22/10	0.2062	22.701	0.0135
cApr17	0 to 0.5mm	04/23/10	NA	NA	NA
cApr17	0 to 0.5mm	04/24/10	0.1956	20.048	NA
cApr17	0 to 0.5mm	04/25/10	0.2492	21.9258	0.0536
cApr17	0 to 0.5mm	04/26/10	0.2542	24.0219	0.005
cApr17	0 to 0.5mm	04/27/10	0.2551	24.9448	9.00E-04

Continued on next page

Table B.3 – continued from previous page

Cohort	Size Fraction	Date	Size (mm)	Abundance (Ind.m^{-3})	Growth (mm.day^{-1})
cApr17	0 to 0.5mm	04/28/10	0.3331	62.3996	0.078
cApr17	0 to 0.5mm	04/29/10	0.3443	45.7486	0.0112
cApr17	0 to 0.5mm	04/30/10	0.3538	46.1697	0.0095
cApr17	0 to 0.5mm	05/01/10	0.3431	87.4172	NA
cApr17	0 to 0.5mm	05/02/10	0.3512	31.6764	0.0081
cApr17	0 to 0.5mm	05/03/10	0.3616	95.8574	0.0104
cApr17	0 to 0.5mm	05/04/10	0.3996	63.5719	0.0484
cApr17	0 to 0.5mm	05/05/10	0.406	148.979	0.0064
cApr17	0 to 0.5mm	05/06/10	0.4318	79.0986	0.0258
cApr17	0 to 0.5mm	05/07/10	0.4821	193.8972	0.0503
cApr22	0 to 0.5mm	04/22/10	0.1614	22.7294	NA
cApr22	0 to 0.5mm	04/23/10	NA	NA	NA
cApr22	0 to 0.5mm	04/24/10	0.1491	0.0973	NA
cApr22	0 to 0.5mm	04/25/10	0.1887	22.0466	0.0396
cApr22	0 to 0.5mm	04/26/10	0.1938	28.6268	0.0041
cApr22	0 to 0.5mm	04/27/10	0.1909	25.1008	NA
cApr22	0 to 0.5mm	04/28/10	0.2352	49.9609	0.0414
cApr22	0 to 0.5mm	04/29/10	0.2637	67.158	0.0285
cApr22	0 to 0.5mm	04/30/10	0.2798	52.0172	0.0161
cApr22	0 to 0.5mm	05/01/10	0.265	70.6579	NA
cApr22	0 to 0.5mm	05/02/10	0.2583	25.5809	NA
cApr22	0 to 0.5mm	05/03/10	0.2557	45.8706	NA
cApr22	0 to 0.5mm	05/04/10	0.2628	67.3435	0.0071
cApr22	0 to 0.5mm	05/05/10	0.2364	75.547	NA
cApr22	0 to 0.5mm	05/06/10	0.2547	87.6874	0.0183

Continued on next page

Table B.3 – continued from previous page

Cohort	Size Fraction	Date	Size (mm)	Abundance (Ind.m^{-3})	Growth (mm.day^{-1})
cApr22	0 to 0.5mm	05/07/10	0.2612	164.6008	0.0065
cApr22	0 to 0.5mm	05/08/10	0.3385	58.2074	0.0773
cApr22	0 to 0.5mm	05/09/10	0.3374	144.2505	NA
cApr22	0 to 0.5mm	05/10/10	0.3933	167.3239	0.0559
cApr22	0 to 0.5mm	05/11/10	0.436	120.6809	0.0427
cApr22	0 to 0.5mm	05/12/10	0.4809	225.2285	0.0876
cApr28	0 to 0.5mm	04/28/10	0.1602	18.6459	NA
cApr28	0 to 0.5mm	04/29/10	0.1987	45.1226	0.0385
cApr28	0 to 0.5mm	04/30/10	0.2084	52.2286	0.0097
cApr28	0 to 0.5mm	05/01/10	0.1954	47.3499	NA
cApr28	0 to 0.5mm	05/02/10	0.199	6.6321	0.0036
cApr28	0 to 0.5mm	05/03/10	0.2557	45.8706	0.0567
cApr28	0 to 0.5mm	05/04/10	0.2628	67.3435	0.0071
cApr28	0 to 0.5mm	05/05/10	0.3141	122.7697	0.0513
cApr28	0 to 0.5mm	05/06/10	0.3393	79.3091	0.0252
cApr28	0 to 0.5mm	05/07/10	0.3565	245.8426	0.0172
cApr28	0 to 0.5mm	05/08/10	0.429	110.8607	0.0725
cApr28	0 to 0.5mm	05/09/10	0.4211	269.7289	NA
cApr28	0 to 0.5mm	05/10/10	0.4842	186.4933	NA
cApr28	0 to 0.5mm	05/11/10	NA	NA	NA
cApr28	0 to 0.5mm	05/12/10	0.4809	225.2285	NA
cApr29	0 to 0.5mm	04/29/10	0.1549	56.6661	NA
cApr29	0 to 0.5mm	04/30/10	0.1525	41.7312	NA
cApr29	0 to 0.5mm	05/01/10	0.1602	114.2373	0.0077
cApr29	0 to 0.5mm	05/02/10	0.1581	21.4198	NA

Continued on next page

Table B.3 – continued from previous page

Cohort	Size Fraction	Date	Size (mm)	Abundance (Ind.m^{-3})	Growth (mm.day^{-1})
cApr29	0 to 0.5mm	05/03/10	0.1688	143.9464	0.0107
cApr29	0 to 0.5mm	05/04/10	0.1866	109.9226	0.0178
cApr29	0 to 0.5mm	05/05/10	0.1795	186.6858	NA
cApr29	0 to 0.5mm	05/06/10	0.175	143.0933	NA
cApr29	0 to 0.5mm	05/07/10	0.2009	123.8884	0.0259
cApr29	0 to 0.5mm	05/08/10	0.229	100.1688	0.0281
cApr29	0 to 0.5mm	05/09/10	0.2751	233.9228	0.0461
cApr29	0 to 0.5mm	05/10/10	0.3089	77.6639	0.0338
cApr29	0 to 0.5mm	05/11/10	0.3745	143.5213	0.0656
cApr29	0 to 0.5mm	05/12/10	0.3761	101.2723	0.0016
cApr29	0 to 0.5mm	05/13/10	0.4793	132.1383	0.1032
cApr29	0 to 0.5mm	05/14/10	0.4841	96.305	0.0048
cApr29	0 to 0.5mm	05/15/10	0.4744	142.0013	NA
cApr29	0 to 0.5mm	05/16/10	0.484	220.9958	0.0096
cApr29	0 to 0.5mm	05/17/10	0.4642	131.2378	NA
cMay07	0 to 0.5mm	05/07/10	0.1581	134.8172	NA
cMay07	0 to 0.5mm	05/08/10	0.1683	67.6996	0.0102
cMay07	0 to 0.5mm	05/09/10	0.1832	412.1687	0.0149
cMay07	0 to 0.5mm	05/10/10	0.2533	189.1069	0.0701
cMay07	0 to 0.5mm	05/11/10	0.2864	269.6928	0.0331
cMay07	0 to 0.5mm	05/12/10	0.2833	231.948	NA
cMay07	0 to 0.5mm	05/13/10	0.3557	246.3021	0.0724
cMay07	0 to 0.5mm	05/14/10	0.3802	33.3594	0.0245
cMay07	0 to 0.5mm	05/15/10	0.3858	73.2094	0.0056
cMay07	0 to 0.5mm	05/16/10	0.3719	171.9983	NA

Continued on next page

Table B.3 – continued from previous page

Cohort	Size Fraction	Date	Size (mm)	Abundance (Ind.m^{-3})	Growth (mm.day^{-1})
cMay07	0 to 0.5mm	05/17/10	0.3521	182.5217	NA
cMay07	0 to 0.5mm	05/18/10	0.3618	1009.6116	0.0097
cMay07	0 to 0.5mm	05/19/10	0.3552	457.0698	NA
cMay07	0 to 0.5mm	05/20/10	0.377	888.7034	0.0218
cMay07	0 to 0.5mm	05/21/10	NA	NA	NA
cMay07	0 to 0.5mm	05/22/10	0.3927	53.9599	0.0078
cMay07	0 to 0.5mm	05/23/10	0.4289	235.6525	0.0362
cMay10	0 to 0.5mm	05/10/10	0.1703	192.8726	NA
cMay10	0 to 0.5mm	05/11/10	0.2236	257.1379	0.0533
cMay10	0 to 0.5mm	05/12/10	0.2069	217.5518	NA
cMay10	0 to 0.5mm	05/13/10	0.2464	164.7412	0.0395
cMay10	0 to 0.5mm	05/14/10	0.2746	81.4858	0.0282
cMay10	0 to 0.5mm	05/15/10	0.288	186.5169	0.0134
cMay10	0 to 0.5mm	05/16/10	0.2921	260.7507	0.0044
cMay10	0 to 0.5mm	05/17/10	0.2846	230.6837	NA
cMay10	0 to 0.5mm	05/18/10	0.3618	1009.6116	0.0772
cMay10	0 to 0.5mm	05/19/10	0.3552	457.0698	NA
cMay10	0 to 0.5mm	05/20/10	0.377	888.7034	0.0218
cMay10	0 to 0.5mm	05/21/10	NA	NA	NA
cMay10	0 to 0.5mm	05/22/10	0.3927	218.0299	0.0078
cMay10	0 to 0.5mm	05/23/10	0.4289	235.6525	0.0362
cMay11	0 to 0.5mm	05/11/10	0.1576	537.9561	NA
cMay11	0 to 0.5mm	05/12/10	0.1531	206.6579	NA
cMay11	0 to 0.5mm	05/13/10	0.1665	335.2995	0.0134
cMay11	0 to 0.5mm	05/14/10	0.17	176.7625	0.0035

Continued on next page

Table B.3 – continued from previous page

Cohort	Size Fraction	Date	Size (mm)	Abundance (Ind.m^{-3})	Growth (mm.day^{-1})
cMay11	0 to 0.5mm	05/15/10	0.1884	336.9296	0.0184
cMay11	0 to 0.5mm	05/16/10	0.2042	296.2878	0.0158
cMay11	0 to 0.5mm	05/17/10	0.2031	225.7144	NA
cMay11	0 to 0.5mm	05/18/10	0.2576	898.8277	0.0545
cMay11	0 to 0.5mm	05/19/10	0.2739	454.4722	0.0163
cMay11	0 to 0.5mm	05/20/10	0.2477	1572.5983	NA
cMay11	0 to 0.5mm	05/21/10	NA	NA	NA
cMay11	0 to 0.5mm	05/22/10	0.277	244.9266	0.0146
cMay11	0 to 0.5mm	05/23/10	0.3158	206.4234	0.0388
cMay11	0 to 0.5mm	05/24/10	0.3231	469.2192	0.0073
cMay11	0 to 0.5mm	05/25/10	0.3324	128.604	0.0093
cMay11	0 to 0.5mm	05/26/10	0.3467	274.956	0.0143
cMay11	0 to 0.5mm	05/27/10	0.4241	82.371	0.0774
cMay11	0 to 0.5mm	05/28/10	0.4376	144.2691	0.0135
cMay11	0 to 0.5mm	05/29/10	0.4492	102.9545	0.0116
cMay11	0 to 0.5mm	05/30/10	0.4689	220.2494	0.0197
cMay16	0 to 0.5mm	05/16/10	0.1488	83.1853	NA
cMay16	0 to 0.5mm	05/17/10	0.1526	129.6669	0.0038
cMay16	0 to 0.5mm	05/18/10	0.1817	445.1131	0.0291
cMay16	0 to 0.5mm	05/19/10	0.192	562.0603	0.0103
cMay16	0 to 0.5mm	05/20/10	0.1604	465.3858	NA
cMay16	0 to 0.5mm	05/21/10	NA	NA	NA
cMay16	0 to 0.5mm	05/22/10	0.1876	561.6681	0.0136
cMay16	0 to 0.5mm	05/23/10	0.2233	196.1085	0.0357
cMay16	0 to 0.5mm	05/24/10	0.2279	286.1311	0.0046

Continued on next page

Table B.3 – continued from previous page

Cohort	Size Fraction	Date	Size (mm)	Abundance (Ind.m^{-3})	Growth (mm.day^{-1})
cMay16	0 to 0.5mm	05/25/10	0.2384	141.6408	0.0105
cMay16	0 to 0.5mm	05/26/10	0.2367	324.4567	NA
cMay16	0 to 0.5mm	05/27/10	0.326	124.0343	0.0893
cMay16	0 to 0.5mm	05/28/10	0.3248	306.4684	NA
cMay16	0 to 0.5mm	05/29/10	0.3648	129.8016	0.04
cMay16	0 to 0.5mm	05/30/10	0.3939	321.1713	0.0291
cMay16	0 to 0.5mm	05/31/10	0.4439	66.7577	0.05
cMay16	0 to 0.5mm	06/01/10	0.4241	353.5336	NA
cMay16	0 to 0.5mm	06/02/10	0.4038	10.5602	NA
cMay16	0 to 0.5mm	06/03/10	0.4889	19.9923	0.0851
cMay20	0 to 0.5mm	05/20/10	0.1604	465.3858	NA
cMay20	0 to 0.5mm	05/21/10	NA	NA	NA
cMay20	0 to 0.5mm	05/22/10	0.1876	561.0681	0.0136
cMay20	0 to 0.5mm	05/23/10	0.2233	196.1085	0.0357
cMay20	0 to 0.5mm	05/24/10	0.2279	286.1311	0.0046
cMay20	0 to 0.5mm	05/25/10	0.2384	141.6408	0.0105
cMay20	0 to 0.5mm	05/26/10	0.2367	324.4567	NA
cMay20	0 to 0.5mm	05/27/10	0.326	124.0343	0.0893
cMay20	0 to 0.5mm	05/28/10	0.3248	306.4684	NA
cMay20	0 to 0.5mm	05/29/10	0.3648	129.8016	0.04
cMay20	0 to 0.5mm	05/30/10	0.3939	321.1713	0.0291
cMay20	0 to 0.5mm	05/31/10	0.4439	66.7577	0.05
cMay20	0 to 0.5mm	06/01/10	0.4241	353.5336	NA
cMay20	0 to 0.5mm	06/02/10	0.4038	10.5602	NA

Continued on next page

Table B.3 – continued from previous page

Cohort	Size Fraction	Date	Size (mm)	Abundance (Ind.m^{-3})	Growth (mm.day^{-1})
cMay20	0 to 0.5mm	06/03/10	0.4889	19.9923	0.0851
cMay23	0 to 0.5mm	05/23/10	0.1484	254.3484	NA
cMay23	0 to 0.5mm	05/24/10	0.1512	190.3226	0.0028
cMay23	0 to 0.5mm	05/25/10	0.1668	162.6051	0.0156
cMay23	0 to 0.5mm	05/26/10	0.1596	93.8876	NA
cMay23	0 to 0.5mm	05/27/10	0.2366	137.9554	0.077
cMay23	0 to 0.5mm	05/28/10	0.2293	161.7999	NA
cMay23	0 to 0.5mm	05/29/10	0.2851	153.6297	0.0558
cMay23	0 to 0.5mm	05/30/10	0.3203	288.8206	0.0352
cMay23	0 to 0.5mm	05/31/10	0.3429	44.9819	0.0226
cMay23	0 to 0.5mm	06/01/10	0.3438	285.5686	9.00E-04
cMay23	0 to 0.5mm	06/02/10	0.3307	3.6816	NA
cMay23	0 to 0.5mm	06/03/10	0.4196	78.531	0.0898
cMay23	0 to 0.5mm	06/04/10	NA	NA	NA
cMay23	0 to 0.5mm	06/05/10	0.4729	420.8423	0.0266
cMay23	0 to 0.5mm	06/06/10	NA	NA	NA
cMay23	0 to 0.5mm	06/07/10	0.4906	251.0487	0.0088
cMay23	0 to 0.5mm	06/08/10	0.4716	99.9266	NA
cMay23	0 to 0.5mm	06/09/10	0.4675	235.1282	NA
cMay27	0 to 0.5mm	05/27/10	0.1463	129.883	NA
cMay27	0 to 0.5mm	05/28/10	0.1449	159.1271	NA
cMay27	0 to 0.5mm	05/29/10	0.1595	142.6032	0.0146
cMay27	0 to 0.5mm	05/30/10	0.2195	169.3804	0.06
cMay27	0 to 0.5mm	05/31/10	0.2314	64.8604	0.0119
cMay27	0 to 0.5mm	06/01/10	0.2679	99.7786	0.0365

Continued on next page

Table B.3 – continued from previous page

Cohort	Size Fraction	Date	Size (mm)	Abundance (Ind.m^{-3})	Growth (mm.day^{-1})
cMay27	0 to 0.5mm	06/02/10	0.2831	1.577	0.0152
cMay27	0 to 0.5mm	06/03/10	0.3252	54.2273	0.0421
cMay27	0 to 0.5mm	06/04/10	0.3718	40.1178	0.0466
cMay27	0 to 0.5mm	06/05/10	0.4	175.9306	0.0282
cMay27	0 to 0.5mm	06/06/10	0.4129	123.1989	0.0129
cMay27	0 to 0.5mm	06/07/10	0.3632	165.3025	NA
cMay27	0 to 0.5mm	06/08/10	0.3672	48.7603	0.004
cMay27	0 to 0.5mm	06/09/10	0.3581	142.5525	NA
cMay27	0 to 0.5mm	06/10/10	0.4996	150.7339	0.1415
cMay27	0 to 0.5mm	06/11/10	0.474	95.7034	NA
cMay27	0 to 0.5mm	06/12/10	0.4905	148.5535	0.0165
cMay30	0 to 0.5mm	05/30/10	0.1516	221.8395	NA
cMay30	0 to 0.5mm	05/31/10	0.1566	31.6916	0.005
cMay30	0 to 0.5mm	06/01/10	0.2081	129.5009	0.0515
cMay30	0 to 0.5mm	06/02/10	0.2183	1.1427	0.0102
cMay30	0 to 0.5mm	06/03/10	0.2178	78.4112	NA
cMay30	0 to 0.5mm	06/04/10	0.2693	33.2847	0.0515
cMay30	0 to 0.5mm	06/05/10	0.3211	125.4321	0.0518
cMay30	0 to 0.5mm	06/06/10	0.2945	128.7586	NA
cMay30	0 to 0.5mm	06/07/10	0.2689	78.0765	NA
cMay30	0 to 0.5mm	06/08/10	0.2871	41.3156	0.0182
cMay30	0 to 0.5mm	06/09/10	0.2789	111.5163	NA
cMay30	0 to 0.5mm	06/10/10	0.3673	114.1064	0.0884
cMay30	0 to 0.5mm	06/11/10	0.3885	67.4515	0.0212
cMay30	0 to 0.5mm	06/12/10	0.3764	32.5118	NA

Continued on next page

Table B.3 – continued from previous page

Cohort	Size Fraction	Date	Size (mm)	Abundance (Ind.m^{-3})	Growth (mm.day^{-1})
cMay30	0 to 0.5mm	06/13/10	0.4327	163.9304	0.0563
cMay30	0 to 0.5mm	06/14/10	0.4621	206.9976	0.0294
cJun01	0 to 0.5mm	06/01/10	0.1491	171.8846	NA
cJun01	0 to 0.5mm	06/02/10	0.2183	1.1427	0.0692
cJun01	0 to 0.5mm	06/03/10	0.2178	78.4112	NA
cJun01	0 to 0.5mm	06/04/10	0.2693	33.2847	0.0515
cJun01	0 to 0.5mm	06/05/10	0.3211	125.4321	0.0518
cJun01	0 to 0.5mm	06/06/10	0.2945	128.7586	NA
cJun01	0 to 0.5mm	06/07/10	0.2689	78.0765	NA
cJun01	0 to 0.5mm	06/08/10	0.2871	41.3156	0.0182
cJun01	0 to 0.5mm	06/09/10	0.2789	111.5163	NA
cJun01	0 to 0.5mm	06/10/10	0.3673	114.1064	0.0884
cJun01	0 to 0.5mm	06/11/10	0.3885	67.4515	0.0212
cJun01	0 to 0.5mm	06/12/10	0.3764	32.5118	NA
cJun01	0 to 0.5mm	06/13/10	0.4327	163.9304	0.0563
cJun01	0 to 0.5mm	06/14/10	0.4621	206.9976	0.0294
cJun03	0 to 0.5mm	06/03/10	0.1534	37.5376	NA
cJun03	0 to 0.5mm	06/04/10	0.184	14.901	0.0306
cJun03	0 to 0.5mm	06/05/10	0.2292	88.2037	0.0452
cJun03	0 to 0.5mm	06/06/10	0.1963	160.3634	NA
cJun03	0 to 0.5mm	06/07/10	0.2063	41.7804	0.01
cJun03	0 to 0.5mm	06/08/10	0.2871	41.3156	0.0808
cJun03	0 to 0.5mm	06/09/10	0.2789	111.5164	NA
cJun03	0 to 0.5mm	06/10/10	0.3673	114.1064	0.0884
cJun03	0 to 0.5mm	06/11/10	0.3885	67.4515	0.0212

Continued on next page

Table B.3 – continued from previous page

Cohort	Size Fraction	Date	Size (mm)	Abundance (Ind.m^{-3})	Growth (mm.day^{-1})
cJun03	0 to 0.5mm	06/12/10	0.3764	32.5118	NA
cJun03	0 to 0.5mm	06/13/10	0.4327	163.9304	0.0563
cJun03	0 to 0.5mm	06/14/10	0.4621	206.9976	0.0294
cJun05	0 to 0.5mm	06/05/10	0.1467	361.0203	NA
cJun05	0 to 0.5mm	06/06/10	0.1351	167.1623	NA
cJun05	0 to 0.5mm	06/07/10	0.1457	121.1904	0.0106
cJun05	0 to 0.5mm	06/08/10	0.1907	67.9686	0.045
cJun05	0 to 0.5mm	06/09/10	0.2073	87.3148	0.0166
cJun05	0 to 0.5mm	06/10/10	0.2846	69.8635	0.0773
cJun05	0 to 0.5mm	06/11/10	0.2837	69.0567	NA
cJun05	0 to 0.5mm	06/12/10	0.301	39.1541	0.0773
cJun05	0 to 0.5mm	06/13/10	0.2991	103.0388	NA
cJun05	0 to 0.5mm	06/14/10	0.3567	169.2531	0.0576
cJun05	0 to 0.5mm	06/15/10	0.3851	621.0002	0.0284
cJun05	0 to 0.5mm	06/16/10	0.4659	373.337	0.0808
cJun08	0 to 0.5mm	06/08/10	0.1307	344.024	NA
cJun08	0 to 0.5mm	06/09/10	0.1533	192.1387	0.0226
cJun08	0 to 0.5mm	06/10/10	0.1982	111.8403	0.0449
cJun08	0 to 0.5mm	06/11/10	0.2021	97.421	0.0039
cJun08	0 to 0.5mm	06/12/10	0.2455	78.0197	0.0434
cJun08	0 to 0.5mm	06/13/10	0.2249	138.2639	NA
cJun08	0 to 0.5mm	06/14/10	0.253	212.8395	0.0281
cJun08	0 to 0.5mm	06/15/10	0.3172	356.3698	0.0642
cJun08	0 to 0.5mm	06/16/10	0.4183	256.232	0.1011
cJun08	0 to 0.5mm	06/17/10	0.4138	302.3025	NA

Continued on next page

Table B.3 – continued from previous page

Cohort	Size Fraction	Date	Size (mm)	Abundance (Ind.m^{-3})	Growth (mm.day^{-1})
cJun08	0 to 0.5mm	06/18/10	0.4152	268.6145	0.0014
cJun08	0 to 0.5mm	06/19/10	0.4671	203.8399	0.0519
cJun08	0 to 0.5mm	06/20/10	0.4427	239.6861	NA
cJun08	0 to 0.5mm	06/21/10	0.4533	148.3587	0.0106
cJun08	0 to 0.5mm	06/22/10	0.4868	91.3773	0.0335
cJun08	0 to 0.5mm	06/23/10	0.4725	157.8899	NA
cJun08	0 to 0.5mm	06/24/10	0.4995	834.5411	0.027
cJun08	0 to 0.5mm	06/25/10	0.4512	171.3592	NA
cJun08	0 to 0.5mm	06/26/10	0.4773	225.8542	0.0261
cJun08	0 to 0.5mm	06/27/10	0.4653	147.2581	NA
cJun10	0 to 0.5mm	06/10/10	0.1377	275.5233	NA
cJun10	0 to 0.5mm	06/11/10	0.148	193.2448	0.0103
cJun10	0 to 0.5mm	06/12/10	0.1632	220.6136	0.0152
cJun10	0 to 0.5mm	06/13/10	0.1501	172.2454	NA
cJun10	0 to 0.5mm	06/14/10	0.172	234.0911	0.0219
cJun10	0 to 0.5mm	06/15/10	0.2333	711.944	0.0613
cJun10	0 to 0.5mm	06/16/10	0.2707	305.8637	0.0374
cJun10	0 to 0.5mm	06/17/10	0.3189	133.1588	0.0482
cJun10	0 to 0.5mm	06/18/10	0.3159	242.3292	NA
cJun10	0 to 0.5mm	06/19/10	0.3788	328.2438	0.0629
cJun10	0 to 0.5mm	06/20/10	0.3784	43.4878	NA
cJun10	0 to 0.5mm	06/21/10	0.377	203.5538	NA
cJun10	0 to 0.5mm	06/22/10	0.3379	93.5547	NA
cJun10	0 to 0.5mm	06/23/10	0.337	308.74234	NA
cJun10	0 to 0.5mm	06/24/10	0.3493	303.3966	0.0123

Continued on next page

Table B.3 – continued from previous page

Cohort	Size Fraction	Date	Size (mm)	Abundance (Ind.m^{-3})	Growth (mm.day^{-1})
cJun10	0 to 0.5mm	06/25/10	0.3868	90.7059	0.0375
cJun10	0 to 0.5mm	06/26/10	0.391	610.2823	0.0042
cJun10	0 to 0.5mm	06/27/10	0.3793	476.7445	NA
cJun10	0 to 0.5mm	06/28/10	NA	NA	NA
cJun10	0 to 0.5mm	06/29/10	0.4053	268.4662	0.013
cJun10	0 to 0.5mm	06/30/10	0.4212	290.4696	0.0159
cJun10	0 to 0.5mm	07/01/10	NA	206.3434	0.084
cJun10	0 to 0.5mm	07/02/10	0.4713	78.4593	NA
cJun15	0 to 0.5mm	06/15/10	0.1394	502.6999	NA
cJun15	0 to 0.5mm	06/16/10	0.1396	195.1853	2.00E-04
cJun15	0 to 0.5mm	06/17/10	0.1348	568.6407	NA
cJun15	0 to 0.5mm	06/18/10	0.194	190.4142	0.0592
cJun15	0 to 0.5mm	06/19/10	0.2202	314.5058	0.0262
cJun15	0 to 0.5mm	06/20/10	0.2222	75.9381	0.002
cJun15	0 to 0.5mm	06/21/10	0.2482	117.4577	0.026
cJun15	0 to 0.5mm	06/22/10	0.2626	116.6371	0.0404
cJun15	0 to 0.5mm	06/23/10	0.2568	413.5747	NA
cJun15	0 to 0.5mm	06/24/10	0.2651	396.3535	0.0083
cJun15	0 to 0.5mm	06/25/10	0.3225	83.0074	0.0574
cJun15	0 to 0.5mm	06/26/10	0.3161	440.6433	NA
cJun15	0 to 0.5mm	06/27/10	0.3259	182.9022	0.0098
cJun15	0 to 0.5mm	06/28/10	NA	NA	NA
cJun15	0 to 0.5mm	06/29/10	0.3265	737.951	3.00E-04
cJun15	0 to 0.5mm	06/30/10	0.336	731.9183	0.0095
cJun15	0 to 0.5mm	07/01/10	0.3813	241.2633	0.0453

Continued on next page

Table B.3 – continued from previous page

Cohort	Size Fraction	Date	Size (mm)	Abundance (Ind.m^{-3})	Growth (mm.day^{-1})
cJun15	0 to 0.5mm	07/02/10	0.3872	126.8319	0.0059
cJun15	0 to 0.5mm	07/03/10	0.399	64.3687	0.0118
cJun15	0 to 0.5mm	07/04/10	0.4502	62.2922	0.0512
cJun18	0 to 0.5mm	06/18/10	0.1347	674.074	NA
cJun18	0 to 0.5mm	06/19/10	0.1386	483.0263	0.0039
cJun18	0 to 0.5mm	06/20/10	0.1401	232.5862	0.0015
cJun18	0 to 0.5mm	06/21/10	0.1408	469.3132	7.00E-04
cJun18	0 to 0.5mm	06/22/10	0.1429	363.871	0.0021
cJun18	0 to 0.5mm	06/23/10	0.1897	279.336	0.0468
cJun18	0 to 0.5mm	06/24/10	0.2051	245.4146	0.0154
cJun18	0 to 0.5mm	06/25/10	0.2566	190.15	0.0515
cJun18	0 to 0.5mm	06/26/10	0.2578	468.5311	0.0012
cJun18	0 to 0.5mm	06/27/10	0.2505	768.5653	NA
cJun18	0 to 0.5mm	06/28/10	NA	NA	NA
cJun18	0 to 0.5mm	06/29/10	0.2486	864.7582	NA
cJun18	0 to 0.5mm	06/30/10	0.2638	936.798	0.0152
cJun18	0 to 0.5mm	07/01/10	0.3162	465.5012	0.0524
cJun18	0 to 0.5mm	07/02/10	0.3202	572.357	0.004
cJun18	0 to 0.5mm	07/03/10	0.3138	139.3227	NA
cJun18	0 to 0.5mm	07/04/10	0.3323	194.8929	0.0185
cJun18	0 to 0.5mm	07/05/10	0.4214	103.6838	0.0891
cJun18	0 to 0.5mm	07/06/10	0.3708	130.6914	NA
cJun23	0 to 0.5mm	06/23/10	0.1379	524.4488	NA
cJun23	0 to 0.5mm	06/24/10	0.1433	571.8843	0.0054
cJun23	0 to 0.5mm	06/25/10	0.2059	355.1538	0.0626

Continued on next page

Table B.3 – continued from previous page

Cohort	Size Fraction	Date	Size (mm)	Abundance (Ind.m^{-3})	Growth (mm.day^{-1})
cJun23	0 to 0.5mm	06/26/10	0.2094	713.9926	0.0035
cJun23	0 to 0.5mm	06/27/10	0.2099	719.6211	5.00E-04
cJun23	0 to 0.5mm	06/28/10	NA	NA	NA
cJun23	0 to 0.5mm	06/29/10	0.1935	1356.899	NA
cJun23	0 to 0.5mm	06/30/10	0.2109	1309.2196	0.0174
cJun23	0 to 0.5mm	07/01/10	0.2576	509.6728	0.0467
cJun23	0 to 0.5mm	07/02/10	0.2727	393.434	0.0151
cJun23	0 to 0.5mm	07/03/10	0.2712	68.7547	NA
cJun23	0 to 0.5mm	07/04/10	0.2816	318.2766	0.0104
cJun23	0 to 0.5mm	07/05/10	0.2564	291.529	NA
cJun23	0 to 0.5mm	07/06/10	0.2679	287.9916	0.0115
cJun23	0 to 0.5mm	07/07/10	0.2751	166.387	0.0072
cJun25	0 to 0.5mm	06/25/10	0.1381	631.814	NA
cJun25	0 to 0.5mm	06/26/10	0.1423	1598.9801	0.0042
cJun25	0 to 0.5mm	06/27/10	0.1416	1251.5875	NA
cJun25	0 to 0.5mm	06/28/10	NA	NA	NA
cJun25	0 to 0.5mm	06/29/10	0.1466	1392.7986	0.005
cJun25	0 to 0.5mm	06/30/10	0.1441	0.0156	NA
cJun25	0 to 0.5mm	07/01/10	0.2009	944.3732	0.0568
cJun25	0 to 0.5mm	07/02/10	0.1877	867.7245	NA
cJun25	0 to 0.5mm	07/03/10	0.1895	288.9121	0.0018
cJun25	0 to 0.5mm	07/04/10	0.1963	623.0448	0.0068
cJun25	0 to 0.5mm	07/05/10	0.2021	642.9493	0.0058
cJun25	0 to 0.5mm	07/06/10	0.1969	601.0934	NA

Continued on next page

Table B.3 – continued from previous page

Cohort	Size Fraction	Date	Size (mm)	Abundance (Ind.m^{-3})	Growth (mm.day^{-1})
cJun25	0 to 0.5mm	07/07/10	0.2122	153.2514	0.0153

B.8 Seaonal Growth Rate

Based on the time series for each component identified and tracked (Table B.3), the daily growth rate was calculated by averaging the daily growth rate for each cohort tracked. Linear regressions were fitted to the time periods showing an increase in growth rate. The full statistical results are presented in the table on the following page.

Table B.4: Statistical results for the linear regressions of shell size growth for the population. The modal shell size (mm) is regressed over the observed periods of increasing shell size for the population of *L. helicina*. Note that the values of the shell growth for the population were the averaged daily growth rates of each component, tracked throughout the daily time series. Refer to Figure 3.2D. Standard errors of the slope and constant/intercpet are displayed in parenthesis with the level of significance for each component displayed beside the slope estimate. The number of observations, R^2, Adjusted R^2, Residual Std. Errors and F statistics are displayed at the bottom of each table.

	Dependent variable:		
	Population Growth Rate	Population Growth Rate	Population Growth Rate
	$mm.day^{-1}$	$mm.day^{-1}$	$mm.day^{-1}$
1 May to 13 May	0.004^{***}		
	(0.001)		
26 May to 16 June		0.001^{**}	
		(0.001)	
7 June to 16 June			0.005^{***}
			(0.001)
Constant	-57.309^{***}	-19.265^{**}	-77.798^{***}
	(8.347)	(7.761)	(21.602)
Observations	13	19	9
R^2	0.811	0.267	0.650
Adjusted R^2	0.794	0.224	0.600
Residual Std. Error	$0.008(df = 11)$	$0.015(df = 17)$	$0.013(df = 7)$
F statistic	$47.187^{***}(df = 1; 11)$	$6.183^{**}(df = 1; 17)$	$12.983^{***}(df = 1; 7)$
Note:			*p<0.1; **p<0.05; ***p<0.01

Table B.5: Statistical results for the linear regressions of shell size growth for the population. The modal shell size (mm) is regressed over the observed periods of increasing shell size for the population of *L. helicina*. Note that the values of the shell growth for the population were the averaged daily growth rates of each component, tracked throughout the daily time series. Refer to Figure 3.2D. Standard errors of the slope and constant/intercpet are displayed in parenthesis with the level of significance for each component displayed beside the slope estimate. The number of observations, R^2, Adjusted R^2, Residual Std. Errors and F statistics are displayed at the bottom of each table.

	Dependent variable:	
	Population Growth Rate mm.day^{-1}	Population Growth Rate mm.day^{-1}
26 May to 16 June	0.001	
	(0.001)	
7 June to 16 June		0.004
		(0.003)
Constant	−10.960	−61.605
	(11.630)	(38.000)
Observations	22	10
R^2	0.043	0.248
Adjusted R^2	−0.005	0.153
Residual Std. Error	0.023($df = 20$)	0.023($df = 8$)
F statistic	0.895($df = 1; 20$)	2.632($df = 1; 8$)
Note:		*p<0.1; **p<0.05; ***p<0.01

B.9 Environmental Connection

The results from Chapter 2 indicated that the temporal resolution may have been too coarse to discern any clear relation between chlorophyll abundance and *L. helicina* population variation. Despite using daily data, there were still no clear relations found between chlorophyll and *L. helicina* growth. It is probable that the high grazing influence of the zooplankton community in Rivers Inlet had kept chlorophyll levels at low concentrations, such that any increase in *L. helicina* abundance or growth rate was not seen.

Results from the linear regressions testing the relation between daily chlorophyll and *L. helicina* abundance for each month, are presented in the table below.

Table B.6: Statistical results of linear regressions testing the relation between chlorophyll and the daily variation in population abundance, for each month. Standard errors of the slope and constant/intercpet are displayed in parenthesis with the level of significance for each component displayed beside the slope estimate. The number of observations, R^2, Adjusted R^2, Residual Std. Errors and F statistics are displayed at the bottom of each table.

	Dependent variable:			
	log-Abundance	log-Abundance	log-Abundance	log-Abundance)
	(April)	(May)	(June)	(July, 1–7)
chl_apr	−0.020			
	(0.034)			
chl_may		0.015		
		(0.031)		
chl_jun			−0.073	
			(0.050)	
chl_jul				−0.004
				(0.071)
Constant	4.265***	6.640***	7.504***	7.482***
	(0.341)	(0.223)	(0.331)	(0.464)
Observations	28	30	29	7
R^2	0.014	0.009	0.072	0.001
Adjusted R^2	−0.024	−0.026	0.038	−0.199
Residual Std. Error	0.751($df = 26$)	0.741($df = 28$)	0.986($df = 27$)	0.660($df = 5$)
F statistic	0.357($df = 1; 26$)	0.253($df = 1; 28$)	2.102($df = 1; 27$)	0.004($df = 1; 5$)
Note:				*p<0.1; **p<0.05; ***p<0.01

B.10 Seasonal Mortality

Seasonal mortality was analyzed from the component level as it was felt that seasonal variation would be potentially masked, from analysis at the population level. The daily abundance of each component tracked was log-transformed and linear regressions were fitted to the perceived periods of notable decrease in abundance for each component

The statistical tables were produced using the `stargazer` package (Hlavac, 2013) for the `R` programming environment. Regression results (slope) for each component tracked is listed with applicable significance codes listed (see the *Note*: at the bottom of the table), as well as the standard errors (in parentheses). The time periods of perceived abundance declines were regressed for each component is listed on the left side of each table. The remaining statistical results (no. observations, R^2, Adjusted R^2, Residual Std. Errors, and F statistics) are listed at the bottom area of each table.

Table B.7: Statistical results of linear regressions testing for periods of increased mortality, for cohorts identified and followed in the daily time series. Standard errors of the slope and constant/intercpet are displayed in parenthesis with the level of significance for each component displayed beside the slope estimate. The number of observations, R^2, Adjusted R^2, Residual Std. Errors and F statistics are displayed at the bottom of each table.

	Dependent Variable:	
	Instantaneous Mortality (fraction dying per unit time)	Instantaneous Mortality (fraction dying per unit time)
7 May to 31 May	−2.911	
	(6.050)	
1 June to 7 July		−3.172
		(2.590)
Constant	42,952.920	46,859.600
	(89,221.450)	(38,276.910)
Observations	23	35
R^2	0.011	0.043
Adjusted R^2	−0.036	0.014
Residual Std. Error	216.944($df = 21$)	164.354($df = 33$)
F statistic	0.231($df = 1; 21$)	1.500($df = 1; 33$)
Note:		*p<0.1; **p<0.05; ***p<0.01